Universidad Politécnica de Cartagena | Campus de Excelencia Internacional

PhD THESIS

CHARACTERISING AN ANCIENT STORAGE AREA OF PHOSPHOGYPSUM BY COMBINING GEOPHYSICAL, GEOCHEMICAL AND STATISTICAL TECHNIQUES

PhD PROGRAM

TECHNOLOGY AND MODELING IN CIVIL, MINING AND ENVIRONMENTAL ENGINEERING

Supervisors:

MARCOS ANTONIO MARTÍNEZ SEGURA

JOSE ALBERTO ACOSTA AVILÉS

MARCO DAVID VÁSCONEZ MAZA

Cartagena, 2020

This PhD thesis uses the compendium of publications mode under article 23 of the Regulation of official doctoral studies of the Universidad Politécnica de Cartagena of December 17, 2015.

Publications

1. **Vásconez-Maza, M.D.**, Martínez-Segura, M.A., Bueso, M.C., Faz, Á., García-Nieto, M.C., Gabarrón, M., Acosta, J.A., 2019. Predicting spatial distribution of heavy metals in an abandoned phosphogypsum pond combining geochemistry, electrical resistivity tomography and statistical methods. J. Hazard. Mater. 374, 392–400. https://doi.org/10.1016/j.jhazmat.2019.04.045; Q1; IF: 9.038

2. Martínez-Segura, M.A., **Vásconez-Maza, M.D.**, García-Nieto, M.C., 2020. Volumetric characterisation of waste deposits generated during the production of fertiliser derived from phosphoric rock by using LiDAR and electrical resistivity tomography. Sci. Total Environ. 716, 137076. https://doi.org/10.1016/j.scitotenv.2020.137076; Q1; IF: 6.551

3. **Vásconez-Maza, M. D.**, Bueso, M.C., Faz, A., Acosta, J.A., Martínez-Segura, M.A., 2021. Assessing the behaviour of heavy metals in abandoned phosphogypsum deposits combining electrical resistivity tomography and multivariate analysis. J. Environ. Manage. 278, 301–4797. https://doi.org/10.1016/j.jenvman.2020.111517; Q1; IF: 5.647

Universidad Politécnica de Cartagena

DT-16

CONFORMIDAD DE SOLICITUD DEAUTORIZACIÓN DE DEPÓSITO DE TESIS DOCTORAL POR EL DIRECTOR DE LA TESIS

D. Marcos Antonio Martínez Segura Director de la Tesis doctoral: "Characterising an ancient storage area of phosphogypsum by combining geophysical, geochemical and statistical techniques."

INFORMA:

Que la referida Tesis Doctoral, ha sido realizada por D. Marco David Vásconez Maza, dentro del Programa de Doctorado Tecnología y Modelización en Ingeniería Civil, Minería y Ambiental, dando mi conformidad para que sea presentada ante el Comité de Dirección de la Escuela Internacional de Doctorado para ser autorizado su depósito.

[x] Informe positivo sobre el plan de investigación y documento de actividades del doctorando emitido por el Director y Tutor (**RAPI**).

La rama de conocimiento en la que esta tesis ha sido desarrollada es:

- [ ] Ciencias
- [ ] Ciencias Sociales y Jurídicas
- [x] Ingeniería y Arquitectura

En Cartagena, a 14 de octubre de 2020

EL DIRECTOR DE LA TESIS

MARCOS ANTONIO|MARTINEZ|SEGURA

Firmado digitalmente por MARCOS ANTONIO|MARTINEZ|SEGURA
Nombre de reconocimiento (DN): cn=MARCOS ANTONIO|MARTINEZ|SEGURA, serialNumber=[redacted], givenName=MARCOS ANTONIO, sn=MARTINEZ SEGURA, ou=CIUDADANOS, o=ACCV, c=ES
Fecha: 2020.10.14 19:01:55 +02'00'

Fdo.: Marcos Antonio Martínez Segura

COMITÉ DE DIRECCIÓN ESCUELA INTERNACIONAL DE DOCTORADO

Universidad Politécnica de Cartagena

DT-16

CONFORMIDAD DE SOLICITUD DEAUTORIZACIÓN DE DEPÓSITO DE TESIS DOCTORAL POR EL CODIRECTOR DE LA TESIS

D. Jose Alberto Acosta Avilés Codirector de la Tesis doctoral: "Characterising an ancient storage area of phosphogypsum by combining geophysical, geochemical and statistical techniques."

INFORMA:

Que la referida Tesis Doctoral, ha sido realizada por D. Marco David Vásconez Maza, dentro del Programa de Doctorado Tecnología y Modelización en Ingeniería Civil, Minería y Ambiental, dando mi conformidad para que sea presentada ante el Comité de Dirección de la Escuela Internacional de Doctorado para ser autorizado su depósito.

[x] Informe positivo sobre el plan de investigación y documento de actividades del doctorando emitido por el Director y Tutor (**RAPI**).

La rama de conocimiento en la que esta tesis ha sido desarrollada es:

- [ ] Ciencias
- [ ] Ciencias Sociales y Jurídicas
- [x] Ingeniería y Arquitectura

En Cartagena, a 14 de octubre de 2020

EL CODIRECTOR DE LA TESIS

JOSE ALBERTO| ACOSTA| AVILES

Firmado digitalmente por JOSE ALBERTO| ACOSTA|AVILES
Nombre de reconocimiento (DN): cn=JOSE ALBERTO|ACOSTA|AVILES, serialNumber=[redacted], givenName=JOSE ALBERTO, sn=ACOSTA AVILES, ou=Ciudadanos, o=ACCV, c=ES
Fecha: 2020.10.15 07:45:02 +02'00'

Fdo.: Jose Alberto Acosta Avilés

COMITÉ DE DIRECCIÓN ESCUELA INTERNACIONAL DE DOCTORADO

Universidad Politécnica de Cartagena

DT-17

CONFORMIDAD DE DEPÓSITO DE TESIS DOCTORAL

POR LA COMISIÓN ACADÉMICA DEL PROGRAMA

Ángel Faz Cano, Presidente de la Comisión Académica del Programa de Doctorado Tecnología y Modelización en Ingeniería Civil, Minería y Ambiental.

INFORMA:

Que la Tesis Doctoral titulada, "Characterising an ancient storage area of phosphogypsum by combining geophysical, geochemical and statistical techniques", ha sido realizada, dentro del mencionado Programa de Doctorado, por D. Marco David Vásconez Maza, bajo la dirección y supervisión del Dr. Marcos Antonio Martínez Segura y el Dr. Jose Alberto Acosta Avilés.

En reunión de la Comisión Académica, visto que en la misma se acreditan los indicios de calidad correspondientes y la autorización de los directores de la misma, se acordó dar la conformidad, con la finalidad de que sea autorizado su depósito por el Comité de Dirección de la Escuela Internacional de Doctorado.

[x] Evaluación positiva del plan de investigación y documento de actividades por el Presidente de la Comisión Académica del programa (**RAPI**).

La Rama de conocimiento por la que esta tesis ha sido desarrollada es:

- [ ] Ciencias
- [ ] Ciencias Sociales y Jurídicas
- [x] Ingeniería y Arquitectura

En Cartagena, a 18 de octubre de 2020

EL PRESIDENTE DE LA COMISIÓN ACADÉMICA

ANGEL|FAZ|CANO

Firmado digitalmente por ANGEL|FAZ|CANO
Nombre de reconocimiento (DN): cn=ANGEL|FAZ|CANO, serialNumber=[redacted], givenName=ANGEL, sn=FAZ CANO, ou=CIUDADANOS, o=ACCV, c=ES
Fecha: 2020.10.18 19:27:40 +02'00'

COMITÉ DE DIRECCIÓN ESCUELA INTERNACIONAL DE DOCTORADO

Universidad Politécnica de Cartagena

Sr. D. Marco David Vásconez Maza

Visto el informe favorable del Director de Tesis y el Vº Bº de la Comisión Académica del Programa de Doctorado "Tecnología y Modelización en Ingeniería Civil, Minera y Ambiental" para la presentación de la Tesis Doctoral titulada: **"Characterising an ancient storage area of phosphogypsum by combining geophysical, geochemical and statistical techniques"** solicitada por D. MARCO DAVID VÁSCONEZ MAZA, el Comité de Dirección de la Escuela Internacional de Doctorado de la Universidad Politécnica de Cartagena, en reunión celebrada el 26 de octubre de 2020, considerando lo dispuesto en el artículo 23 del Reglamento de Estudios Oficiales de Doctorado de la UPCT, aprobado en Consejo de Gobierno el 17 de diciembre de 2015,

ACUERDA

Autorizar la presentación de la Tesis Doctoral a D. Marco David Vásconez Maza en la modalidad de "compendio de publicaciones".

Contra el presente acuerdo, que no agota la vía administrativa, podrá formular recurso de alzada ante el Sr. Rector-Magnífico de la Universidad Politécnica de Cartagena, en el plazo de un mes a partir de la notificación de la presente.

Cartagena, 26 de octubre de 2020

EL DIRECTOR DE LA ESCUELA
INTERNACIONAL DE DOCTORADO

SANCHEZ PALMA PEDRO - [redacted]

Firmado digitalmente por SANCHEZ PALMA PEDRO - [redacted]
Fecha: 2020.10.28 11:29:42 +01'00'

Fdo.: Pedro Sánchez Palma

To: Lucila and Adolfo, Cristina and Sergio

for their unconditional

Love.

AGRADECIMIENTOS

En primer lugar; quiero agradecer a mi director de tesis, el Doctor Marcos Antonio Martínez Segura, quien ha sido el pilar fundamental en la realización de esta tesis. No tengo palabras suficientes para agradecer su implicación, su paciencia, sus consejos, su guía, su motivación, su confianza y su manera de enseñar. Quiero agradecer también; cada momento dedicado, las incontables reuniones, cada salida de campo e incluso aquellos momentos fuera del ámbito académico ya que, en esos instantes es cuando las lecciones más grandes se aprenden.

A La Cátedra de desarrollo urbano sostenible y estudios de suelos contaminados del Ayuntamiento de Cartagena y a su director Ángel Faz Cano. También, a Jose Alberto Acosta, codirector y a María del Carmen Bueso por su colaboración para el desarrollo de esta tesis.

A mis padres, Lucila y Adolfo, luchadores incansables. Gracias por haberme brindado todo su apoyo. Me siento muy orgulloso de ustedes ya que, sin apenas haber asistido a las aulas, apostaron por la educación y lograron educar a todos sus hijos. Gracias por ser tan responsables, por su tenacidad y por buscar siempre días mejores para nosotros; incluso, cuando eso significó viajar muy lejos... Su migración fue una etapa muy dura; pero, la supieron sobrellevar y mantener la familia unida especialmente, cuando hubo un océano de distancia entre nosotros. Todo su esfuerzo ha dado buen fruto.

A mi hermana, Elizabeth Cristina, la pieza clave de mi vida. Gracias a ti he llegado a esta etapa. Tú has sido el motor y la guía; porque cuando la vida nos impuso retos enormes, tú encontraste la manera de superarlos y llevarnos a buen puerto. Eres lo máximo hermana mía, gracias por forjar en mi la confianza y enseñarme a perseverar hasta conseguirlo.

A Sergio, mi compañero de vida. Llegaste en el momento justo, la vida nos unió de la forma más inusual y lo agradezco ya que, eres lo que más amo en este mundo. El haberte conocido y poder construir nuestro futuro es lo más grande de esta vida. Gracias por tu entrega, por tu amor, por tu apoyo y por todo lo que nos queda por vivir.

También, quiero agradecer a todos y a cada uno de los miembros de mi familia quienes han estado allí para brindarme una palabra de aliento e impulsándome a continuar en la vida académica y profesional.

Finalmente quiero agradecer a todos los miembros de la universidad, a todos mis amigos y amigas quienes han estado presentes durante este proceso.

RESUMEN

Los fertilizantes fosfóricos han tenido un impacto positivo en la industria agrícola. Sin embargo, este tipo de fertilizante, además del fertilizante, genera una cantidad significativa de fosfoyeso como subproducto. Dependiendo del ácido utilizado en el proceso industrial del fertilizante se pueden producir hasta cinco toneladas de fosfoyeso. En la zona de estudio se empleó el proceso de ácido húmedo que consiste en atacar la roca fosfórica con un ácido fuerte, generalmente ácido sulfúrico.

Las investigaciones previas de fosfoyeso lo han estudiado con la ayuda de análisis químicos y radiológicos, pero no con tomografía eléctrica. Por lo tanto, la tesis pretende caracterizar una antigua zona de fosfoyeso ubicada en la Región de Murcia, en el sureste de España, utilizando la tomografía eléctrica como principal herramienta para la caracterización y así, establecer una metodología eficiente para evaluar áreas de residuos.

La presente tesis doctoral utiliza la modalidad de compendio de publicaciones. Tres publicaciones científicas componen este documento. Inicialmente, se caracteriza físicamente el área de estudio; calculando el volumen existente en los depósitos de residuos. En segundo lugar, se realiza una caracterización geoquímica; determinando que el cromo es el metal más presente en los residuos. Finalmente, se establece una metodología eficiente para identificar y clasificar el depósito más contaminado por metales pesados.

La primera publicación utiliza LiDAR y tomografía de eléctrica para determinar con alta precisión el volumen de los depósitos en el área de estudio. Esta combinación no solo mejora la precisión del volumen, sino que también establece una metodología para calcular el volumen en este tipo de depósitos. El estudio presentado mejoró los resultados de estudios previos realizados algunos años antes por otra empresa.

La segunda publicación determina la distribución espacial de los metales pesados presentes en los depósitos de fosfoyeso. La tomografía eléctrica y los datos geoquímicos se combinaron utilizando modelos de regresión no lineal; logrando un modelo predictivo confiable. La combinación de las técnicas geofísicas, geoquímicas y estadísticas arrojan resultados muy significativos.

La última publicación evalúa el comportamiento de los metales pesados de los depósitos de fosfoyeso. La caracterización física y química reveló que los depósitos contienen un tipo diferente de residuo. Por lo tanto, se realizó un análisis de componentes principales y un análisis discriminante de mínimos cuadrados parciales para clasificar y discriminar ambas poblaciones.

Por tanto, la investigación ha logrado con éxito los objetivos planteados. Los resultados mostraron que la combinación de tomografía eléctrica con análisis químico es adecuada y confiable para caracterizar depósitos de desechos. Adicionalmente, incorporar herramientas estadísticas han demostrado resultados satisfactorios y confirman matemáticamente los resultados obtenidos.

Finalmente, esta tesis se estructura en capítulos de la siguiente manera: el capítulo uno presenta los objetivos, el capítulo dos analiza el estado del arte. Posteriormente, los capítulos tres, cuatro y cinco contienen las publicaciones científicas que componen esta tesis. Finalmente, el capítulo seis trata de las conclusiones de esta tesis doctoral.

SUMMARY

Phosphoric fertilisers have impacted positively on the agricultural industry. Nevertheless, this type of fertiliser, apart from the fertiliser itself, also generates a significant quantity of phosphogypsum as a by-product. Per one ton of fertiliser, five tonnes of phosphogypsum are generated. This occurs due to the industrial process followed in the study area. The factory employed the wet acid process which consists in attacking the phosphoric rock with a strong acid, usually, sulphuric acid.

Previously, phosphogypsum has not been studied with electrical resistivity tomography but rather radiological and chemical analysis. Therefore, the thesis intends to characterise an ancient phosphogypsum area located in the Murcia Region in the Southeast of Spain with ERT as the principal tool to set an efficient methodology to assess waste areas.

The present doctoral thesis uses the compendium of publications mode. Three scientific publications compose this document. Initially, it assesses the whole area volumetrically with significant accuracy. Next, it evaluates geochemically one specific pond determining that chromium is the most present metal in the waste. Finally, an efficient methodology is established to identify and classify the deposit most contaminated by heavy metals.

The first publication uses LiDAR and electrical resistivity tomography for determining the volume of the deposits in the study area accurately. Not only does this combination enhances the precision of the results, but it also sets a methodology for calculating the volume of the deposits. The presented study improved the results of previous studies carried out some years before by another company.

The second publication determines the spatial distribution of the heavy metals presents within deposits of phosphogypsum. Electrical resistivity tomography and geochemical data were merged by using non-linear regression models, achieving a reliable predictive model. The combination of the geophysical, geochemical and statistical techniques yields significant results.

The last publication assesses the behaviour of heavy metals of phosphogypsum deposits. Physical and chemical characterisation revealed that deposits hold a different type of waste.

Therefore, it was performed principal component analysis and partial least squares discriminant analysis to classify and discriminating both populations.

Consequently, the research has successfully achieved the objectives. Results showed that combining electrical resistivity tomography with chemical analysis is suitable and reliable to characterise waste deposits. Additionally, incorporating statistic tools have demonstrated satisfactory results and support the obtained results mathematically.

Finally, this thesis is structured in chapters as follows: chapter one presents the objectives, chapter two analyse state of the art. Later, chapters three, four, and five holds the scientific publications that compose this thesis. Finally, chapter six deals with the conclusions of this doctoral thesis.

CONTENTS

CONTENTS

List of tables

List of Figures

CHAPTER 1

1. OBJECTIVES

The main objective of this doctoral thesis is characterising an ancient storage area of phosphogypsum by using electrical resistivity tomography as a transversal tool to set an efficient methodology of waste assessment. The work in this dissertation is intended to seek suitable synergic combinations of electrical resistivity tomography with other techniques for obtaining more new information.

Therefore, the present dissertation promotes the use of electrical resistivity tomography in combination with chemical analysis incorporating statistic tools to structure models, yielding useful and readable information to researchers and scientists. Hence this doctoral thesis is developed in three phases.

The first stage deals with the physical characterisation proposing the following specific objectives which aim to:

- Scan the industrial area to figure out the physical distribution and possible variants of the waste deposits.
- Determine the volume contained in the chosen deposits by merging Electrical Resistivity Tomography with LiDAR point cloud.

The second stage focuses on the chemical characterisation with two specific objectives that intend to:

- Perform the physical and chemical characterisation of phosphogypsum using geophysical and geochemical techniques.
- Predict the heavy metals spatial distribution through statistical models.

Finally, the third stage defines the most contaminated deposit by heavy metals; introducing a specific objective that pretends to:

- Conduct unsupervised and supervised techniques to identify and classify the existing chemical population within phosphogypsum deposits.

The present PhD thesis is organised as follows. Chapter two analyse state of the art and mention the methodology followed in the publications. Chapter three, four and five contain the three publications, respectively. Conclusions are given in Chapter six. Chapter 7 is devoted to references. Finally, the appendixes present the correspondence with the journals and the impact factor these.

CHAPTER 2

2. STATE OF THE ART AND METHODOLOGY

Industrial production brings many benefits to the economy around the world. However, industrial production, in most of the cases, generates by-products. These by-products, owing to its chemical composition, are sometimes non-reusable or hazardous. Then, it was necessary to store these residues. Since the environmental regulations in the past were fewer rigours than now. By-products were stored in the factory or simple threw to the environment.

According to the European Environmental Agency (2015), there are around 4,000,000 hectares contaminated spread in Europe. One representative example is the case of Huelva; during many years, liquid waste was thrown to the ocean, and the solid phosphogypsum was a store near the marshes. Nowadays, there are about 440 hectares plenty of phosphogypsum. Another example is Portman in the Southeast of Spain with 57 million tonnes of mining tailings.

By 1991, the European Union promoted new environmental regulations (European Communities, 1991). Spain adopted the new environmental law by 1998. Environmental liabilities on waste generated by the industry were established as well as the requirement to create management plans for the existing waste and contaminated soils (Juan Carlos I Rey de España, 1998). Spain, by 2005, established the activities that cause soil contamination as well as set the standard and criteria for establishing the thresholds to declare a site as contaminated. The Spanish Royal Decree 9/2005 holds the reference concentration levels which are unique for each province of the country. During the research, these levels of reference are referred to as “NGR” (BOE, 2005b).

One of these potentially contaminated areas is “El Hondón”, an abandoned industrial area adjacent to Cartagena in the Murcia Region in Spain. This area covers approximately 110 hectares. This area was an economic pole of the city (2018). Nowadays, the A-30 motorway divides the property into two halves. The Southeast of Spain has semi-arid Mediterranean weather featured by mild winter and hot summers. The geological composition of the study area is composed of a deposition of three main components: conglomerates (Tortonian), limestone (Messianian) and sandstone (Pliocene).

Various factories have performed their activity at "El Hondón", by 1950 the metallurgical company "Española del Zinc" refined zinc for about a decade. "Sociedad General de Industria y Comercio", "Unión Española de Explosivos", "Explosivos Río Tinto S.A.", "Fertilizantes Españoles S.A." and "Potasas y Derivados S.A." are some other factories that have passed by the industrial area. Even though owners and legally were different factories have followed the same scheme of production, which consist of obtaining phosphoric fertiliser by attacking phosphoric rock with sulphuric acid. This process generated phosphogypsum and pyrite acid as by-products.

"Potasas y Derivados" was the last factory to work on the study area. The factory had three lines of production: the plant of sulphuric acid, the plant of phosphoric fertiliser and the plant of potassium sulphate.

The sulphuric acid plant used as raw materials pyrite, air, dehydrating, water and vanadium as a catalyst. This plant generated as by-products: pyrite ashes, gaseous emissions, wastewater. Next, the plant of phosphoric fertiliser used as raw materials: phosphoric rock and the previously obtained sulphuric acid. The plant generates some by-products: phosphate powder, gaseous emissions, wastewater, hydrofluoric acid and phosphogypsum. Finally, the plant of potassium sulphate needed potassium sulphate, sulphuric acid, and calcium hydroxide. The by-product generated were hydrochloric acid which will be used for attacking the phosphoric rock.

The aforementioned industrial area before was in the peripheries of the urban nuclei, but the city expansion has enveloped it. Nowadays, the ancient industrial area is an abandoned place where there only remains the wastes of the former factories. Debris and several deposits are spread all over the industrial area. The majority of the deposits hold phosphogypsum waste and the rest pyrite ashes. This abandoned area poses two main issues. The most visible is the interruption of the urban expansion and the other that is less visible, but it could represent more danger than the first one. The area houses potentially hazardous waste that was generated during the synthesising of phosphoric fertiliser derived from the phosphoric rock.

Phosphogypsum has been studied since several years ago; it contains trace elements, natural radioactive isotopes such as ^{238} U, ^{232} Th, ^{40}K and its daughters. Most of the components of phosphogypsum could be dangerous for both human health and the environment.

Phosphogypsum is a complex waste; it is featured for being acidic and high in saline. This waste appears in huge amounts. Five tonnes of phosphogypsum are generated per one ton of fertiliser. Phosphogypsum poses an environmental issue not only for the quantity produced but also for its chemical composition. Phosphogypsum was obtained through the wet acid process; which concentrates heavy metals, trace materials, and some natural radioactive isotopes. The fertiliser process production employed the widely known, wet acid process, which reacts as follows: $Ca_{10}(PO_4)6X_2 + 10H_2SO_4 + 20H_2O = 6H_3PO_4 + 10CaSO_4 \cdot 2H_2O + 2HX$ where X = Cl, F, OH. Thus, long time exposure to this waste could affect the environment and human health (Rutherford, Dudas, & Samek, 1994).

Besides, phosphogypsum is present around the world from Tunisia to Florida. The management of this waste is a worldwide environmental issue. Not only does the management of phosphogypsum present a problem, but also phosphogypsum is difficult to reuse. Several researchers have been carried out various studies for reusing phosphogypsum. Ma et al. (2018) studied a better synthesis for cleaner phosphogypsum. Some authors study the way to reuse phosphogypsum as raw material (Mashifana, Ntuli, & Okonta, 2018; Romero-Hermida et al., 2018).

Phosphogypsum is a source of trace elements that could move from one place to another. Pérez-López et al. (2016) studied the mobility of the trace elements of phosphogypsum of Huelva; the study concluded that the surroundings of the stacking place were polluted. El Zrelli et al. (2019) found that a vast quantity of contaminants was transferred to the aquatic environment.

Heavy metals exposure could promote the appearance of several illnesses, according to the Agency for toxic substances and disease registry (2011). For instance, arsenic affects the neurological and respiratory system. Cadmium could affect several human systems such as: neurological, respiratory, renal and reproductive mostly if the exposition occurs during the development stadium of the organs. Lead affects the renal and neurological system as

well. The list is long and continues; some of them are catalogued as a probable cause of cancer.

Also, the chemical composition of the phosphogypsum offers an important range of reuse possibilities. In agriculture, it could be used as amend for soils (Papastefanou, Stoulos, Ioannidou, & Manolopoulou, 2006). Cardenas-Escudero et al. (2011) used phosphogypsum for CO_2 sequestration. Sadiqul et al. (2017) have studied the effects of phosphogypsum on Portland cement.

Future and new investigation lines are already open with phosphogypsum and their possible applications. For example, phosphogypsum could be a source of minerals or elements (Walawalkar, Nichol, & Azimi, 2016). Virolainen et al. (2019) studied the use of the resin-in-leach process for recovering rare earths from phosphogypsum. Since trace and radioactive elements are present in the phosphogypsum composition and due to the amount of phosphogypsum that already exist around the world; it could become suitable to exploit from a mineral point of view. Lin et al. (2018) recover uranium from phosphogypsum by using new technologies.

The bibliographic revision yielded the same conclusion: phosphogypsum represents risks for both human health and the environment. Before, phosphogypsum has not been studied with electrical resistivity tomography (ERT) but rather chemical and radiological analysis.

Applied geophysics is a well-known and widely proven science; it is composed of several non-invasive techniques. Due to the high prices and the complex software demanded, geophysics has been utilised almost only in the phase of exploration of extractable industries. Cutting-edge technology has opened a wide range of application for geophysics. The new and powerful computers permit invert data with a velocity that before was inconceivable. Nowadays, it has become common and affordable to use geophysics as a primary tool to assess mining tailings, urban areas or examining the underground of an archaeological venue (Drahor, 2011; Perrone, Lapenna, & Piscitelli, 2014).

One of the techniques most employed in the field is the electrical resistivity tomography (ERT) due to it offers accurate and fast results. Electrical resistivity tomography technique is easy to deploy in the field and not require significant resources investment. Another positive aspect of ERT is the versatility; it adapts to almost any field of study. Martínez-Pagán (2006) applied electrical resistivity tomography to assess mining tailings as well as pig farming industry. Various authors used it as the primary tool to perform their studies (Samouëlian, Cousin, Tabbagh, Bruand, & Richard, 2005; Tsokas, Tsourlos, Vargemezis, & Novack, 2008; Chambers et al., 2014).

1D and 2D pseudosection were employed to infer information previously. Currently, electrical resistivity tomography (ERT) is on the crest of the wave. 3D and 4D models are computed with novel and very sophisticated software and hardware. Geophysics provide important information at every scale, from local studies to global measures. ERT offers the possibility of monitoring 24 hours, 365 in a year. These data might help to compute an accurate model that would become vital for the decision-making process (British Geological Survey, 2020).

Consequently, this dissertation analysis it is using Electrical Resistivity Tomography in combination with some other complementary techniques, yielding a methodology that efficiently locates polluted areas and pollutant type. The premise of this work is providing updated information for a management plan or future remedy actions. Knowing where and how pollutant are distributed in an area is an imperative step prior to any environmental remediation.

2.1. Techniques employed

Electrical resistivity tomography

Electrical resistivity tomography (ERT) is quintessentially a non-invasive technique. This technique bases on the principle of the four electrodes array. There is a total of four electrodes. Two of them are the current electrodes, usually referred to as A – B, that inject the current. The other pair referred to as M – N, are the potential electrodes, which measure the difference in potential created (Everett, 2013).

The process of gathering information is divided into two stages. In the field, the apparent resistivity was gathered by using a Syscal R1 Switch 72 resistivimeter from IRIS. Wenner-Schlumberger array was employed to gather the measures due to it offers good vertical resolution, depth penetration and high signal-to-noise ratio.

The final stage is to invert the field data to true resistivity. RES2DINV software was employed to invert the data.

Chemical laboratory analysis

Before running the chemical analysis, samples passed by a preparation stadium. This preparation stadium consists of drying the samples during 72 hours at 35º C. Next, sieving it with a 2 mm sieve and ground with a Retsch RM grinder. The physical properties potential of hydrogen (pH) and electrical conductivity (EC) were measured with deionised water with the following portions. For pH one part of the sample into 2.5 parts of deionised water (1:2.5 w/v). While for EC one part of the sample with 5 parts of deionised water (1:5 w/v).

Determining the concentration of metals of the samples, the laboratory followed the standardised US-EPA method 3051. First, it is mandatory to digest the sample with nitric acid following fixed portions; 0.5 g of sample in 10 ml of nitric acid 65%. The process of digestion is performed with a MARS 6 microwave. Next, an inductively coupled plasma mass spectrometer (ICP-MS) measures the metallic concentration of the digested samples.

The ICP-MS is sophisticated equipment for quantifying metals; it performs the measures with lower limits of detection in the order of one part per trillion to one part per quadrillion. A total of eight metal were analysed: arsenic, cadmium, chromium, copper, lead, nickel, mercury and zinc.

Reagent blanks and a certificated material of reference (BAM-U110) verified the accuracy and dependability of the laboratory results. BAM-U110 is a commercial certificated material of reference for contaminated soil, it contains known mass fraction of

arsenic, cadmium, cobalt, chromium, copper, mercury, magnesium, nickel, lead, and zinc (*Certified Reference Material BAM-U110 Contaminated Soil Certified Values*, 2006).

Statistical software

R free software is conceived as an environment where statistical techniques are performed. Not only does R is a powerful statistical tool, but it also promotes sharing knowledge in public domain forums (R Core Team, 2020). This doctoral thesis used R for computing and graphing the whole statistic study.

In the first stage, descriptive statistics helped figured out global behaviour. Next, sophisticated statistic tools were employed; the first publication used non-linear regression models (nls function) as the main tool for predicting the spatial distribution of chromium. The third publication aimed to recognise and classify the populations; then, it was employed principal component analysis (PCA) and partial least squares-discriminant analysis (PLS-DA). R contains a vast range of libraries and resources that accelerated the process of statistical computing and interpretation.

2.2. Methodology

This doctoral thesis bases on the use of electrical resistivity tomography, chemical analysis and as merging tool, the statistic. This PhD thesis is developed in three phases.

In the article entitled “Volumetric characterisation of waste deposits generated during the production of fertiliser derived from phosphoric rock by using LiDAR and electrical resistivity tomography”. This paper deals with the volume calculation of the four deposits of the whole study area. The research work is divided into two stages: field data gathering and treatment of the data at the office.

The study area is composed of several deposits of waste from phosphoric fertiliser synthesis and roasting pyrite process. Since the thesis is focused on providing utile information for a future management plan; it was necessary to develop an efficient methodology for calculating the volume of the existing waste.

There are various methods to calculate or estimate volume either geometrically or with some GPS coordinates and mathematical work. However, these methods showed a low

level of accuracy or even worse, it was not any manner to prove its accuracy. Hence, we utilised the LiDAR point cloud merged with electrical resistivity tomography to calculate the volume of the deposit assuring metric precision.

LiDAR point cloud covers the whole surface of Spain with a density of at least 0.5 points per square meter (IGN, 2020), which allows creating a superficial surface model with enough points of reference. The main idea of the methodology is to create accurate surface models one on the top of the deposit and the other on the bottom.

The electrical resistivity tomography originated 2D geoelectrical profiles what allowed estimating the geometry of the deposit. Next, five boreholes were drilled for extracting samples to run the chemical analysis. Not only does the boreholes provide chemical samples but also verifies the thickness of the waste layer exactly. Knowing the exact point where the natural soil appears in five different points of the deposit permitted to delimit the subsurface.

Merging the boreholes information with the geometry obtained from the electrical resistivity tomography study yielded an accurate surface model of the subsurface of the deposit. Once both surfaces were completed, the volume calculation become in a mathematical problem; calculating what is in between the two layers what we solved by using a commercial software “Surfer”.

The next article, “Predicting spatial distribution of heavy metals in an abandoned phosphogypsum pond combining geochemistry, electrical resistivity tomography and statistical methods” the fieldwork was developed at “El Hondón”. Basically, it was performed the electrical resistivity tomography campaign as the first step. Next, with the resulting geoelectrical profiles, it was planned the most suitable place to drill the boreholes from which the core samples for performing the chemical analysis were extracted.

Once all data were acquired, the desk work started. Chemical results were analysed to figure out the distribution of the heavy metals along the borehole. For the first publication, it was relatively easy to find out the behaviour of chromium owing to it presented a well-defined distribution. Next, both geoelectrical and chemical data were merged to infer new information.

Statistical tools were used to recognise relationships among variables. In this case, regression models were the principal tool for assessing correlations between heavy metals and electrical resistivity tomography. Several non-linear regression models were carried out considering the electrical resistivity tomography as the independent variable. The accuracy of the models was measured with the root mean square error (RMSE), but it only supported the model goodness. Therefore, the relationship measure between observed and fitted values was the coefficient of correlation of Pearson.

The last scientific publication of the present thesis was entitled "Assessing the behaviour of heavy metals in abandoned phosphogypsum deposits combining electrical resistivity tomography and multivariate analysis". This publication conjugated all the lessons previously learned.

During the production of the two previous papers, we have noticed that phosphogypsum deposit presented a different metallic concentration, but the same analysed elements. Thereby, we decided to analyse the origin of the waste what opened a new line of investigation. Next, we employed unsupervised and supervised techniques to identify and classify the existing population in the waste.

Finally, the methodology was able to distinguish waste that was generated with hydrochloric acid and the other waste that was generated with sulphuric acid. This differentiation might bring several benefits at the moment of remediation due to waste generated with hydrochloric acid contain significant lower metallic concentration; thereby, it must be treated differently, saving time and reducing costs.

CHAPTER 3

3. VOLUMETRIC CHARACTERISATION OF WASTE DEPOSITS GENERATED DURING THE PRODUCTION OF FERTILISER DERIVED FROM PHOSPHORIC ROCK BY USING LIDAR AND ELECTRICAL RESISTIVITY TOMOGRAPHY

This paper is published as: Martínez-Segura, M.A., **Vásconez-Maza, M.D.**, García-Nieto, M.C., 2020. Volumetric characterisation of waste deposits generated during the production of fertiliser derived from phosphoric rock by using LiDAR and electrical resistivity tomography. Sci. Total Environ. 716, 137076. https://doi.org/10.1016/j.scitotenv.2020.137076

The author of the present PhD thesis has contributed significantly to this publication. Since the beginning of this scientific work, initial draft, writing and final publication of the paper. All work was done under the direction of the supervisors.

Abstract

Industrial production is an indicator of the economy. Producing industrially boosts economies; but along with the economic growth, the industrial production comes with intrinsically two main parts: the product itself and a long-term issue, the by-product, that most of the time are non-recyclables or, even worse, that are hazardous. Fertiliser derived from phosphoric rock industry produces five tonnes of phosphogypsum per one tonne of fertiliser produced. Acid sulphuric synthesising from roasting pyrite generates ashes enriched in heavy metals that are toxic to human health. In Europe, before 1998, there were not any legal measures in place, bringing about significant environmental consequences. Western Europe, especially Mediterranean countries, there have been 4 000 000 hectares identified that are potentially contaminated because of abnormal salinity and alkalinity values spread in approximately 300 000 sites. The majority of the potentially contaminated sites are entirely unknown in terms of volume, geometry, chemical content, etcetera.

Therefore, this study aims to develop a fast and efficient methodology to assess in geometric and volumetric terms that would help enormously at the moment of planning the remediation of the site or waste treatment. The study of different waste deposits allowed having enough materials and variants for proving the effectiveness of the methodology for calculating an accurate volume. The Electrical Resistivity Tomography and boreholes core samples ensure the depth and the thickness of the waste layer, while LiDAR point cloud guarantees the exactness of the digital terrain model created for the surface of the pond/landfill, yielding an accurate volume calculation, with the consequent reduction of assessing time.

3.1. Introduction

Industrial production is an indicator of the economy in any country; a direct relationship exists between them (The Conference Board, 2019). Producing industrially boosts economies; but along with the economic growth, the industrial production comes with intrinsically two main parts: the product itself and a long-term issue, the by-product, that most of the time are non-recyclables or, even worse, that are hazardous. Fertiliser derived from phosphoric rock industry produces five tonnes of phosphogypsum, which it carries radiological risks, per one tonne of fertiliser produced (Cánovas et al., 2018). Acid sulphuric synthesising from roasting pyrite generates ashes enriched in heavy metals that are toxic to human health (Macías et al., 2017).

Besides, before 1998, there were not any legal measures in place bringing about significant environmental consequences. Western Europe, especially Mediterranean countries there have been 4,000,000 hectares identified that are potentially contaminated because of abnormal salinity and alkalinity values spread in approximately 300,000 sites

(European Environment Agency, 1998). France, Italy, Romania, Spain, have used pyrite for producing sulphuric acid (Oliveira et al., 2012a).

Consequently, by-products are still there; for instance, 440 hectares are covered in phosphogypsum in Huelva Spain (Guerrero et al., 2019). About 57 million tonnes of waste from metallic mining is in Portman in SE Spain (Gómez-García et al., 2015).

Besides, the configuration of the cities was utterly different during the 70s from the current one. The waste deposits were far away from the urban nuclei, yet urban expansion has caused cities to envelop them. Nowadays, they are located in the middle of the town, promoting an environmental issue and an impediment to continuing urban development.

Therefore, Spanish legislation promotes the recovery of the contaminated soils (BOE, 2005). The majority of the potentially contaminated sites are entirely unknown in terms of volume, geometry, chemical content, and age. This lack of information adds to the issue when dealing with the planning of the site remediation or waste treatment. To comply with the law, it has become mandatory to find a methodology to assess the site accurately.

The branch of the Geophysics science devoted to investigating the near-surface and the crust of the Earth is the *Applied Geophysics*. Not only does it make measures of Earth's physical properties, but it also interprets them. Frequently, this science is applied looking for a specific analyte. This science is composed of several techniques which quintessentially are non-invasive (Everett, 2013).

Also, applied geophysics is very versatile and adapts easily according to the needs of the researchers. Each technique utilises different principles, from acoustic waves to electrical current, to register the underground features. Some distinct studies have been

carried out accomplishing good enough results. Evangelista et al. (2017a) characterised the subsoil of a cultural heritage site. Carderelli et al. (2018) performed the reconstruction of the building masonry. García-Mendez et al. (2018) monitored the management of an aquifer.

Thereby, this study uses Electrical Resistivity Tomography owing to the nature of the study area, the versatility of the technique, and its efficient performance detecting contaminates in the field, e.g. (Caterina et al., 2017; Bortnikova et al., 2018; Vásconez-Maza et al., 2019).

Light Detection and Ranging (LiDAR) utilises signals at optical frequencies. These signals improve the spatial resolution of the imaging. This improvement has opened new fields of application of this technology, akin terrain mapping, autonomous driving, and robotics (Isaac, Song, Pinna, Coldren, & Klamkin, 2019).

Also, LiDAR point cloud that has shown good results with very high accuracy. For instance, an ancient Mayan metropole was found in the middle of a narrow jungle in Central America (Clynes, 2018). Chalupa et al. (2018) have reached a spatial resolution of 1 mm and 0.3 m. of elevation error in their geotechnical study.

Consequently, this study aimed: i) scan the industrial area selected to identify the distribution and possible variants of the waste to make up the configuration of geoelectrical profiles and boreholes. ii) assess the selected waste ponds trough electrical resistivity tomography. iii) contrast the geoelectrical profiles with the borehole core samples to calculate the volume contained in the selected site to provide reliable information of the quantity of waste that would help enormously at the moment of planning the remediation of the site or waste treatment.

3.2. Material and methods

Study area

Cartagena city in southeast Spain has semi-arid Mediterranean weather characterised by mild winters and hot summers, the annual average temperature of 18 ºC, precipitation of 275 mm, and evapotranspiration of 900 mm (AEMET, 2018). According to Köppen-Geiger (2006), Cartagena climate is a BSh (Hot semi-arid climate). The area of Cartagena geologically is configured by the accumulation of conglomerates, limestone and sandstones which belong to a different geologic period: Tortorian, Messianian, and Pliocene respectively.

This study focused on "El Hondón", an ancient industrial area, near to Cartagena city which was the scene of many industries from tannery to fertiliser. At "El Hondón" it was manufactured: Sulphuric acid from pyrite and fertiliser from a phosphoric rock. The whole area was full of distinct industrial wastes, which can be divided by colour: purple (pyrite ashes) and white (phosphogypsum). "El Hondón" has an area of approximately 113 ha; the A-30 highway crosses it. Nowadays, it is a forsaken industrial area, see figure 1 (Concejalía de Nuevas Tecnologías, 2018).

Electrical Resistivity Tomography

Electrical resistivity tomography (ERT) also known as electrical resistivity imaging (ERI) is a non-invasive geophysical method. It measures the distribution of the subsurface resistivity. The resistivity contrast between materials, components, and contaminates allow ERI detecting complex geological forms and subsoil material changes. The array election and the electrode spacing determine the investigation depth and vertical/horizontal resolution.

The traditional four-electrode array tenet is utilised frequently in ERI studies. A - B electrodes are usually those which injects current and M - N electrodes measure the difference of potential between themselves. This array does not acquire the true resistivity of the ground; it acquires apparent resistivity, which assumes that the Earth has a uniform resistivity. The apparent resistivity is a function of voltage(V), current (I), and a geometrical factor (a) (Halihan, Sefa, Sale, & Lyverse, 2017).

Besides, Electrical Resistivity Tomography has been used for decades in different fields such as: environmental assessment (Martínez Pagán, 2006), soil characterisation (Sudha et al., 2009), mine tailing characterisation (Gómez-Ortiz et al., 2010), or even looking for a specific contaminant (Rosales Aranda, 2013), agriculture (Vanella et al., 2018), and so forth.

In this study, four ERT profiles were performed over the entire surface of each deposit. Two ponds and two landfills were selected to ensure to analyse one of each type. Ponds contain solid waste while landfills house loose materials. Ponds are located at a higher bound than landfills. Also, five boreholes and four geoelectrical profiles were mapped out for each deposit. Table 1 shows the distribution used in the study (Figure 2).

Field data were acquired with a resistivimeter from IRIS-Instruments house. It is composed of four multicore cables; each cable can house eighteen stainless electrodes, the maximum space between electrodes is 5 meters. Investigation depth depends on the length of the profile as well as the type of the array employed. Investigation depth increases according to profile horizontal distance. The Wenner-Schlumberger array was applied because it provides a high signal-to-noise ratio, good vertical resolution, depth penetration, and has successful results in previous studies (Winters et al., 2015).

Subsequently, PROSYS II software removes data that do not follow the acceptation threshold previously defined. Data are inverted by RES2DINV software where the primary statistical algorithm utilised is the least-squares method (Loke & Barker, 1996). Resulting in the 2D geoelectrical section where the GPS coordinates are included; these were previously obtained from each electrode through a Leica GPS device (±1 cm accuracy). Hence, all data will be plotted in a map properly georeferenced.

Light detection and ranging (LiDAR) and Volume calculation software

The remote-sensing main aim is to acquire the geometric information from an object without touching it physically. One good representative of this technique is LiDAR that fixes laser light and a set of receivers to any flying device (aeroplane, drone) to sample an object/surface while the flight, obtaining a highly accurate point cloud in system x,y,z (Esri, 2016).

Spain is digitalising its whole territory progressively by using LiDAR. The national Spanish government funds this project, the project manager since 2008, is the National Geographic Institute referred to as “Instituto Geográfico Nacional (IGN)” in Spanish. The project has been developed in two phases; the first one has covered the whole territory in 2015. However, the technology and accuracy have improved; thus, a second cover is being performed currently. This second cover goes from RMSE of 0.2 m to RMSE 0.15 m; point density enhances from 0.5 point/m^2 to 1 point/m^2.

Besides, the point cloud is available in .laz extension, which is a public file for the exchange point cloud dataset. Despite the fact that this extension was primarily conceived for LiDAR point cloud, it allows working with almost any three-dimensional (x,y,z)

dataset. This format keeps with the information for LiDAR, yet it does not need sophisticated software.

Nevertheless, the point cloud is composed must pass first by a processing stage before being utilisable in this study. The data acquired from distinct sources must be meshed and plotted in a consistent format. Hence, it is mandatory to employ robust software that uses mathematical algorithms to triangulate surfaces and create models. Surfer software is a powerful and versatile and allows the dataset to be treated and deployed in a featured map.

The volume calculation consists of computing two surfaces (layers) and find the quantity of material that exists in-between. In the first stage, LiDAR provides the information to create the superficial layer referred to as the "Topographic layer". Secondly, an underground layer referred to as the "Geophysics layer" is computed by using the geoelectrical sections which show the different values of resistivity. These values vary according to underground components.

Also, the contrast between one material and another marks the boundaries between the natural terrain and the fillings of the deposit. The (CAD) computer-aided design software ensures the accuracy of measures. By using CAD boreholes depth and resistivity sections were compared and measured. All graphical approaches were performed at real scale in meters.

Therefore, both layers have a different altitude; thus, to know the volume existing in-between becomes in an integrating mathematical problem. The accuracy of the volume calculation lies in the difference among three numerical integration algorithms (extended trapezoidal rule, extended Simpson's Rule, and extended Simpson's 3/8 rule).

The accuracy of the volume calculation lies in the difference between these three methods; the net value reported is an average of the three results. These three results have to be very close one to another; otherwise, the result will not be accepted (Golden Software, 2018).

3.3. Results and discussion

As expected, results divide the waste into two categories, nature of the waste and type of the deposit. Parallelly, it was also performed chemical analysis, table 2 and 3 summarise the physic-chemical properties of the waste grouped by type of waste. The abnormal values of pH, electrical conductivity, and the elevated concentration of heavy metals revel the complexity of the pyrite ash and phosphogypsum.

However, to make it easier to understand; the successive results will be explained by deposits type. Phosphogypsum and pyrite ash would vary according to the industrial process followed and geneses of the ore employed. Additionally, RMSE (root-mean-square error) is a quality indicator for Electrical Resistivity Tomography profiles that must be below 10 % (Rosales et al., 2012).

Electrical resistivity imaging

Phosphogypsum and pyrite ponds

We have named the ponds as F1 for phosphogypsum and P1 for pyrite ash. The four geoelectrical profiles obtained from the pond F1 have revealed the existence of two layers: One in the top that runs all over the surface of the pond with a relatively constant thickness, and one another in the bottom that is mainly constituted of clay (see figure 3a-d). Within the four profiles, it was observed that some values might belong to the top layer, but they are located below the marked border. They probably are leaching traits.

Besides, the laboratory analyses exposed two well-differentiated materials in the pond (waste and clay). The thickness range of the top layer (waste) goes from 2 m. to 3 m. The stratigraphic column obtained from those boreholes shows that the three first boreholes have the same distribution because they have the same thickness; yet, the fourth and fifth reach deeper (Figure 3e). A possible explanation could be that the terrain was not prepared adequately due to the fact that an environmental law did not exist when this waste was stored as Domènech et al. (2017) pointed out in their study.

On the whole, the information from the five boreholes strongly supports the geoelectrical profiles. The depth of the boreholes fit coherently with the resistivity values distribution. Based on that information, the dashed line was drawn for marking the border between the waste and the clay. There is a high contrast between the top and bottom layer. The top layer has an average resistivity value of < 17 Ω.m while in the bottom layer >124 Ω.m (Figure 3).

The similar characteristics from F1 were found in the pyrite pond P1. The similarity lies in the complexity of the waste due to its apparent metal concentration that inhibits the growth of vegetation on the pond surfaces (García-Carmona et al., 2019) (Figure 4f). Two layers are well identified, the top one where the waste is concentrated has as resistivity average of 10 Ω.m while at the bottom layer > 200 Ω.m.

Subsequently, the zone marked by a dashed line is known as the transition area. In this area, the resistivity varies from 10 to 70 Ω.m approximately. This line follows strictly the measures provided by ERT and contrasted with the depth of the boreholes. Boreholes mainly provided stratigraphic information. It is observed that the waste (pyrite ashes) are concentrated in the top of the pond (Figure 4a-d). The thickness of the layer is variable; it runs from ≈2.5 m to ≈4 m (Figure 4e).

Phosphogypsum and pyrite landfills

As above mentioned, F2 corresponds to phosphogypsum landfill and P2 to pyrite landfill. The F2 landfill presented different characteristics from F1 as expected. According to EMGRISA report (1998), there were two processes to produce the fertiliser; the first one used sulphuric acid (probably F1), while the second one used Hydrochloride acid (probably F2). F2 infillings are loose and apparently dry, there even is some vegetation spread within the landfill surface (Figure 5f), which is surprising because of the relative absence of water and the acidic nature of the phosphogypsum (Bisone et al., 2017).

Furthermore, ERT profiles reveal the presence of a layer in the top with variable thickness and another layer in the bottom. The resistivity value in the top layer is <10 Ω.m while at the bottom is >20 Ω.m.

The resistivity values of the bottom layer are lower than expected for a clay. Thus, the layers are not well differentiated as it was in the pond (F1).

Nevertheless, the borehole core samples showed that the natural terrain is indeed clay and that the water table is below 8 m. in deep. A possible explanation can be that the highway construction has changed the original topography of the ground, and the runoff of the highway was directed to the south (landfills). Electrical values on soil depend on the presence of water, clay content (Pedrera-Parrilla et al., 2017).

Consequently, the top layer (waste) is about 6 meters thick on average, this layer regularly continues until five meters in deep; then, in random places, it gets thicker (Figure 5e). The borehole core samples provided a precise depth to mark the borderline between waste and natural terrain (see Figure 5a-d). Borehole provided stratigraphic column shows that the bottom is constituted mainly by clay.

Even though the landfills house a different kind of waste, the landfill P2 presents similar characteristics to landfill F2. This time it appears as a heterogeneous layer of the waste with an average of resistivity of ≈5 Ω.m. As happened before, the waste and natural terrain layer are not well defined. The presence of water in the natural terrain makes the resistivity values decrease (<5 Ω.m).

Finally, the boreholes have provided the depth for marking the border between waste and natural terrain. Here boreholes play a crucial role to delimitate and make up the "Geophysics layer". The stratigraphy shows a thin layer with a variable thickness from ≈1 m to ≈2.5 m. P2 is the smallest landfill studied (Figure 6f).

Volume calculation

Previously, other scientific methods have been applied to estimate the volume of waste deposits. Martínez-Pagán et al. (2009) assessed the volume of two mine tailings by using Digital Model Terrain (DMT). Martín-Crespo et al. (2018a) have estimated a volume of toxic mine tailings by using cartography and ERT; neither of these techniques assures a millimetric accuracy of the results.

At "El Hondón" a volume calculation was performed by FCC (Local construction company) during 2012. It was delimitated two areas (top and bottom). The top one was obtained by delimitating the perimeter of the site, taking some GPS coordinates, where it was walking accessible, and the bottom one was considered as a flat and regular area. With the resulting surfaces, the volume was calculated trough prismoidal method; results are displayed in table 4.

Contrastingly, the method used in this study yielded more accurate results than those from the 2012 FCC study, demonstrating the significant discrepancies when comparing the two studies. In F1 and F2 (phosphogypsum), we have calculated a higher quantity of material, yet the gap is affordable. Nonetheless, for P1 and P2 (pyrite ashes) the gap is notable; the 2012 volume for P1 is about double of the current one as well as in P1 that in 2012 the volume calculated is three times higher than 2017's. Table 4 summarises the difference between both techniques.

In this study, we used the second cover of LiDAR, which assures 0.2 m of $RMSE_Z$ (Dirección General del Instituto Geográfico Nacional, 2016). The second cover data in the Murcia Region (SE Spain) were gathered with ALS 60 (Airborne Laser Scanning). Data

follow the European Terrestrial Reference System of 1989 (ERTS89) in the whole territory (Iberian Peninsula) but the Canary Islands.

Thus, every single electrode used for geoelectrical profiles was geo-referenced with a high accuracy GPS device. Then, these coordinates were matched to LiDAR point cloud resulting in a layer closest to the reality (upper layer), referred to as "Topographic layer" (Figure 7 left). The combination of data from the borehole (depth) and electrical resistivity from the profiles generate the lower layer, referred to as "Geophysics layer" (Figure 7 right).

Subsequently, data are treated in Surfer software where first both layers pass by a gridding process. To calculate the volume the software runs its three algorithms to calculate the difference existing between the two created layers, Topographic layer & Geophysics layers, resulting in a volume of 35,600 m^3 and 17,320 m^3 for phosphogypsum and pyrite ashes ponds respectively (Figure 7a-b). Following the same process, the result for phosphogypsum landfill F2 is 59,300 m^3 and 4,900 m^3 in landfill P2 (see figure 8a-b).

3.4. Conclusions

Although there was a significant distinct origin of the waste, the volumetric characterisation was performed successfully. Previously, deposit volume characterisation has not been studied with LiDAR but rather Electrical Resistivity Tomography and borehole core samples. Nevertheless, this methodological study is using LiDAR point cloud in combination with Electrical Resistivity Tomography and boreholes core samples to volumetrically assess the deposits, yielding an accurate methodology that efficiently determines the volume existent in a waste deposit.

The presented methodology is completely exportable to any material deposit and we have used commonly used software to develop this study; then, it could be applied anyplace beyond "El Hondón" without a considerable investment. The 300 000 potentially contaminated sites that are spread in Western Europe need to be assessed urgently to start the site remediation. Hence, being able to predict the volume accurately and what the deposit geometry is is valuable information in environmental remediation.

Tables

Table 1: Nomenclature of the study area.

Nomenclature	Type	Waste	Geoelectrical profiles	Electrodes	Spacing (m)	Length (m)
F1	Pond	Phosphogypsum	1	72	3	213
			2	72	3	213
			3	72	1.5	106.5
			4	36	2.5	87.5
F2	Landfill	Phosphogypsum	1	72	2	142
			2	72	2.5	177.5
			3	72	1.5	106.5
			4	36	2.5	87.5
P1	Pond	Pyrite Ashes	1	72	2	142
			2	72	1.5	106.5
			3	36	2.5	87.5
			4	36	2.5	87.5
P2	Landfill	Pyrite Ashes	1	36	2.5	87.5
			2	72	1.5	106.5
			3	54	1.5	79.5
			4	36	1.5	52.5

Distribution of the selected sites ponds/landfills & Configuration of the geoelectrical profiles

Table 2: Chemical result from superficial sampling in phosphogypsum deposits.

F1											F2										
	mg kg^{-1}									dS m^{-1}		mg kg^{-1}									dS m^{-1}
Sample	Cd	As	Cr	Cu	Ni	Pb	Zn	Hg	pH	CE	Sample	Cd	As	Cr	Cu	Ni	Pb	Zn	Hg	pH	CE
F1-1	9.7	38	179	51	26.4	49	125	3.7	3.6	7.9	F2-1	12.9	31	275	40	28.0	27	190	3.9	3.8	21.3
F1-2	51.4	94	793	124	140.4	48	449	13.1	3.8	15.3	F2-2	4.8	29	217	44	34.5	35	202	6.7	6.3	24.1
F1-3	10.9	40	364	46	59.2	18	111	6.3	3.4	20.0	F2-3	8.0	22	139	32	43.8	19	154	2.5	6.7	28.1
F1-4	11.0	41	356	45	56.2	15	103	5.5	3.7	18.5	F2-4	11.1	25	256	33	31.3	24	128	2.7	4.4	23.2
F1-5	7.6	38	344	49	26.9	25	135	4.5	4.3	3.8	F2-5	20.3	30	270	50	56.5	22	124	2.0	4.1	13.6
F1-6	13.7	41	364	43	26.0	15	115	4.4	4.1	6.1	F2-6	9.7	27	204	47	49.6	34	285	2.2	7.1	12.5
F1-7	19.2	49	393	49	46.6	22	150	5.1	4.1	7.0	F2-7	4.1	22	290	36	16.0	17	102	3.3	3.8	20.3
F1-8	11.2	39	348	39	18.6	17	105	4.0	4.3	3.9	F2-8	27.1	31	253	35	73.3	25	196	3.5	6.7	25.8
F1-9	14.2	31	289	36	29.0	17	147	8.8	3.8	13.4	F2-9	14.3	24	279	50	28.6	18	174	7.9	5.0	23.8
F1-10	33.5	41	320	47	31.3	18	219	5.1	4.2	4.5	F2-10	5.5	13	187	38	30.3	17	169	2.7	5.8	14.1
Mean	18.2	45	375	53	46.1	24	166	6	4	10	Mean	11.8	25	237	40	39.2	24	172	4	5	21
SD	13.8	17.6	158.6	25.5	35.9	13.1	105.3	2.9	0.3	6.2	SD	7.3	5.5	48.8	6.8	16.8	6.5	51.7	2.0	1.3	5.5
Max	51.4	93.8	793.2	124.2	140.4	48.8	449.5	13.1	4.3	20.0	Max	27.1	31.3	290.4	49.8	73.3	34.8	285.0	7.9	7.1	28.1
Min	7.6	31.1	179.2	35.8	18.6	14.7	102.5	3.7	3.4	3.8	Min	4.1	13.4	138.9	31.5	16.0	17.0	101.6	2.0	3.8	12.5
NGR*	0.6	12	67	23	37	43	96	1.6			NGR*	0.6	12	67	23	37	43	96	1.6		

F1 phosphogypsum pond. F2 phosphogypsum landfill. *NGR is the local legal thresholds for heavy metal concentrations.

Table 3: Chemical result from superficial sampling in pyrite deposits.

P1										
	mg kg^{-1}									dS m^{-1}
Sample	Cd	As	Cr	Cu	Ni	Pb	Zn	Hg	pH	EC
P1-1	18.7	2518	8.5	1708	14.2	6720	7307	24	3.98	2.91
P1-2	7.3	7137	8.4	564	3.8	5577	1839	31	3.08	4.97
P1-3	5.3	7354	5.1	449	3.8	8768	1733	150	2.76	4.93
P1-4	5.5	6859	7.0	345	4.9	6264	2045	43	3.39	5.35
P1-5	4.1	4356	5.0	720	3.2	5399	1839	95	3.51	3.01
P1-6	7.0	21423	7.9	527	23.6	10352	1849	87	2.66	5.4
P1-7	14.7	3132	6.3	852	17.3	6380	7945	16	5.9	6.85
P1-8	1.5	2231	3.2	419	2.3	8841	1002	108	3.43	1.676
P1-9	4.4	6002	9.9	205	14.2	2996	1445	13	6.97	3.14
P1-10	1.2	4538	5.1	678	5.7	8878	1409	49	3.38	1.138
Mean	7	6555	7	647	9	7018	2841	62	4	4
SD	6	5558	2	418	7	2183	2544	46	1	2
Max	19	21423	10	1708	24	10352	7945	150	7	7
Min	1	2231	3	205	2	2996	1002	13	3	1
NGR*	1	12	67	23	37	43	96	2		

P2										
	mg kg^{-1}									dS m^{-1}
Sample	Cd	As	Cr	Cu	Ni	Pb	Zn	Hg	pH	EC
P2-1	10.4	2524	25.5	490	20.6	1837	2828	23.2	7.59	2.97
P2-2	7.9	2456	24.2	648	10.0	3545	3597	76.2	6.18	3.62
P2-3	5.4	1180	6.6	319	7.1	15016	3285	3.4	6	3.26
P2-4	13.2	1674	31.0	352	13.6	1841	2170	26.5	6.56	7.38
P2-5	10.6	906	6.7	356	6.0	21161	5495	0.9	5.93	2.93
P2-6	4.1	3968	22.8	650	9.4	11478	2839	3.7	4.56	4.2
P2-7	11.4	2181	31.1	470	24.2	2376	3838	25.6	7.78	3.56
P2-8	8.9	713	4.5	826	9.2	7450	4477	27.9	4.48	8.63
P2-9	5.7	3249	12.4	243	4.2	4814	961	47.2	2.74	3.98
P2-10	4.8	1521	33.9	448	5.3	1850	1852	37.1	2.55	6.23
Mean	8	2037	20	480	11	7137	3134	27	5	5
SD	3	1043	11	180	7	6690	1316	23	2	2
Max	13	3968	34	826	24	21161	5495	76	8	9
Min	4	713	4	243	4	1837	961	1	3	3
NGR*	1	12	67	23	37	43	96	2		

P1 pyrite pond. P2 pyrite landfill. *NGR is the local legal thresholds for heavy metal concentrations.

Table 4: Volume results

	GPS	LiDAR	
	2012	2017	Difference
	m^3	m^3	m^3
F1	33 660	35 600	+1 940
P1	30 400	17 320	-13 080
P2	15 055	4 900	-10 155
F2	50 225	59 300	+9 075

Figure captions

Figure 1: Location of the study area "El Hondón". Selected study sites are highlighted in white for phosphogypsum and in red for pyrite.

Figure 2: Configuration of the geoelectrical profiles and distribution of the boreholes a) Phosphogypsum pond "F1" b) Phosphogypsum landfill "F2" c) Pyrite pond "P1" d) Pyrite landfill "P2"

Figure 3: Phosphogypsum pond "F1" a-d) Geoelectrical profiles. e) Stratigraphy column suite from the five boreholes. f) Aerial view.

Figure 4: Pyrite pond "P1" a-d) Geoelectrical profiles. e) Stratigraphy column suite from the five boreholes. f) Aerial view.

Figure 5: Phosphogypsum landfill "F2"a-d) Geoelectrical profiles. e) Stratigraphy column suite from the five boreholes. f) Aerial view.

Figure 6: Pyrite landfill "P2" a-d) Geoelectrical profiles. e) Stratigraphy column suite from the five boreholes. f) Aerial view.

Figure 7: Left: The topographic layer (Upper layer) Right: The Geophysics layer (Lower layer). a) Phosphogypsum pond "F1" b) Pyrite pond "P1"

Figure 8: Left: The topographic layer (Upper layer) Right: The Geophysics layer (Lower layer). a) Phosphogypsum landfill "F2" b) Pyrite landfill "P2"

Figure 1.

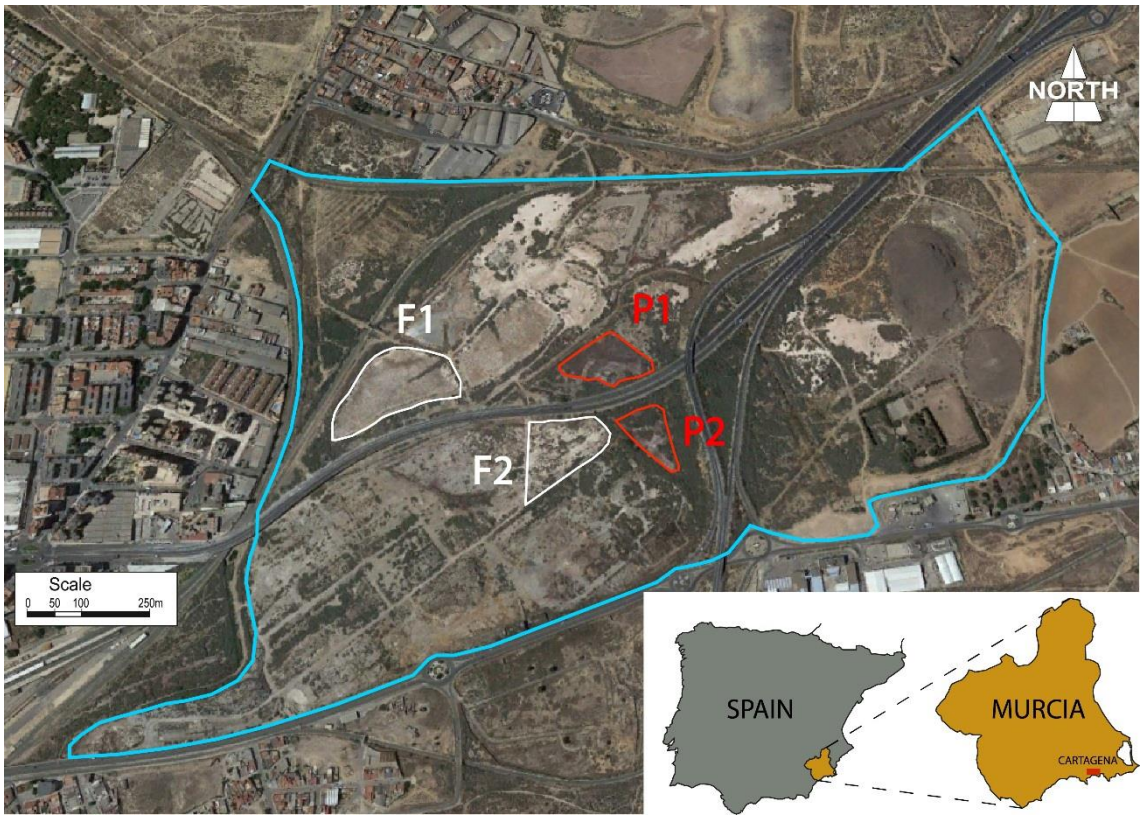

Figure 2.


Profile 4
Profile 2
Profile 1
Profile 3
S1
S2
S3
S4
S5
a
Profile 1
Profile 4
Profile 2
Profile 3
c
Profile 1
Profile 4
Profile 2
Profile 3
b
Profile 3
Profile 2
Profile 4
Profile 1
d
= Borehole
Electrical Tomography Profile
Scale
0
25
50
100 m

Figure 3.

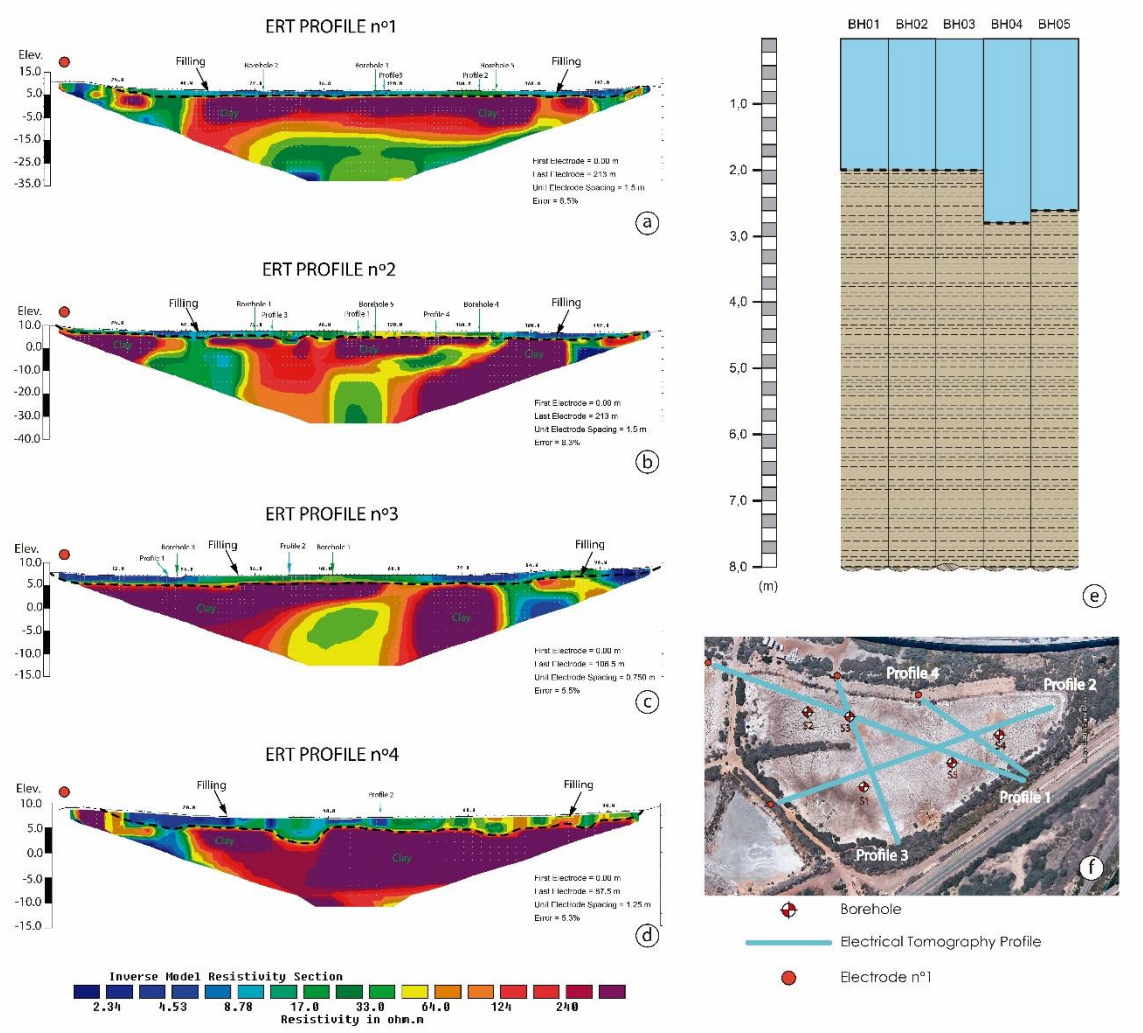
ERT PROFILE nº1
ERT PROFILE nº2
ERT PROFILE nº3
ERT PROFILE nº4
Elev.
Filling
Clay
a
b
c
d
Inverse Model Resistivity Section
2.34 4.53 8.78 17.0 33.0 64.0 124 240
Resistivity in ohm.m
BH01 BH02 BH03 BH04 BH05
1,0
2,0
3,0
4,0
5,0
6,0
7,0
8,0
(m)
e
Profile 4
Profile 2
Profile 1
Profile 3
S1
S2
S3
S4
S5
f
Borehole
Electrical Tomography Profile
Electrode nº1

Figure 4.

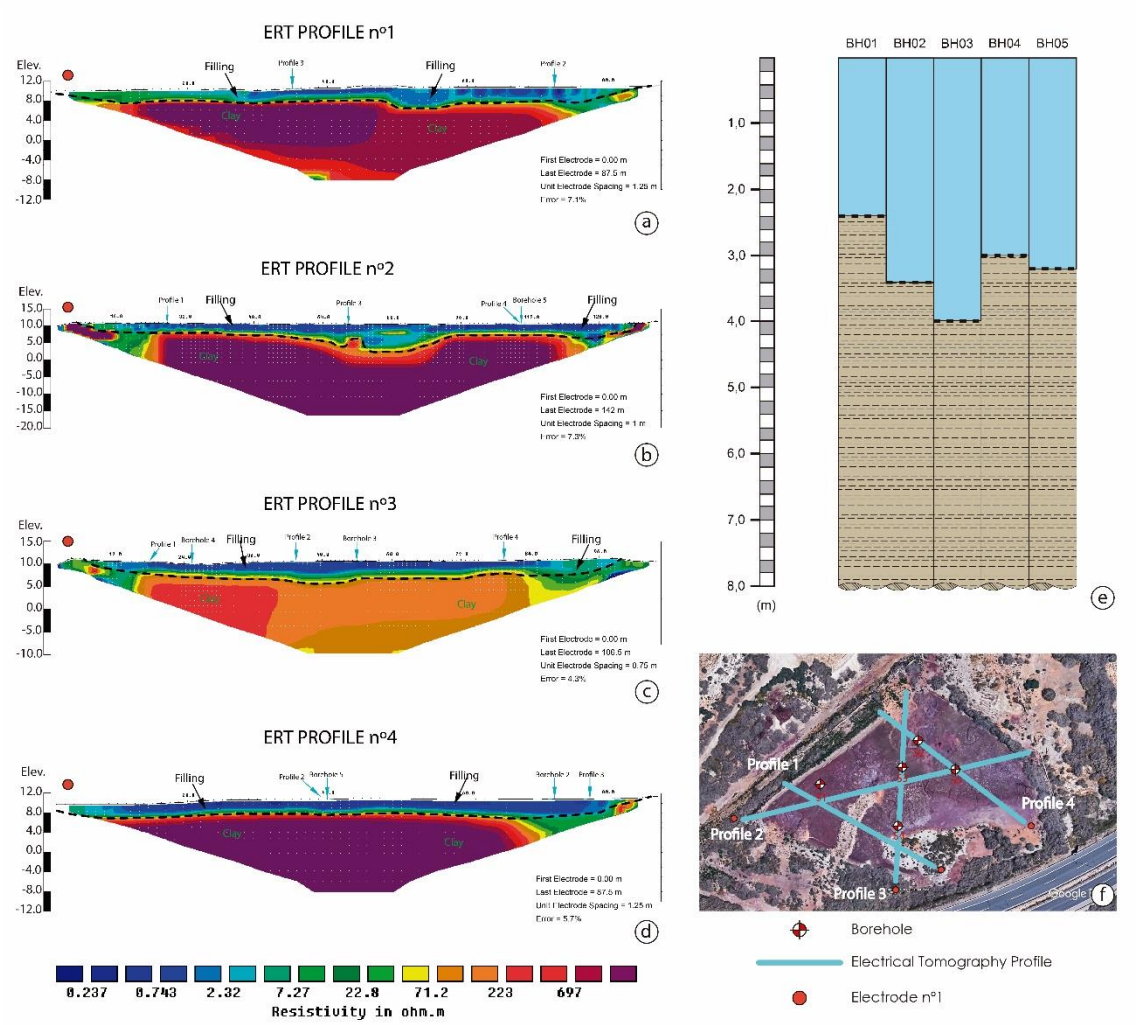
ERT PROFILE nº1
Elev.
Filling
Clay
First Electrode = 0.00 m
Last Electrode = 87.5 m
Unit Electrode Spacing = 1.25 m
a
ERT PROFILE nº2
Filling
Clay
First Electrode = 0.00 m
Last Electrode = 142 m
Unit Electrode Spacing = 1 m
b
ERT PROFILE nº3
Filling
Clay
First Electrode = 0.00 m
Last Electrode = 166.5 m
Unit Electrode Spacing = 0.75 m
c
ERT PROFILE nº4
Filling
Clay
First Electrode = 0.00 m
Last Electrode = 87.5 m
d
0.237 0.743 2.32 7.27 22.8 71.2 223 697
Resistivity in ohm.m
BH01 BH02 BH03 BH04 BH05
(m)
e
Profile 1
Profile 2
Profile 3
Profile 4
Google
f
Borehole
Electrical Tomography Profile
Electrode nº1

Figure 5.

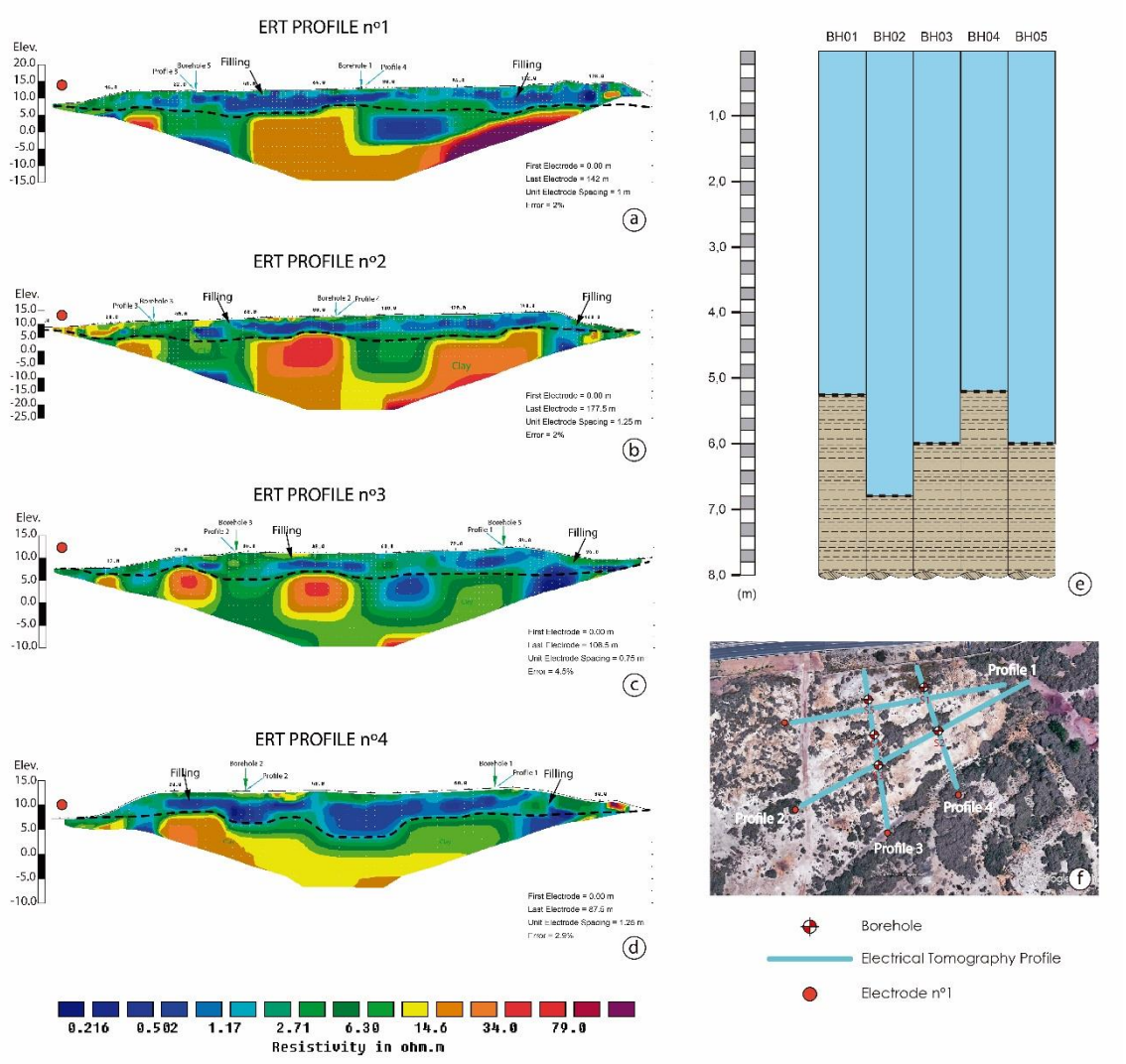
ERT PROFILE nº1
ERT PROFILE nº2
ERT PROFILE nº3
ERT PROFILE nº4
Elev.
Filling
Clay
a
b
c
d
0.216
0.502
1.17
2.71
6.30
14.6
34.0
79.0
Resistivity in ohm.m
BH01
BH02
BH03
BH04
BH05
(m)
e
Profile 1
Profile 2
Profile 3
Profile 4
f
Borehole
Electrical Tomography Profile
Electrode nº1

Figure 6.

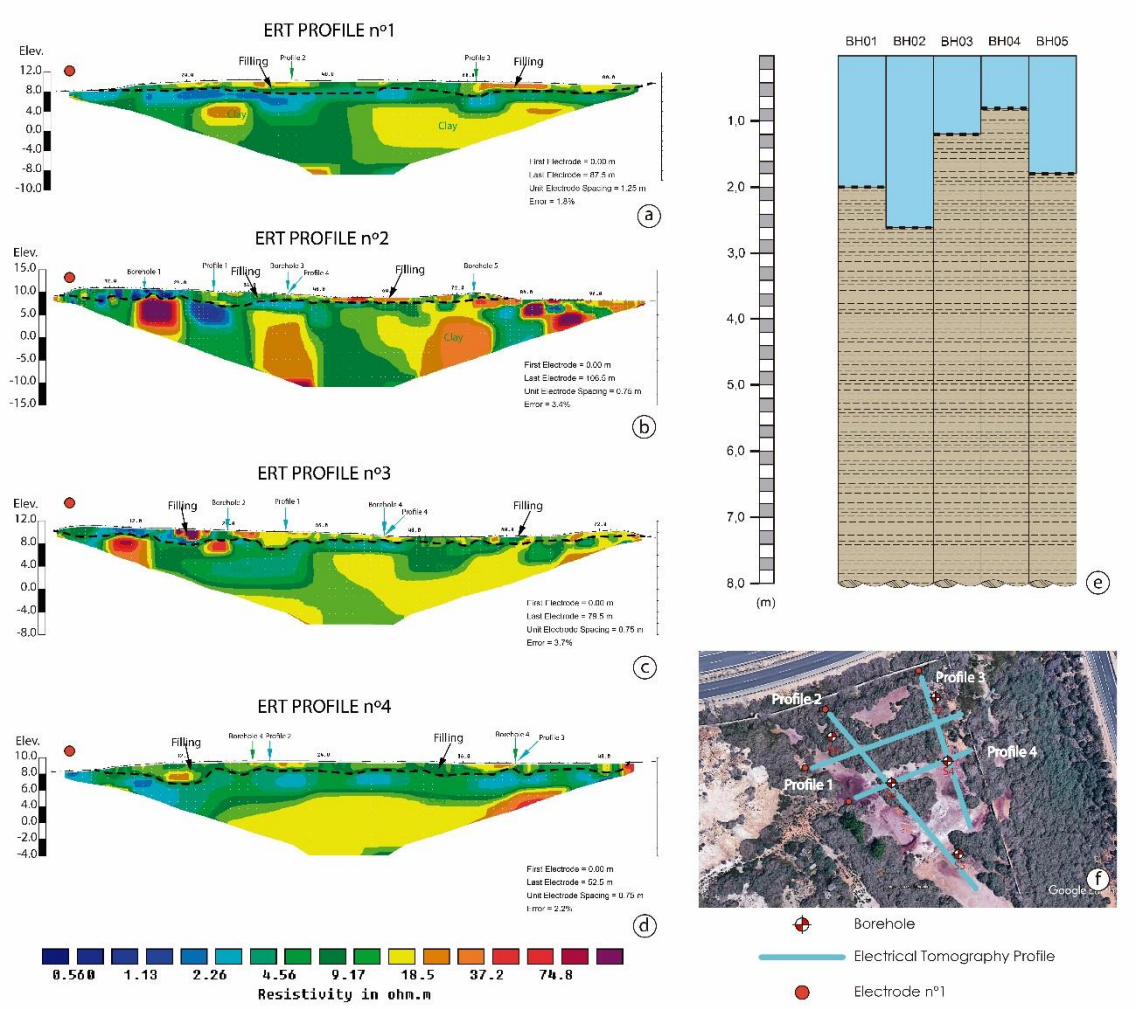
ERT PROFILE nº1
Elev.
Filling
Clay
ERT PROFILE nº2
Borehole 1
Borehole 3
Borehole 5
ERT PROFILE nº3
Borehole 2
Borehole 4
ERT PROFILE nº4
0.560
1.13
2.26
4.56
9.17
18.5
37.2
74.8
Resistivity in ohm.m
BH01
BH02
BH03
BH04
BH05
(m)
Profile 1
Profile 2
Profile 3
Profile 4
Borehole
Electrical Tomography Profile
Electrode nº1

Figure 7.

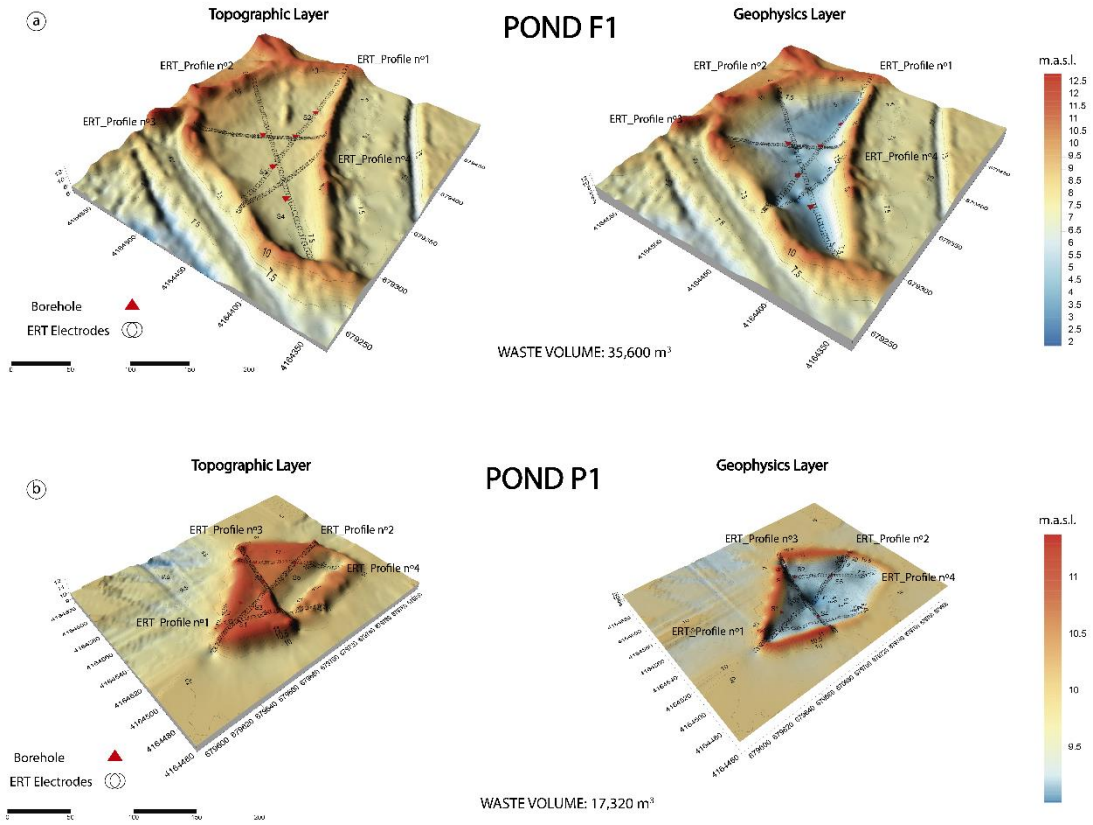
a
Topographic Layer
ERT_Profile nº2
ERT_Profile nº1
ERT_Profile nº3
ERT_Profile nº4
Borehole
ERT Electrodes
POND F1
Geophysics Layer
WASTE VOLUME: 35,600 m³
m.a.s.l.
12.5
12
11.5
11
10.5
10
9.5
9
8.5
8
7.5
7
6.5
6
5.5
5
4.5
4
3.5
3
2.5
2
b
Topographic Layer
ERT_Profile nº3
ERT_Profile nº2
ERT_Profile nº4
ERT_Profile nº1
Borehole
ERT Electrodes
POND P1
Geophysics Layer
WASTE VOLUME: 17,320 m³
m.a.s.l.
11
10.5
10
9.5

Figure 8.

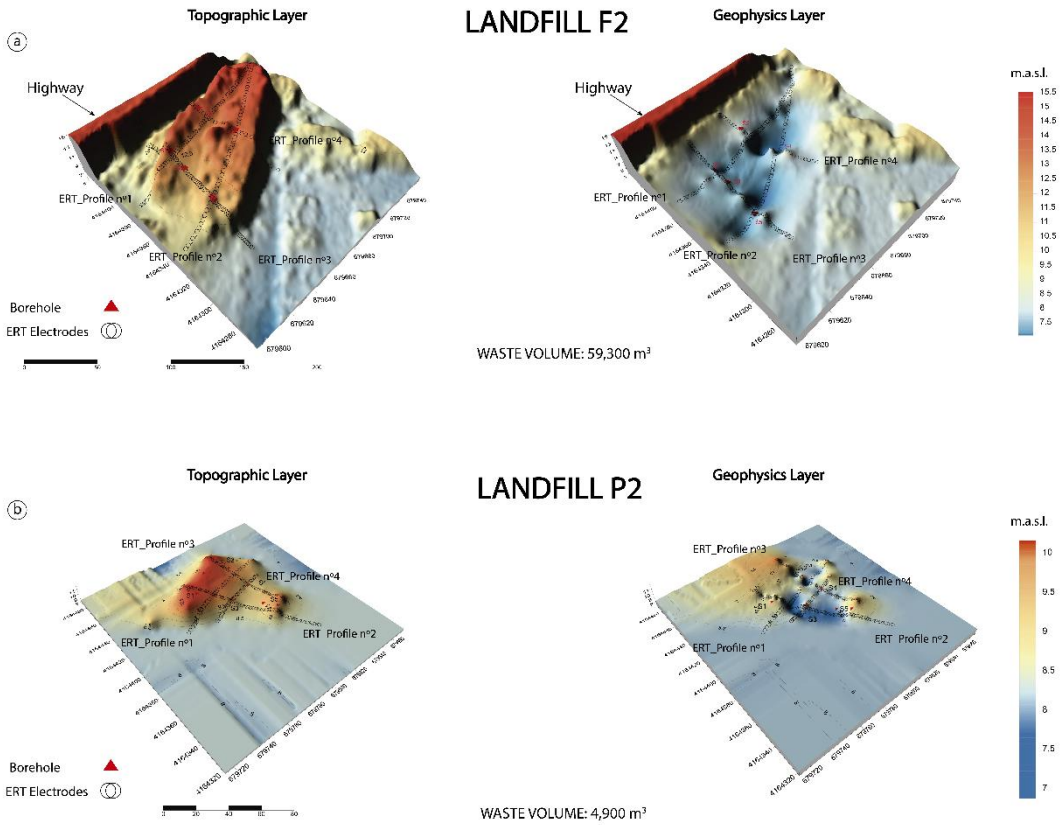
a
Topographic Layer
LANDFILL F2
Geophysics Layer
Highway
ERT_Profile nº1
ERT_Profile nº2
ERT_Profile nº3
ERT_Profile nº4
Borehole
ERT Electrodes
m.a.s.l.
15.5
15
14.5
14
13.5
13
12.5
12
11.5
11
10.5
10
9.5
9
8.5
8
7.5
WASTE VOLUME: 59,300 m³
b
Topographic Layer
LANDFILL P2
Geophysics Layer
ERT_Profile nº1
ERT Profile nº2
ERT_Profile nº3
ERT_Profile nº4
Borehole
ERT Electrodes
m.a.s.l.
10
9.5
9
8.5
8
7.5
7
WASTE VOLUME: 4,900 m³

CHAPTER 4

4. PREDICTING SPATIAL DISTRIBUTION OF HEAVY METALS IN AN ABANDONED PHOSPHOGYPSUM POND COMBINING GEOCHEMISTRY, ELECTRICAL RESISTIVITY TOMOGRAPHY AND STATISTICAL METHODS

This paper is published as: **Vásconez-Maza, M.D.**, Martínez-Segura, M.A., Bueso, M.C., Faz, Á., García-Nieto, M.C., Gabarrón, M., Acosta, J.A., 2019. Predicting spatial distribution of heavy metals in an abandoned phosphogypsum pond combining geochemistry, electrical resistivity tomography and statistical methods. J. Hazard. Mater. 374, 392–400. https://doi.org/10.1016/j.jhazmat.2019.04.045

The author of the present PhD thesis has contributed significantly to this publication. Since the beginning of this scientific work, initial draft, writing and final publication of the paper. All work was done under the direction of the supervisors.

Abstract

One of the waste generated in the production of fertilisers from phosphoric rock is phosphogypsum, whose mismanagement could cause environmental and health risks due to its high concentration of heavy metals and acidity. Therefore, a detailed evaluation of the chemical composition of phosphogypsum is necessary for correct control and management of this waste. However, due to the high amount of generated waste, the cost and time consumed for this characterisation by chemical analysis is prohibitive. For this reason, new, fast, and low-cost tools should be developed to predict chemical composition of this waste. Consequently, the objectives of this study are: 1) determine the physic-chemical characterisation of phosphogypsum pond using geochemical and geophysical techniques and 2) predict the heavy metals spatial distribution through statistical models. The laboratory results from borehole core samples and the Electrical Resistivity Tomography (ERT) profiles were combined by applying statistical regression models and

confronting log-resistivity with heavy metal concentrations. An accurate model for prediction chromium concentration was achieved. This model was used for revealing the location and spatial distribution of the highest Cr concentrations in the pond, with the consequent reduction of expensive traditional methods as mechanical drilling, sampling and chemical analysis.

4.1. Introduction

Fertilisers from phosphoric rock are globally spread bringing unquantifiable agricultural benefits. However, the production of one tonne of phosphoric fertiliser through wet acid process generates five tonnes of phosphogypsum (Cánovas et al., 2018; Rutherford et al., 1994; Sahu, Ajmal, Bhangare, Tiwari, & Pandit, 2014). This waste is an important environmental issue due to its high concentration of heavy metals and acidity, which could contaminate the proximal water resources and soil. In addition, the radiological risk can be significantly increased due to phosphogypsum concentrate trace elements, which increases the values of natural radiation; and therefore, human health can be affected by long term exposure to this kind of waste (Rutherford et al., 1994).

The management and treatment of phosphogypsum vary around the world, from Tunisia where Tayibi (2009) studied the phosphogypsum being thrown directly into the sea to Spain where there are 1200 hectares of phosphogypsum piled next to Medraña marsh in Huelva (CHAREYRON Bruno, 2007). In United States of America, 19 Mt of phosphoric rock is mined every year for manufacturing fertiliser in Florida which intrinsically leads to the production of this by-product (Liang, Jin, & Depaoli, 2018).

Moreover, for future use of the areas polluted by phosphogypsum, the remediation process is an inaudible step to decrease environmental and human health risks; therefore,

assessing the composition of this waste would help to make a decision for its treatment. However, the large amount of these materials generated during the production process and the different physical-chemical characteristics observed (Mahmoud & Abd El-Kader, 2015; Rychkov et al., 2018) make it difficult the fully assess of this waste.

State of the art software has opened new application fields for geophysics which were previously employed almost exclusively in the exploration of extractable industries. Geophysics is utilised in the field due to its versatility, low cost and accurate results. Currently, it is possible and affordable to apply geophysics, for example, Electrical Resistivity Tomography (ERT) for characterising landfills from an environmental point of view (Vladimir Frid, Sharabi, Frid, & Averbakh, 2017) and determine preferential drainage paths or in obtaining soil information for foundation planning (Y. Chen, Wei, Irfan, Xu, & Yang, 2018), or in archaeology for guiding an excavation (Evangelista et al., 2017b) and so forth.

Consequently, although for characterising the phosphogypsum ponds, drilling boreholes every single meter would be no contestable way to reveal all materials which are present in the waste landfill; the cost would be economically unviable. However, combination of geochemical techniques, with a reasonable number of boreholes, and ERT would give very a reliable characterisation of the whole site (P. Martínez-Pagán, Faz, Acosta, Carmona, & Martínez-Martínez, 2011).

Once all data is acquired, the interpretation phase is a critical stage where statistics plays a crucial role, which enormously helps researchers reporting objective results with a goodness of fit acceptable (V. Frid, Averbach, Frid, Dudkinski, & Liskevich, 2017). Statistical techniques have been applied to data acquired to detect inter-relationships among

the different observed variables. In particular, regression models have been used for evaluating correlations between, mainly, ERT and soil properties (Siddiqui & Osman, 2012). Statistics is transversally present in the interpretation of data, in a laboratory case, some phosphate tailings were assessed where geotechnical soil properties and ERT matched with a reliable fit (Y. Chen et al., 2018).

The objectives of the study were: 1) determine the physic-chemical characterisation of phosphogypsum pond using geochemical and geophysical techniques and 2) predict the heavy metals spatial distribution through statistical models, which could be fundamental in a decision making for a future site remediation.

4.2 Materials and methods

Study area

The city of Cartagena in southeast Spain has been historically a regional economic pole where either commercial or industrial activities have been developed (Espejo Marín, 2005). From the environmental point of view, these activities have left behind a huge amount of waste linked intrinsically to the industrial process. Some years ago, "El Hondón" was an industrial area located near Cartagena, where the main factories were fertiliser producers (Concejalía de Nuevas Tecnologías, 2018). Nowadays this site is an abandoned area where there are several ponds of phosphogypsum.

In this study, the biggest pond was selected (Figure 1), which does not have any kind of protection against wind and water erosion. This zone has a semi-arid Mediterranean climate, with an annual average temperature of 18 ºC, precipitation of 275 mm and evapotranspiration of 900 mm (Climate-data.org, 2018). Geology of the area is formed by

conglomerates (Tortonian), limestone (Messinian) and sandstones (Pliocene) (Región de murcia digital, 2009).

Geochemistry techniques

For physic-chemical pond characterisation, sampling was divided in surface and subsurface sampling. Ten composite superficial samples (0.5 m depth) were collected following a regular grid covering whole pond surface (Figure 1), each sample was composed by mixing and homogenising of 5 subsamples. The subsurface sampling corresponded to five boreholes distributed in the pond, matching one borehole with at least one geoelectrical profile previously arranged (Figure 1). All boreholes reached bedrock and were drilled 3 meters below the surface of the waste. Composite samples were collected every meter directly from the undisturbed waste extracted from each borehole core sample. Samples were taken to the laboratory and dried for 72 h at 35 °C. Dried samples were sieved to 2 mm and ground (Retsch RM 100). Samples were analysed for the following properties: pH (Soil Survey Staff, 2011) and electrical conductivity (EC) (Andrades, 1996) were measured in deionised water (1:2.5 w/v and 1:5 w/v, respectively). To assess the total metal concentration (Cd, As, Cr, Ni, Cu, Pb and Zn), 0.5 g of each sample was transferred into vessels with 10 ml of nitric acid (65%) and digested in a MARS 6 microwave according to US-EPA method 3051 (US-EPA, 2007). The metal concentrations were measured by Inductively Coupled Plasma-Mass Spectrometer (ICP-MS) (Agilent Technologies, 2006). Certified reference material (BAM-U110) from the Federal Institute for Materials Research and Testing and reagent blanks were used as quality control samples during the analyses. We obtained recoveries of 95-102% for Cd, 96-98% for Cu, 94-101% for Pb, 92-99% for Zn, 96-104% for Cr, 98-103% for As and 93-101% for Ni.

Geophysics technique: Electrical Resistivity Tomography (ERT)

Electrical resistivity tomography is a non-invasive geophysical method which combines simultaneously vertical electrical sounding and profiling techniques that allows the gathering of significant underground information, complex geological formations and phase changes (Acosta et al., 2014). Apparent resistivity measures were retrieved through a Syscal R1 Switch 72 resistivimeter (IRIS Instruments, 2018). Every single electrode was georeferenced employing a GPS device. Four ERT profiles were performed covering the surface of the pond. For profile number one and two, there were 72 stainless electrodes connected, separating each electrode by 3 m, reaching 213 m long. Profile 3 needed 72 electrodes too, but the separation was 1.5 m, with 106.5 m long. Finally, profile 4 due to the pond geometry, only needed 36 electrodes 2.5 m apart reaching 87.5 m long (Figure 1). In this study the Wenner-Schlumberger array was used because it provides good vertical resolution, depth penetration, and high signal-to-noise ratio. Moreover, many authors in similar studies have employed this array achieving excellent results (Acosta et al., 2014; Evangelista et al., 2017b; Martín-Crespo et al., 2018a).

The dataset must first eliminate anomalous measures (background noise) by using PROSYS II software. Then GPS coordinates are added; thus, data can be deployed in a georeferenced map with their proper height (z). The next step is the inversion by RES2DINV software. This process follows the least-squares method (Loke & Barker, 1996) as its primary statistical algorithm.

Statistical analysis

Graphical exploratory analysis of data was carried out by using box-plot graphics and scatterplots of pairs of variables to visualise the global behaviour of the data. Descriptive statistics (mean, standard deviation, maximum, and minimum) were used to detect values above legal thresholds (Table 1). Correlation heatmaps were displayed to identify inter-relationships among the different geochemical and geophysical parameters evaluated in heavy metal-contaminated soils. In order to find relationships between the chemical data from borehole core samples and resistivity values from ERT profiles, scatterplots were done confronting one by one leaving resistivity as the independent variable. Different non-linear regression models were analysed to find relationships between concentration of Cd, As, Cr, Cu, Ni, Pb and Zn in the phosphogypsum and ERT. Finally, among the fitted models, the non-linear model considered in this study was given by the following equation:

$$\log(y) = \frac{a}{1 + b \cdot \log(Re)}$$

Where *y* represents the response variable (the metal content), *Re* the electrical resistivity assumed to be the explanatory variable, and, *a* and *b* are unknown constants to be estimated from experimental data. To evaluate the goodness of the fit of each estimated model, the root mean square error (*RMSE*) is computed, defined as:

$$RMSE = \sqrt{\frac{\sum_{i=1}^{n}\left(\log(y_i) - \widehat{\log(y_i)}\right)^2}{n}}$$

Where $\log(y_i)$ and $\widehat{\log(y_i)}$ are the observed and fitted values, respectively, and n is the number of observed data. The RMSE value corresponds to the standard deviation between observed and fitted values, and the lower RMSE values indicate better fit.

This error performance measure depends on the units in which the response variable is measured, and it is only useful to compare the accuracy of different fitted models. For this reason, Pearson correlation coefficient between observed and fitted values (r) is evaluated as measure of the relationship between both. All statistical analyses were conducted by using R free software (R Core Team, 2019). In particular, the estimation of the parameters involved in the non-linear models was performed using the nonlinear least squares fit function *nls* available in *stats* R package.

4.3 Results and discussion

Geochemistry of phosphogypsum

Superficial samples show the phosphogypsum is highly acidic and high in saline (Bisone et al., 2017) with mean values of 3.9 and 10 $ds.m^{-1}$, respectively; which explains the absence of vegetation in this pond. All metals analysed, except lead, exceed the limit allowed by the local law (BOE, 2005a). Nonetheless, it highlights the concentration of chromium (375 $mg.kg^{-1}$) exceeding more than five times the maximum level allowed by the legislation (NRG in Table 1). During the fertilizer process production, apatite interacts with sulphuric acid also known as the wet acid process: $Ca_{10}(PO_4)6X_2 + 10H_2SO_4 + 20H_2O = 6H_3PO_4 + 10CaSO_4 \cdot 2H_2O + 2HX$ where X = Cl, F, OH (Lin et al., 2018). As a result, acidity is generated and some heavy metals and metalloids are concentrated in the phosphogypsum (Oliveira et al., 2012b).

Chemical analyses result from the five borehole core samples are displayed in Figure 2. Results show that pH remains acidic in the phosphogypsum (< 2 m. deep), whilst in the substrate pH values increase up to ≈8 m., indicating that soil under phosphogypsum are basic (Bisone et al., 2017). However, soils from borehole 1 show a pH value of 4,

indicating that acid leaching from waste accumulation has taken place. In contrast, electrical conductivity was higher in the phosphogypsum than in the soil, with values from 20 to 5 $dS.m^{-1}$ (very saline) and < 5 $dS.m^{-1}$ (slightly saline) respectively. Mahmoud (Mahmoud & Abd El-Kader, 2015) showed how compost decreased the levels of electrical conductivity and increased the pH in a remediation process of phosphogypsum.

Results show that the concentration of Cadmium (Cd) in phosphogypsum is higher than the allowed level (0.6 $mg.kg^{-1}$), which is classified as a cancerogenic element according to European Chemicals Agency (European Chemicals Agency, 2018). The Cd concentration is constant in the five boreholes until the contact soil-waste, 2 m. deep (≈15-23 $mg.kg^{-1}$), after that depth the concentration decreased significantly except for borehole 1 which remains high, supporting that an acid leaching from phosphogypsum has been take place, transferring Cd to subsoil with the subsequent associated environmental and health risks (T. Chen, Chang, Clevers, & Kooistra, 2015).

Legal thresholds of Arsenic (12 $mg.kg^{-1}$) and Nickel (37 $mg.kg^{-1}$) in the pond are easily surpassed. Concentrations are spread in a wide range of values (≈15 – 90 $mg.kg^{-1}$), and they do not follow a marked trend until 2 m. deep. However, below 2 m. a random behaviour has been observed, but after 5 meters deep all boreholes trend to decrease until concentrations near to 10 $mg.kg^{-1}$ in all boreholes. Macias et al. (2017) showed that phosphogypsum has a different concentration of metals depending on the place where it has been produced and the type of industrial process followed.

Chromium (Cr) needed to be observed carefully because its concentration has risen to ≈900 $mg.kg^{-1}$ resulting in a concentration defined curve. From the surface, where the concentration is ≈200 $mg.kg^{-1}$, a systematic continuous increment until ≈800 $mg.kg^{-1}$ can be observed, drawing well-defined curve till reaching 2 m deep. Below 2 meters, the

concentration reduced gradually until reaching values close to zero. It is necessary to highlight that the maximum threshold determinate by the local law is 67 $mg.kg^{-1}$, and Cr could damage human health due to its toxicity (Kargar Shouroki, Shahtaheri, Golbabaei, Barkhordari, & Rahimi-Froushani, 2018).

Copper (legal threshold: 23 $mg.kg^{-1}$) has a concentration in the pond <50 $mg.kg^{-1}$ for all depths, except in borehole 2 that show a higher concentration <150 $mg.kg^{-1}$. Nonetheless, after 2 m. deep all borehole concentrations trend to lower values. Whilst, Zinc (Zn) (legal threshold: 96 mg kg^{-1}) concentrations are below 200 mg kg^{-1}, except for borehole 1 where the Zn concentration reaches up to 2200 $mg.kg^{-1}$. This value significantly has augmented the mean of the Zn concentration, and it shows the possible accumulation of other kinds of waste. Domènech et al. (Domènech et al., 2017) concluded that Zn and other metals are preferentially bound onto Fe-oxy-hydroxides (e.g. pyrites ashes).

Lead (Pb) (legal threshold: 43 $mg.kg^{-1}$) shows a different behaviour. The concentration in the first meter was low (< 10 $mg.kg^{-1}$). However, in the second meter, the Pb concentration started to increase (≈0-40 $mg.kg^{-1}$), and once surpassing 2 m, this trend was higher. Even borehole 5 concentration reached ≈120 mg kg^{-1} at the end of the borehole. This accumulation of Pb in the lowest layers has likely occurred due to its high density (11.34 $g.cm^{-3}$), which is the heaviest metal among all metals analysed (Lenntech, 2018).

Geoelectrical profiles

Electrical Resistivity Tomography (ERT) depth penetration depends on the array (Roy & Apparao, 1971). This technique is versatile and previously as is shown by Simyrdanis et al. (Simyrdanis, Papadopoulos, Soupios, Kirkou, & Tsourlos, 2018) who used this technique to assess subsurface contamination by olive oil; or by Bortnikova et al. (2018) who assessed gold mine tailing applying ERT. Our study has provided data up to ≈45 meters deep in profile 1-2 and profiles 3-4 have only penetrated to ≈ 25 m. Then, after the fourth iteration with 17.5 % RMS error the geoelectrical section was obtained, which displayed a resistivity map coherently fitting with information acquired from boreholes. Rosales et al. (2012) allude to the fact that RMS error below 10% is an indicator of a good electrical section result; however, higher values might be considered if the analysed terrain is complex (as in this study) and presents lower resistivity values. Resistivity values change according to each distinct material, each having a distinct colour assigned in the colorbar (Figure 3). A superficial layer was identified with a relatively constant thickness (≈2.5 m). This layer is common in four profiles, and it presented similar resistivity values (≈17Ω.m), in addition a subsurface layer where resistivity leapt over 124 Ω.m. A dashed line marks the division between both layers (Figure 3).

A corrected and processed geoelectrical section with 8.3% RMS error after the fifth iteration was made up from profile 2 (Figure 3b). Profile 1 (Figure 3a) and profile 2 were planned to cross each other and be parallel at the beginning and end (Figure 1), which accounts for the similarity in the results of resistivity (≈17 Ω.m) and it rises with the depth (≈33-120 Ω.m). Both pseudosections follow a similar pattern and they relate to one another. Frid et al. (2017) puts forward that ERT is a good method to identify preferential leaching

paths. We observed a potential leach, in profile 1 at ≈36 m. of horizontal distance. It also appeared in profile 2 at ≈48 m.

Profile 3 (Figure 3c) and 4 (Figure 3d) are shorter (<100 m) and they are deployed transversely with respect to profile 1 and 2. The geoelectrical section of Profile 3, after the fifth iteration with RMS error of 12.7%, is displayed in Figure 3. The superficial layer appeared with the previous values and a possible leach from ≈80 m up to ≈90 m with a depth of ≈-5 m. There also is a decreasing change of resistivity values; however, the value ranges are above ≈35-124 Ω.m.

As it was expected, in profile 4 (Figure 3d), the superficial layer appeared to contain the same features and resistivity values (≈17Ω.m). A high resistivity zone has been identified from ≈10 m to ≈30 m right below this zone. It can be observed as a blue coloured fringe, which is associated to values < 9 Ω.m. This distribution has brought up the percolation because in its environs there are very different values. It is likely the different values exist due to the presence of heavy metals below the dashed line.

Content estimation. Statistical model and chromium content imaging

As it is previously shown, ERT profiles brought about underground information (15 to 45 m of depth). Since boreholes were only drilled till ≈ 6 m, laboratory data is framed in that range. Eventually, the resistivity range was narrowed, and we have carried out the estimation of the model with just the dataset located in that fringe.

Table 2 summarises the results of the estimated model parameters by predicting each variable in function of the log-resistivity using the model. We have observed three variables which show a strong correlation (R^2>0.5) with the log-resistivity.

However, two of them are soil properties (pH and CE) that provide some features that support the results; the third is the Cr concentration, which has showed a strong correlation (R^2 =0.68) with log-resistivity with a RMSE of 0.81 (Figure 4). The linear regression model has been used successfully in other studies as Alamry et al. (2017) pointed out in their study where soil moisture was correlated with ERT. Likewise, Chen et al. (2018) put forward the relationship between ERT and geotechnical properties always through statistical models.

The Cr prediction model is adjusted in the superficial layer. It accounts for the reduction of resistivity range in the profiles (Figure 5). Few studies have been carried out combining ERT and statistics on characterisation of phosphogypsum ponds. However, ERT has been used for detecting heavy metals as Hazreek et al. (2018) have shown in a miniature field study. In this study they successfully detected artificially injected magnesium. In addition, it has been demonstrated that resistivity values vary with each change in soil properties (Brillante, Mathieu, Bois, Van Leeuwen, & Lévêque, 2015; Friedman, 2005).

The pond has presented a superficial layer where the phosphogypsum is located, which explains the low resistivity values (≈17 Ω m), and as expected the Cr content model fits the resistivity section coherently. The high concentration of Cr is linked directly with low resistivity values (blue colour). The prediction model was calibrated to adjust to the local legal threshold (BOE, 2005a) (Figure 5); any value of Cr below 67 $mg.kg^{-1}$ is considered to be non-contaminated soil. Due to the nature of the pond, the four maps show that the superficial layer is contaminated. However, there are also some areas where the contaminants have percolated beyond the superficial layer.

The highest concentration of Cr (>800 $mg.kg^{-1}$) formed specific areas that can be easily identified in the 4 models. One horizontal segment runs from ≈10 m. to ≈200 m. in the top of Profile 1, two more diagonally oriented from 40 m. until 100 m. and a polygonal body < 3 m. thick that runs from 180 m. to 200 m. approximately. Profile 2 only has punctual areas of >800 $mg.kg^{-1}$ concentration one spread from 35 m. to 50 m. and another from 160 m. to 190 m. Profile 3 shows 4 areas spread along the profile with the mentioned chromium concentration. Three of them are horizontally aligned, the first one runs from 0 m. to ≈25 m, the next from ≈65 m. to ≈82 m. and the last one from ≈98 m. to the end of the profile. There is a body at the bottom of the model from ≈80 m. to ≈90 m. Finally, profile 4 followed the same pattern. In the top layer there also are some punctual areas located at ≈31 m, ≈42 m and ≈49 m. P4 also presents a considerable area of concentration (>800 $mg.kg^{-1}$) of Cr; it is slightly diagonal oriented with 20 m in length and a thickness of < 5 m.

4.4 Conclusions

The characterisation of the pond was successfully completed using geochemical and geophysical analysis. The phosphogypsum studied was highly acidic and highly saline. All the metals analysed (Cd, As, Cu, Cr and Zn), with the exception of Pb exceed the legal limit of these, Chromium concentration is especially high, exceeding 5 times (375 $mg.kg^{-1}$) the legal limit. This explains the absence of vegetation in this pond. ERT provided geometric information and the geoelectrical section classified the pond by material. In addition, a percolation phenomenon was identified in the pond, the geoelectrical profiles have shown the preferential leaching path. Clay has acted as a barrier against heavy metals leaching in the shallow layer, but in the zones where there is no clay, it can be observed in descending leaching paths. Geochemically, Pb is identified as increasing in concentration deeper in the sample profile than the other heavy metals.

This suggested that lead is able to cause the most contamination, but additional studies will need to be done to determine the extent of Pb contamination. Consequently, we can consider that ERT and geochemical analysis are useful and reliable techniques to characterise phosphogypsum waste.

By using statistical modelling, we have determined a strong correlation between log-resistivity and Cr, which allows a relatively easy, cheap, and efficient way to determine the concentration of this metal using values of resistivity. This correlation was very useful for revealing the location and distribution of the highest Cr concentration in the pond without need to make new boreholes. Therefore, it can be concluded that statistical models can be used more efficiently to predict Cr concentrations, the most abundant metal in phosphogypsum, with the consequent reduction of expensive traditional methods as mechanical drilling, sampling and chemical analysis.

Tables

Table 1 Results of chemical analyses in superficial samples.

	mg kg^{-1}								(dS m^{-1})
Sample	**Cd**	**As**	**Cr**	**Cu**	**Ni**	**Pb**	**Zn**	**pH**	**EC**
F1-1	9.7	38	179	51	26	49	125	3.6	7.9
F1-2	51	94	793	124	140	48	449	3.8	15
F1-3	11	40	364	46	59	18	111	3.4	20
F1-4	11	41	356	45	56	15	103	3.7	19
F1-5	7.6	38	344	49	27	25	135	4.3	3.8
F1-6	14	41	364	43	26	15	115	4.1	6.1
F1-7	19	49	393	49	47	22	150	4.1	7.0
F1-8	11	39	348	39	19	17	105	4.3	3.9
F1-9	14	31	289	36	29	17	147	3.8	13
F1-10	34	41	320	47	31	18	219	4.2	4.5
NGR	0.6	12	67	23	37	43	96		
Mean	18	45	**375**	53	46	24	166	3.9	10
SD	14	18	159	256	36	13	105	0.3	6.2
Max	51	94	793	124	140	49	450	4.3	20
Min	7.6	31	179	36	19	15	103	3.4	3.8

NGR: reference concentration (Legal threshold); SD: standard deviation; Max: maximum; Min: minimum

Table 2 Estimated model parameters.

Dependent variable	n	Estimate a	SE(a)	Estimate b	SE(b)	RMSE	r	r^2
Cd	35	5.38	3.19	0.43	0.42	1.15	0.42	0.18
Cr	35	10.6	1.53	0.3	0.08	0.81	0.83	**0.68**
Ni	35	4.69	0.20	0.05	0.01	0.32	0.68	0.47
Cu	35	4.27	0.30	0.03	0.02	0.52	0.32	0.11
As	35	3.97	0.37	0.07	0.03	0.50	0.53	0.28
Pb	35	1.99	0.19	-0.1	0.01	0.72	0.66	0.43
Zn	35	5.17	0.50	0	0.02	1.04	0.03	0
pH	35	1.28	0.06	-0.1	0.01	0.21	0.78	0.61
CE	35	33.2	138.77	5.96	26.37	0.69	0.74	0.54

n: Sample Size; SE: Standard Error; RMSE: Root Mean Square Error; r: Pearson Correlation Coefficient

Figure captions

Figure 1. Location of the study area in southeast Spain. Spatial distribution of the geoelectrical profiles, the boreholes, and the superficial samples.

Figure 2. Results of chemical analyses distribution by borehole. Each line describes the trend followed in the respective borehole.

Figure 3. Geoelectrical pseudosection obtained from profile 1 (a), profile 2 (b), profile 3 (c) and profile 4 (d); where A marks the beginning of the profile and A' marks the end of it.

Figure 4. Chromium content and log-resistivity calibrated model.

Figure 5. Chromium content prediction model. Scale adjusted to the threshold allowed by the legislation (NGR).

Figure 1.

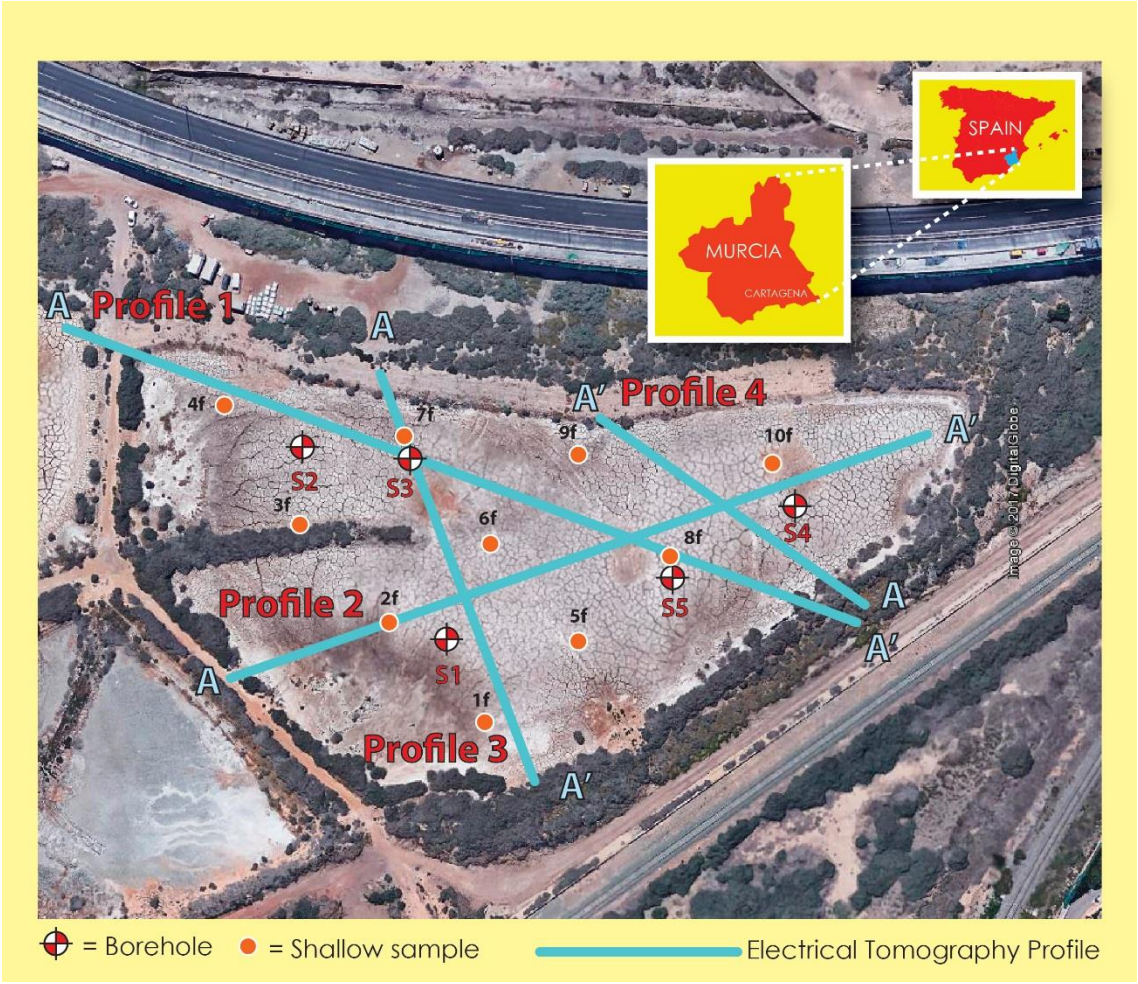
SPAIN
MURCIA
CARTAGENA
Profile 1
Profile 2
Profile 3
Profile 4
A
A′
4f
7f
9f
10f
3f
6f
8f
2f
5f
1f
S1
S2
S3
S4
S5
Image © 2017 DigitalGlobe
= Borehole
= Shallow sample
Electrical Tomography Profile

Figure 2.

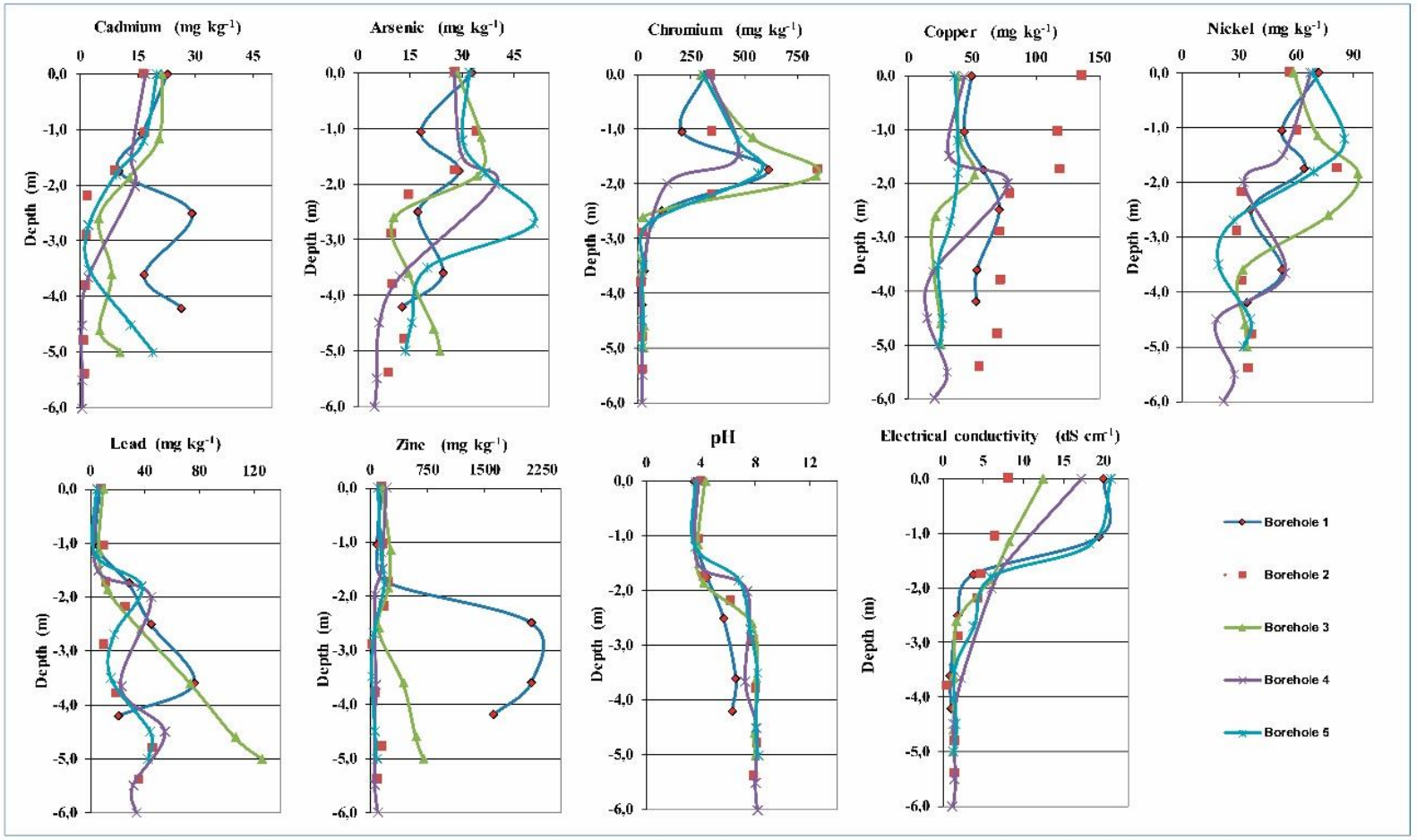
Cadmium (mg kg-1)
Arsenic (mg kg-1)
Chromium (mg kg-1)
Copper (mg kg-1)
Nickel (mg kg-1)
Lead (mg kg-1)
Zinc (mg kg-1)
pH
Electrical conductivity (dS cm-1)
Depth (m)
Borehole 1
Borehole 2
Borehole 3
Borehole 4
Borehole 5

Figure 3.

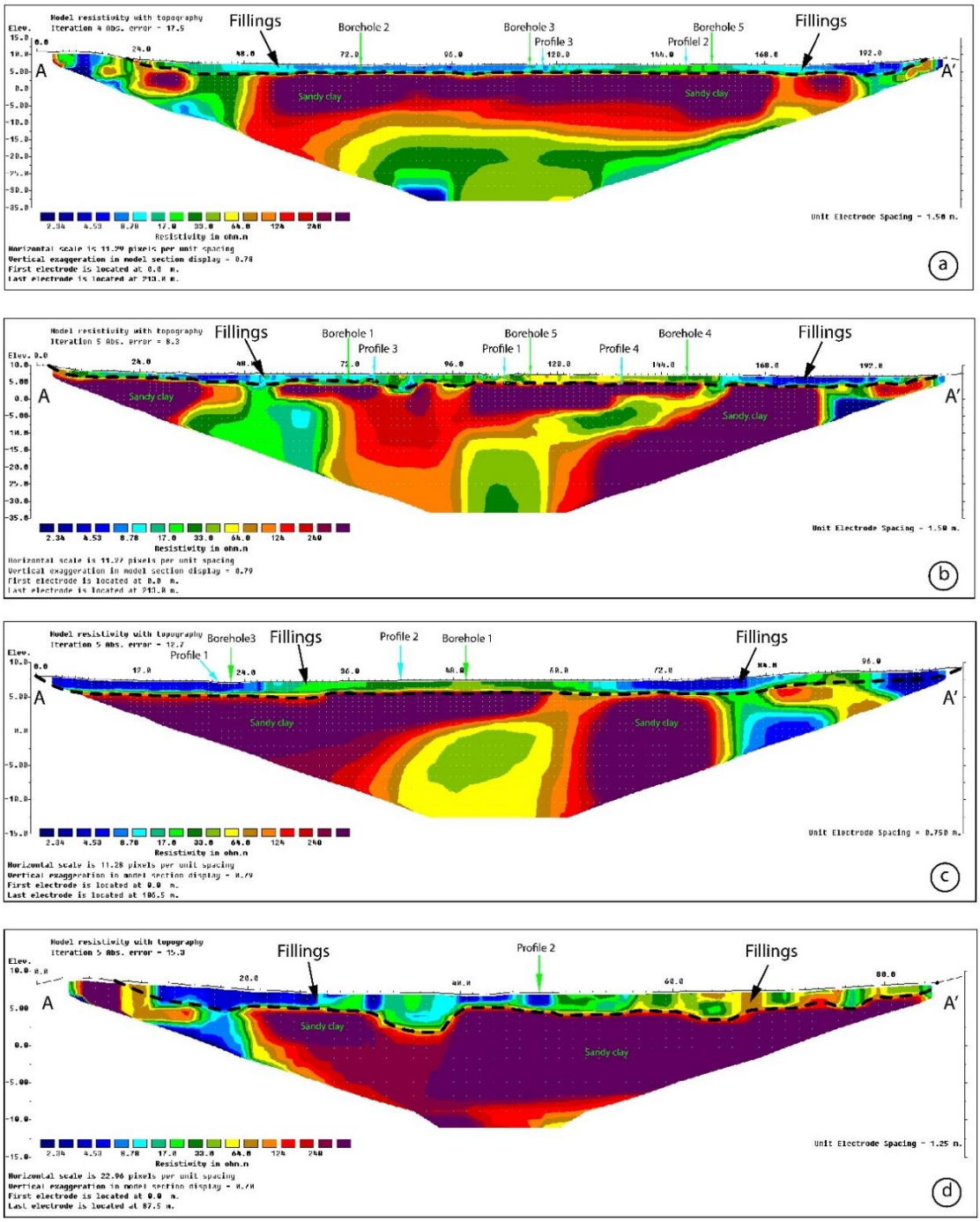
Fillings
Borehole 2
Borehole 3
Profile 3
Borehole 5
Profile 2
Fillings
A
A'
Sandy clay
Sandy clay
Unit Electrode Spacing = 1.50 m.
a
Fillings
Borehole 1
Profile 3
Borehole 5
Profile 1
Profile 4
Borehole 4
Fillings
A
A'
Sandy clay
Sandy clay
Unit Electrode Spacing = 1.50 m.
b
Borehole3
Fillings
Profile 2
Borehole 1
Profile 1
Fillings
A
A'
Sandy clay
Sandy clay
Unit Electrode Spacing = 0.750 m.
c
Fillings
Profile 2
Fillings
A
A'
Sandy clay
Sandy clay
Unit Electrode Spacing = 1.25 m.
d

Figure 4.

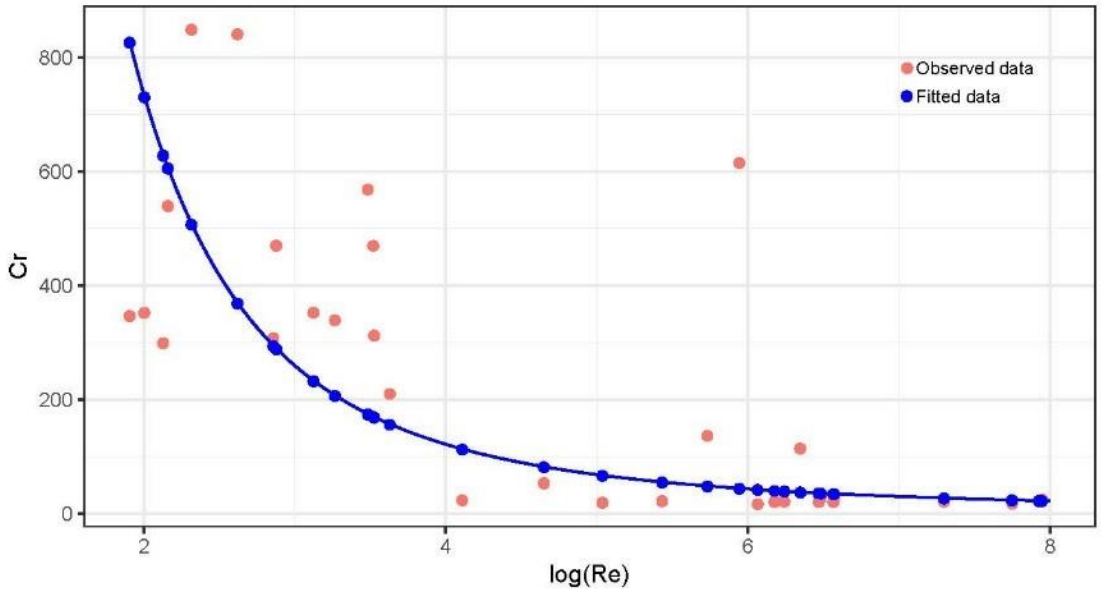

Figure 5.

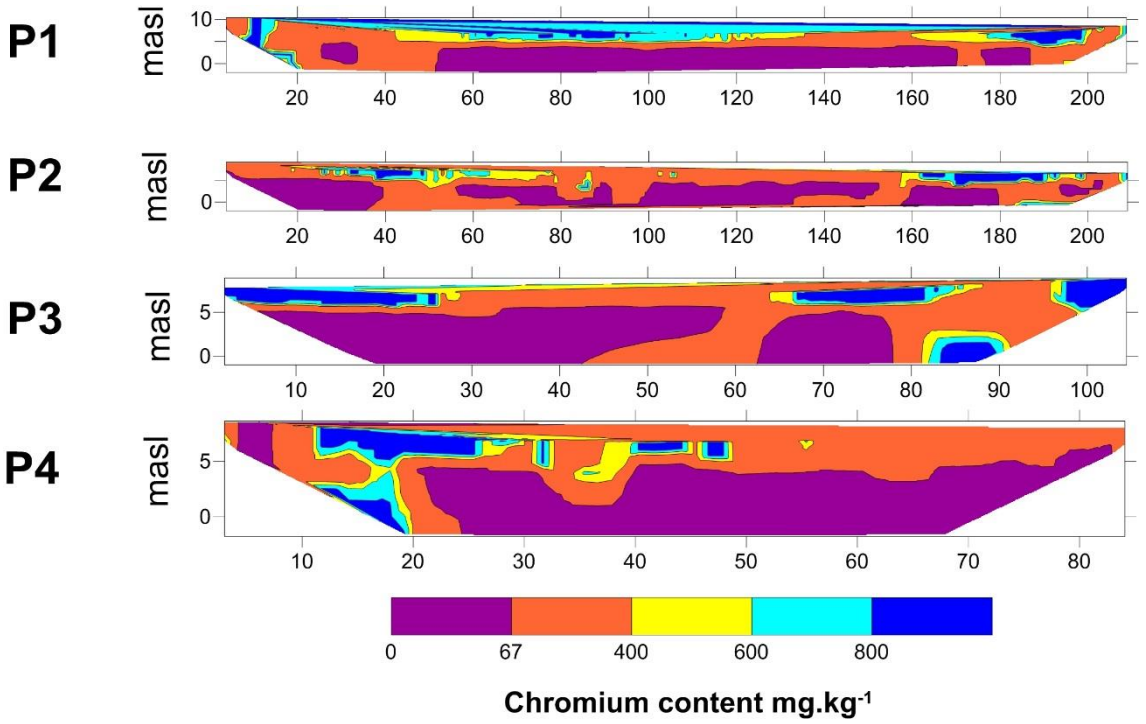
P1
P2
P3
P4
masl
10
0
5
0
20 40 60 80 100 120 140 160 180 200
10 20 30 40 50 60 70 80 90 100
0 67 400 600 800
Chromium content mg.kg-1

CHAPTER 5

5. ASSESSING THE BEHAVIOUR OF HEAVY METALS IN ABANDONED PHOSPHOGYPSUM DEPOSITS COMBINING ELECTRICAL RESISTIVITY TOMOGRAPHY AND MULTIVARIATE ANALYSIS

This paper is published as: **Vásconez-Maza, M. D.**, Bueso, M.C., Faz, A., Acosta, J.A., Martínez-Segura, M.A., 2021. Assessing the behaviour of heavy metals in abandoned phosphogypsum deposits combining electrical resistivity tomography and multivariate analysis. J. Environ. Manage. 278, 301–4797. https://doi.org/10.1016/j.jenvman.2020.111517

The author of the present PhD thesis has contributed significantly to this publication. Since the beginning of this scientific work, initial draft, writing and final publication of the paper. All work was done under the direction of the supervisors.

Abstract

The study presents the results of a physical-chemical characterisation of phosphogypsum deposits generated with hydrochloric and sulphuric acid during the wet acid process. This paper aims to set an efficient methodology based on electrical resistivity tomography (ERT), chemical analyses, and multivariate analysis identifying the most contaminated zones by heavy metals within an old factory of fertiliser derived from phosphoric rock. This fertiliser has provided many benefits to agriculture; however, it generates a vast amount of waste (5 tonnes/fertiliser ton). The chemical composition of this by-product varies according to the industrial process followed. The hydrochloric acid (HCl) recovers above 90% of phosphorus while sulphuric acid (H_2SO_4) about around 30%. Therefore, a chemical assessment of remaining waste before starting any remediation process is an ineludible step. The ERT provided the geometry of the deposits and the distribution of the phosphogypsum. The chemical analyses consistently validated the electrical contrast found within the deposits. We employed a correlation analysis combined with multivariate analysis for identifying the relationships among the metal concentrations and resistivity.

Principal component analysis (PCA) reduced the information contained in all variables into a few principal components. The first three principal components covered 74% of the variability of all the studied variables. Partial least squares-discriminant analysis (PLS-DA) for classification allowed discriminating both populations. Moreover, the electrical resistivity was the most influential variable for separating HCl waste from those of H_2SO_4. The use of the ERT saves time and reduces costs yielding a methodology which facilitates the environmental assessment of large areas.

5.1 Introduction

Several enterprises synthesised fertilisers derived from the apatite (phosphoric rock) during the last century, in Europe. Since there were few environmental regulations before the 70s, industries attacked the apatite with sulphuric acid generating a large quantity of phosphogypsum, especially in western European countries (EEA, 2015).

On the one hand, the configuration of cities was completely different during the 70s compared to today. The waste deposits were once far away from the urban nuclei, yet urban expansion has caused cities to envelop them. Nowadays, they are located in the middle of the city, prompting an environmental issue and an impediment to continuing urban development. The study was performed in an ancient industrial area which is in the southeast of Spain.

On the other hand, Europe promoted new environmental regulations (European Communities, 1991). By 1998, Spain adapted the new environmental law which obliged industry to reduce waste production (Law 10/1998, of April 21). Also, it established environmental liabilities on waste generated by the industry as well as, required them to create management plans for the existing waste and contaminated soils (Juan Carlos I Rey de España, 1998).

At that point, the industry object of this study needed to reduce hazardousness and the amount of by-product. It continued using the wet acid process, but it implemented the use of potassium chloride (KCl) in the process. The sulphuric acid (H_2SO_4) attacked the KCl obtaining potassium sulphate (K_2SO_4) that is also utilised in farming, and as a by-product, it appears hydrochloric acid (HCl). The new acid was used to attack the phosphoric rock

creating phosphoric acid (H_3PO_4) and phosphate slurries as waste. The resulting residue contains fewer heavy metals, optimising the process.

Fertilisers from phosphoric rock can be produced either by the thermal process or by the wet acid process. The wet acid process is the most common process used for synthesising this fertiliser (Tayibi et al., 2009). The wet process consists of the acidulation of phosphoric rock with a strong inorganic acid to recover the phosphorus. Sulphuric acid (H_2SO_4) is the most common acid employed in the industry due to its relatively low cost (Austin, 1992). Attacking the phosphoric rock with sulphuric acid (H_2SO_4) recovers around 30% of phosphorus but generates a vast quantity of waste (5 tonnes per tonne) with high heavy metal concentrations (Pérez-López et al., 2016).

One of the advantages of employing hydrochloric acid (HCl) is the recovery rate. It virtually recovers all the phosphorus (90%). The generated waste presents a lower heavy metal concentration. The employment of HCl instead of H_2SO_4 allows for the use of low-grade rock or reuse of phosphogypsum resulting from sulphuric acid production (U.S. Patent Nº 2,880,063, 1959). However, it is not often used in the industry due to its cost and corrosion issues during the industrial process (Al-Fariss, Ozbelge, & El-Shall, 1992).

In some cases, residues from HCl and H_2SO_4 could coexist as in this study case. But with no previous information. This paper presents the collaborative combination results of electrical resistivity tomography, chemical analyses, and multivariate analysis to differentiate one waste from the other by assessing the extent of contamination by heavy metal in a waste area.

Electrical resistivity tomography (ERT) is a non-invasive geophysical technique. This technique is frequently used in environmental assessments due to its capacity to provide subsurface information rapidly. The underground components respond differently to electrical currents, generating an electrical contrast. The presence of some metals lows the electrical resistivity values generating a significant electrical contrast with the background. In most cases, heavy metals are a sign of contamination. Therefore, ERT makes use of this contrast to identify subsurface heterogeneity, obtaining satisfactory results. Some authors have studied heavy metals with ERT (Martín-Crespo et al., 2012; Acosta et al., 2014; Cortada et al., 2017).

ERT provides indirect information which is validated with chemical analyses (direct measures). The combination of these derives in quantitative estimates of the subsurface. Previously it has been identified the spatial distribution of the chromium within a pond combining these techniques (Vásconez-Maza et al., 2019). This combination is widely known and proven. Several authors have employed it in their studies, showing that ERT is suitable for assessing ponds and mining tailings where the metallic concentration rate is high (Kemna et al., 2002; Martinez-Pagan et al., 2009; Wang et al., 2015; Martín-Crespo et al., 2018; Martínez-Segura et al., 2020).

Additionally, we employed multivariate statistical tools to explore the relationships among the parameters measured from chemical analyses and electrical resistivity values. The heatmaps have shown some strong correlation between some studied variables; therefore, we performed a principal component analysis (PCA) and a partial least squares-discriminant analysis (PLS-DA), for assembling all variables into a few principal components which allowed to discriminate both populations. Grouping variables into components facilitates the analysis and interpretation of data (Gabarrón, Faz, & Acosta, 2018). We studied the two most significant waste deposits in the area. Then, the multivariate techniques separate all the data into two well-defined groups that conveniently belong to the studied deposits.

Consequently, this study aims to: i) characterise the physical and chemical makeup of phosphogypsum deposits by using ERT and chemical analyses and ii) determine a correlation between ERT and heavy metals analysed by using multivariate analysis to identify the most contaminated site.

5.2 Material and methods

Study area

The study area is located in the periphery of Cartagena in southeast Spain (Fig. 1). The annual average temperature is 18ºC, with precipitation of 275 mm, and evapotranspiration of 900 mm. The geologic profile of this site is comprised of an accumulation of conglomerates (Tortonian), limestones (Messinian), and sandstones (Pliocene).

The site where the study was carried out is "El Hondón", which is an abandoned industrial area. Debris and several waste accumulation deposits cover a surface area of approximately 113 ha. These deposits were formed during fertiliser synthesis derived from phosphoric rock. This area is crossed by A-30 motorway which divides into two parts. For the study, there were selected the most significant deposit of each half. One deposit is in the north of the motorway and the other in the south, referred to as F1 and F2, respectively, see Fig. 1.

Electrical resistivity tomography

ERT is a non-invasive geophysical method for measuring the distribution of the subsurface resistivity. The resistivity contrast between materials, components and contaminates allow ERT to detect complex geological forms and change of phases in the subsoil. The leading electrical conduction mechanisms are electrolytic and electronic. In environmental studies, the electrolytic mechanism is frequently employed as the pore/fluid relationship governs the electrical conduction system. Nevertheless, in this study, there are high concentrations of native metals in the assessment area, then the electronic mechanism will govern the conduction of the electricity (Loke, 2015).

Field resistivity measures were retrieved with a Syscal R1 Switch 72 multi-core resistivimeter. This resistivimeter admits four coils; each coil holds eighteen stainless electrodes. These electrodes were georeferenced with a high accuracy GPS device. Also, ten boreholes were strategically dug, five in each site, aiming to acquire the highest quantity of chemical data. The location of boreholes was planned so as to coincide with at least one

profile. In most cases, they were made at the exact crossing point of the profile (see Fig. 1.).

A total of eight ERT profiles were situated throughout the study sites, F1 and F2, covering the surface of them. In deposit F1, Profile 1, Profile 2 used 72 stainless electrodes, spacing each electrode in 3 m, reaching 213 m long. Profile 3 required 72 stainless electrodes as well, but the spacing between electrodes was 1.5 m, with 106.5 m long; and, Profile 4 only required 36 electrodes, separating by 2.5 m, reaching 87.5 m long. For deposit F2, Profile 1, Profile 2 and Profile 3 employed 72 electrodes, separating by 2 m, 2.5 m, and 1.5 m; reaching a length of 142 m, 177.5 m, and 106.5 m, respectively. Finally, Profile 4 only employed 36 electrodes, with 2.5 m of separation between electrodes, reaching a length of 87.5 m.

In this study, the Wenner-Schlumberger array was employed because it offers a high signal-to-noise ratio, good vertical resolution, and depth penetration. Previous studies employed the same array achieving satisfactory results (Matys Grygar et al., 2013; Bortnikova et al., 2017). Before the inversion process, the dataset must be filtered, eliminating anomalous measures by using PROSYS II software and the GPS coordinates of the electrodes are added. Finally, the data is inverted by RES2DINV software, resulting in geoelectrical sections deployed on a 2D map with proper elevation (masl).

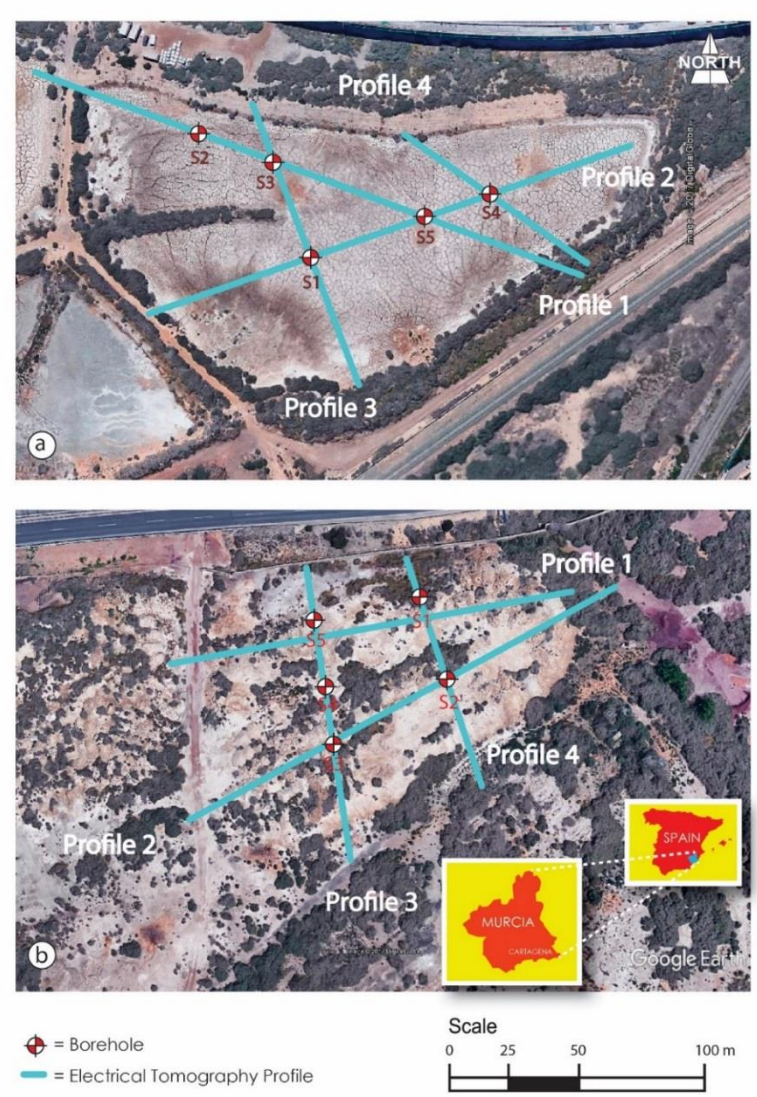

Fig. 1. Boreholes and electrical resistivity tomography profiles design of the study area.

Sampling and chemical results

The laboratory characterisation utilised samples from the subsurface of the deposits. The subsurface sampling was configured according to ERT profiles. As a minimum, each borehole was situated on one geoelectrical profile to guarantee a correlation among the data. This study uses the local legal thresholds as a reference, referred to as NGR. Table 1 summarises the geometry and the sample distribution of the boreholes, see Fig. 1.

The samples passed through a conditioning process before undergoing the laboratory procedure, which mainly consisted of a 72-hour drying process at 35°C. The dried samples were sieved to 2mm and then ground (Retsch RM 100). Physical properties, related to pH and electrical conductivity referred to as CE, were measured in deionised water (1:2.5 w/v and 1:5 w/v).

To determine the metallic concentration, the sample first had to pass through acidic digestion according to the US-EPA method 3051, (i.e. 0.5 g of sample in 10 ml of nitric acid (65%) and digested in a MARS 6 microwave). The metals analysed were Cd, As, Cr, Ni, Cu, Pb, Zn, and Hg. Then, an inductively coupled plasma-mass spectrometer (ICP-MS) measured the concentrations of metals, performing a highly sensitive analysis with lower detection limits that reached the order of one part per trillion to one part per quadrillion.

The accuracy and reliability of the results were supported using certified reference material (BAM-U110) from the Federal Institute for Materials Research and testing and reagent blanks were used as quality control samples during the analyses. We obtained satisfactory levels of recovery of the analysed metal ranging between 92% and 104%.

Table 1. Laboratory results from borehole core samples from F1 and F2.

	F1												F2										
			mg.kg^{-1}									dS.m^{-1}			mg.kg^{-1}								dS.m^{-1}
	Depth		Cu	As	Pb	Zn	Cr	Ni	Cd	Hg	pH	CE	Depth		Cu	As	Pb	Zn	Cr	Ni	Cd	Hg	pH	CE
BH-1	0	0.6	49.4	32.9	7.0	153.4	313.0	72.1	22.7	6.9	3.5	20.0	0	1	32.1	24.8	7.9	236.5	352.6	75.4	26.1	1.4	6.5	10.4
	0.6	1.5	43.8	18.2	5.5	94.6	210.6	52.4	16.3	5.9	3.6	19.5	1	1.9	16.0	10.4	nd	100.3	149.4	43.5	15.0	0.9	12.2	13.1
	1.5	2	58.9	29.2	28.2	232.8	615.6	64.2	10.1	5.9	4.4	3.9	1.9	3.6	31.6	37.0	17.2	253.6	381.4	71.7	33.0	3.4	5.3	11.0
	2	3	71.3	17.4	44.3	2109.0	114.8	36.3	29.1	0.3	5.6	1.9	3.6	4.2	99.7	184.9	475.7	588.7	64.1	30.1	6.8	1.0	10.9	9.4
	3	4.2	54.0	24.5	75.9	2105.8	28.6	52.7	16.8	0.3	6.5	1.0	4.2	4.7	269.8	2304.8	2645.4	1349.4	15.1	10.7	5.3	0.9	6.5	7.0
	4.2		53.2	12.7	20.6	1608.4	20.8	34.2	26.4	0.2	6.3	1.1	4.7	5.7	1810.9	26.1	45.2	40213.1	25.2	105.2	164.5	0.4	7.4	6.4
													5.7	7	1748.9	65.7	13.4	7575.9	20.6	28.9	31.7	0.3	7.6	3.9
													7		4043.1	120.7	15.0	23403.2	24.7	40.7	91.1	0.3	7.4	3.2
BH-2	0	0.6	137.0	28.2	8.0	158.2	347.3	57.3	16.7	9.5	4.0	8.4	0	1	74.3	50.2	137.4	335.8	256.9	68.4	36.1	2.0	7.7	5.8
	0.6	1.5	117.6	34.4	10.1	176.6	352.6	61.0	17.0	6.9	3.9	6.7	1	2	44.8	34.9	9.0	229.8	330.6	90.2	39.2	3.1	7.0	6.4
	1.5	2	119.0	28.2	11.5	233.8	849.4	82.0	9.3	9.2	4.3	4.9	2	2.8	47.2	58.6	334.2	313.5	223.6	45.3	19.7	1.6	6.6	5.7
	2	2.4	80.7	14.8	25.6	182.0	353.2	32.4	2.1	0.5	6.2	4.6	2.8	4	275.4	2038.3	1944.5	1609.0	14.8	15.1	15.3	5.8	3.0	47.5
	2.4	3.4	72.1	9.9	10.5	38.4	21.8	29.4	1.9	0.3	7.9	2.0	4	4.7	583.3	1085.8	3916.3	4225.8	17.8	22.9	19.3	1.2	3.6	13.2
	3.4	4.2	72.5	10.4	19.8	69.5	21.1	32.2	1.6	0.3	8.1	0.8	4.7	6	188.3	31.4	108.8	1441.8	22.6	26.2	5.7	0.4	8.3	8.1
	4.2	5.4	70.2	13.8	45.8	150.9	25.7	37.1	1.1	0.4	8.1	1.6	6	7	19.8	7.3	13.1	50.7	15.7	13.7	0.2	0.2	8.5	1.0
	5.4		56.7	9.0	35.7	103.9	22.7	35.4	1.4	0.1	7.9	1.7	7	8.4	23.7	5.4	27.2	137.8	21.1	20.7	0.3	0.2	8.4	0.5
													8.4		22.2	9.9	45.6	194.1	20.5	21.0	0.5	0.3	8.3	0.7
BH-3	0	0.8	39.1	28.7	9.4	159.3	299.6	58.8	21.3	6.6	4.3	12.6	1	1.2	23.2	10.3	4.1	130.5	124.8	38.3	26.0	1.2	12.2	12.8
	0.8	1.5	39.8	35.4	6.1	265.8	540.0	71.3	20.5	5.5	3.8	8.3	1.2	1.8	30.0	32.8	4.5	195.0	351.6	120.8	69.3	2.8	7.2	8.2
	1.5	2.2	51.9	34.3	12.3	244.9	841.5	92.6	12.8	6.2	4.2	5.9	1.8	3	13.7	4.1	3.6	57.3	46.2	30.8	6.9	0.6	12.4	11.9
	2.2	3	21.0	10.4	36.7	111.7	24.1	76.9	4.8	0.2	7.7	1.8	3	3.5	59.8	176.3	255.4	380.6	90.6	27.4	10.4	3.9	10.0	5.0
	3	4.2	19.9	14.5	73.3	435.9	21.2	32.0	8.1	0.4	8.1	1.4	3.5	4.4	331.8	13231.4	7205.3	804.1	24.4	11.2	12.3	1.5	7.8	4.0
	4.2	5	25.7	22.0	106.0	602.4	28.8	33.4	5.0	0.4	7.9	1.3	4.4	5.1	79.9	359.3	570.0	2156.5	26.5	29.8	10.9	0.5	8.1	3.6
	5		25.8	23.7	125.7	703.1	27.5	34.6	10.4	0.3	8.0	1.3	5.1	6	52.6	725.1	554.6	334.7	21.6	17.0	3.2	0.3	12.3	6.9
													6	7	18.9	51.3	87.1	267.6	24.8	24.4	1.2	0.5	9.1	1.5
													7	8	16.6	10.3	44.5	187.5	24.2	23.9	0.5	0.5	8.2	0.7
													8		15.4	7.9	43.1	113.8	24.5	24.8	0.8	0.7	8.3	0.6
BH-4	0	1	43.9	27.6	4.5	218.2	339.7	67.7	17.1	5.2	3.8	17.3	0	0.6	27.5	21.9	1.9	142.9	287.4	45.3	17.3	2.2	5.5	5.7
	1	2	32.4	30.0	5.6	150.3	470.4	53.0	13.4	4.5	3.8	8.1	0.6	1.5	20.3	19.1	1.7	122.2	250.3	68.8	29.9	1.8	9.1	4.3
	2	3.3	77.8	39.7	44.4	61.7	137.1	32.8	14.2	3.7	7.4	6.1	1.5	2.4	8.2	1.6	nd	20.5	33.9	23.8	1.6	0.6	12.4	11.0
	3.3	4	19.4	12.2	22.5	77.2	21.2	54.4	2.1	0.4	7.2	2.3	2.4	3	22.8	21.2	3.0	296.7	377.7	62.6	26.6	1.8	5.2	7.1
	4	5	15.2	6.1	54.7	58.4	17.6	18.6	0.4	0.6	8.1	1.3	3	4.2	27.3	36.2	16.4	293.2	336.8	55.5	45.2	2.3	4.6	9.2
	5	6	30.4	5.4	31.3	64.9	22.7	27.6	0.4	0.7	8.0	1.5	4.2	4.8	46.8	62.6	170.4	241.5	101.1	39.5	39.8	2.0	12.2	13.0
	6		20.5	4.7	33.7	102.4	20.1	22.1	0.5	0.4	8.1	1.2	4.8	6	159.6	251.5	406.1	515.5	182.0	50.2	19.4	2.6	10.3	8.2
													6	6.8	421.3	634.7	601.4	675.4	74.5	16.5	3.8	2.9	6.9	6.7
													6.8	8	117.6	11.9	8.5	468.4	30.0	35.1	3.4	0.4	7.9	3.8
													8	9	40.5	4.4	18.9	305.9	19.6	36.4	0.1	0.3	8.0	2.4
													9		45.4	4.9	21.6	195.8	23.8	44.9	0.5	0.2	8.0	1.9
BH-5	0	0.6	36.6	32.1	4.6	102.6	308.6	69.0	19.9	7.0	3.6	20.9	0	0.6	21.7	16.3	8.3	133.4	189.4	47.2	14.6	1.6	12.3	12.1
	0.6	1.8	38.6	30.2	3.7	143.3	470.6	85.4	16.5	9.8	3.5	18.4	0.6	1.8	25.6	22.3	7.1	127.6	345.6	45.0	14.6	2.1	6.0	6.5
	1.8	2.4	38.9	36.7	37.6	183.1	569.0	69.4	9.2	7.6	6.8	6.0	1.8	3	21.0	22.4	3.1	106.3	321.9	50.8	13.3	1.4	5.2	8.2
	2.4	3	33.4	50.8	17.4	46.4	53.9	27.2	2.2	0.3	7.6	3.8	3	4	25.7	31.2	7.7	132.8	395.3	58.3	22.3	2.0	4.1	8.3
	3	4	23.0	20.1	15.2	22.3	21.8	19.3	2.2	0.2	8.1	1.4	4	5	28.6	26.3	6.0	162.8	427.2	54.4	14.3	3.0	4.6	7.0
	4	5	26.4	15.5	43.7	64.5	20.9	36.0	13.2	0.4	8.0	1.6	5	5.6	126.7	54.3	553.0	2101.1	22.8	35.1	3.7	2.2	7.6	4.0
	5		24.1	13.7	42.2	83.1	18.5	32.5	19.1	0.4	8.2	1.4	5.6	6.6	22.7	5.1	36.5	240.5	16.5	16.0	1.4	0.3	7.9	4.1
													6.6	7.6	41.1	9.3	37.3	187.7	23.1	24.3	0.8	0.2	8.0	1.5
													7.6	8.6	32.7	3.3	26.4	96.4	15.8	17.1	0.6	0.2	8.1	1.0
													8.6	9.6	12.4	9.2	38.3	114.5	15.6	17.0	0.5	0.1	8.3	0.5
													9.6	10.7	13.5	3.8	31.8	136.2	15.3	15.3	0.2	0.2	8.6	0.4
													10.7		13.4	5.0	34.3	185.7	16.5	16.6	0.5	0.1	8.3	0.5
Mean			49.7	22.2	30.8	323.4	216.3	48.4	11.0	3.1	6.2	5.8			225.9	439.7	428.5	1877.8	124.8	39.1	18.5	1.3	8.0	6.7
Min			15.2	4.7	3.7	22.3	17.6	18.6	0.4	0.1	3.5	0.8			8.2	1.6	1.7	20.5	14.8	10.7	0.1	0.1	3.0	0.4
Max			137.0	50.8	125.7	2109.0	849.4	92.6	29.1	9.8	8.2	20.9			4043.1	13231.4	7205.3	40213.1	427.2	120.8	164.5	5.8	12.4	47.5
NGR			23	12	43	96	67	37	0.6	1.7					23	12	43	96	67	37	0.6	1.7		

Statistical analysis

Data analysis was conducted with the well-known R free software (R Core Team, 2019). The experimental data measured from the deposits were explored using graphical methods (box-and-whisker plots and scatterplots) to figure out their global behaviour, and descriptive statistics summary aided in comparing the dataset with the local legal thresholds of contamination (NGR). Filtering the atypical data and limiting resistivity values to chemical values from borehole core samples.

Besides, the cornerstone of this study lies in the existence of a correlation between metallic concentration (Cd, As, Cr, Cu, Ni, Pb, Zn and Hg) and resistivity (Re). Due to the metrical nature of the variables, Pearson's correlations between all the log-transformed variables were performed in order to recognise interrelationships among geochemical and geoelectrical parameters.

Even though some strong correlations were found among the data; these alone do not determine the origin of one component or another. Thus, a principal component analysis (PCA), applied to the mean-centred log-transformed variables and based on the correlation matrix, was carried out for an unsupervised classification and dimensionality reduction, assembling all variables into a few principal components which explained most of the variability contained in the data.

Finally, as a supervised technique, partial least squares-discriminant analysis (PLS-DA) was performed for discriminating between deposits which allowed to identify the most influential parameters in the classification based on the variable importance in the projection (VIP). As a criterion, the variables with VIP scores greater a given threshold, usually assumed to be greater than one, were selected as the most discriminant variables for the classification. Results were displayed in crown diagrams.

5.3 Results and discussion

Electrical resistivity tomography

In the overall analysis, both F1 and F2 have two layers, with the top layer likely being comprised of the contaminant, and the deepest layer is natural soil. This information fits initial assumptions as the study area is composed of accumulation deposits. The waste was piled one layer on top of another. Thus, the phase change likely is vertical but not horizontal. The background noise level expected is high due to the presence of native metals and sulphides on the top layer and sandy clay with gravels at the bottom. Loke (2015) alludes to that Wenner-Schlumberger array provides a suitable strength signal for a noisy background.

Also, the boreholes core samples confirm that the most contaminating elements lie at the top and the presence of these elements decreases in deeper layers. These findings match those of previous studies such as that found by Martín-Crespo et al. (2018b) in their study of heavy metals in mine tailings. For F1, profiles 1-2, the largest penetrated to a depth of ≈45 metres, while profiles 3-4 only penetrated to ≈25 metres. Similarly, in F2, the maximum depth reached is ≈30 metres in profiles 1-2 and ≈20 metres for profiles 3-4.

Additionally, Rosales et al. (2012) put forward that the root mean squared error (RMSE) below 10% is a good quality indicator. The resulting ERT profiles of this study exhibit an RMSE below the 8.5% meeting the reliability requirements. A dashed line marks the border between the upper and lower layers. This line is drawn following the resistivity patterns and the geometry obtained from the boreholes. This synergetic combination ensures the reliability of the data. The range of colours of the rainbow was used for the scale of colours, with those colours closer to blue being less resistive and those closer to red representing higher resistivity (Fig. 2.).

The top of F1 shows a well-defined layer, which is common for the four geoelectrical sections, with a relatively constant thickness (≈2.5 m), and an average resistivity below ≈17 Ω.m. At the bottom lies another layer composed mainly of sandy clay and gravels. The sum of these materials results in higher resistivity. So, the resistivity here leaps up to >124 Ω.m. In between lies a transition area in which the resistivity range is ≈30-

124 Ω.m; (Fig. 2, left). Lower resistivity values marking a descending path below the dashed line could probably be due to a leach phenomenon.

F2 shows a top layer similar to that of F1. The boreholes and chemical analysis played a crucial role in this deposit because they clarify how the resistivity varies. Consequently, they mark the border (dashed line) between the contaminated layer and the natural soil (figure 2, right). The top layer has a thickness of ≈5 m. The resistivity average of the top layer in F2 is <10 Ω.m and, for the bottom layer, >20 Ω.m, in general. The heterogeneity characterises the deposit F2. Low resistivity values appear below the dashed line. Probably, the materials from the top have leached more than in F1.

ERT study indicates that the contamination is concentrated on the top of the deposits and some metals from the top layer probably have leached, but this does not lie within the scope of this study and might be studied deeply in further studies.

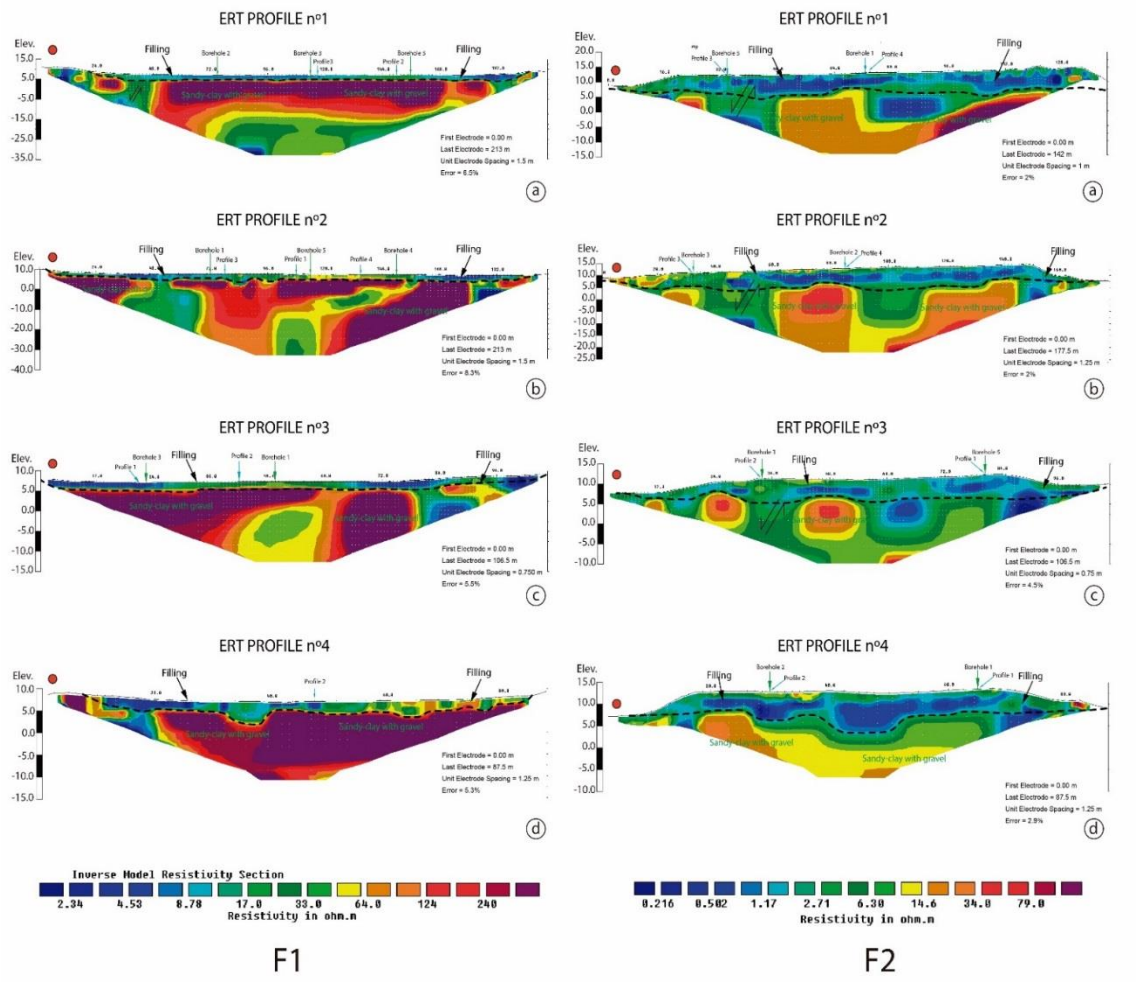

Fig. 2. Geoelectrical sections of deposit F1 and F2.

Properties and chemical composition of the deposits

The initial chemical analysis yields the leading distinctive features between deposits, mainly regarding the metallic concentration. Both deposits far exceed the local legal thresholds (NGR). This behaviour is in line with previous studies of phosphogypsum, as Millán-Becerro et al. (2019) point out in their study. However, it is necessary to analyse the data meticulously. We focus on the top layer previously identified with the ERT study. Thus, we narrow the data down to the top layer for the study.

Besides, based on bibliographic documents about the last factory that worked in the study area; we expect two different by-products. One was resulting from the HCl and another from the H_2SO_4. Fig. 3d. illustrates the mean concentrations of the top layers from both deposits. Particularly, both deposits hold the same metals but follow a distinct descendant concentration trend. For F1, metals were ranked in the order Cr > Zn > Cu > Ni > As > Pb > Cd > Hg, while for F2 in the order As > Pb > Zn > Cr > Cu > Ni > Cd > Hg. This probably occurs due to the attacking acid was different.

The recovery rate of the phosphorous from the phosphoric rock varies according to the attack acid employed, as mentioned in the introduction. The wet acid process is well-known around the world. With the sulphuric acid (H_2SO_4) occurs the following chemical reaction $Ca_{10}(PO_4)_6 + 10H_2SO_4 + 20H_2O = 6H_3PO_4 + 10CaSO_4 \cdot 2H_2O$ while with the hydrochloric acid (HCl) $Ca_{10}(PO_4)_6 + 20HCl = 6H_3PO_4 + 10CaCl_2 + 2H_2O$. In both cases the by-product resulting present, heavy metals, but the mean concentration of these is higher for the sulphuric acid. Table 1 presents the chemical results from the borehole core samples.

The sulphuric acid is widely employed due to the calcium sulphate ($CaSO_4$) is much more insoluble (easier separation) than the calcium chloride ($CaCl_2$). Consequently, in the precipitated $CaSO_4$ remains much more quantity of trace materials among them the heavy metals. This information shows the potential, and the danger of the by-products, as El Zrelli et al. (2018) states the phosphogypsum issues and the possible economic exploitation. The elevated metal concentration shows the danger that phosphogypsum presents within the environment as these metals are available and could migrate to nearby urban nuclei (Gabarrón et al., 2018).

On the one hand, F1 presents chromium (Cr) with 417 $mg.kg^{-1}$ as the metal most concentrated and mercury (Hg) the least concentrated with 6.44 $mg.kg^{-1}$. Waste containing heavy metals represents an environmental problem due to the potential contamination of nearby agricultural soils and the risk of the anomalous heavy metal concentration entering the food chain. Exposure to heavy metals could cause several illnesses. According to the Agency for Toxic Substances and Disease Registry (2011). Both deposits surpass by far the local legal thresholds (NGR), see Fig. 3d.

On the other hand, F2 contains the same metals, but metallic contents are higher than in F1. Arsenic (As), lead (Pb), zinc (Zn) are above 400 $mg.kg^{-1}$. The rest of the metals are below 214 $mg.kg^{-1}$. Mercury is the least concentrated with 2.5 $mg.kg^{-1}$, which is about two times higher than the legal limit. Arsenic affects the skin, liver, and gastrointestinal and respiratory systems. Cadmium exposure during pregnancy affects development, attacking the cardiovascular, gastrointestinal, neurological, renal, respiratory and reproductive systems. Vásconez-Maza et al. (2019) summarise the health effects of the most common metals present in phosphogypsum.

Finally, the chemical study shows that F1 waste is different from those of F2. F1 has a lower average metallic concentration; therefore, the future management plans have to take it into account before any remedial action.

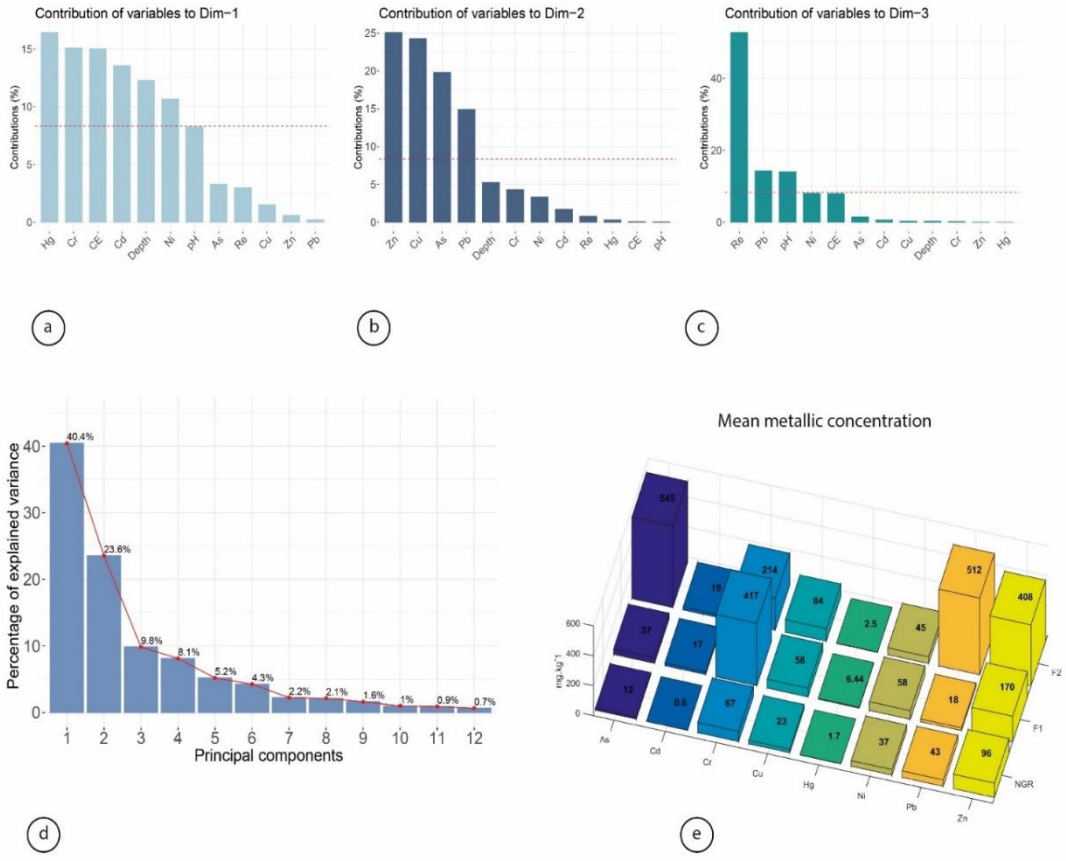

Fig. 3. a-c. Contributions (%) of each variable to each dimension of the PCA. **d.** Scree plot of the components extracted by PCA **e.** Mean metallic concentrations from both studied deposits.

Discrimination between deposits by multivariate analysis

Chemical analysis is limited for borehole penetration; in the case of F1, it reached a depth of ≈6 metres, and a depth of ≈10 metres for F2. ERT provided a range of information to a depth of ≈15-45 metres for both deposits. In order to carry out the statistical analysis, the electrical resistivity data was narrowed down and adapted to the band marked by the borehole core samples. Thus, the direct measures (chemical analysis) validates the indirect measures (ERT)

Fig. 4 graphically represents Pearson's correlation matrices between the log-transformed variables measured from F1 (left) and F2 (right). The strong and positive relationships are highlighted in blue, whereas the opposite appears in red. Weakly correlated variables acquire a degraded range of blue and red, respectively.

These heatmaps reveal that there are several strong correlations within the deposits. We considered significant correlations those that are above 0.60 in absolute value. The electrical conductivity (CE) and pH have a strong correlation with almost all variables but zinc (Zn), copper (Cu), and cadmium (Cd). Lead (Pb), chromium (Cr), nickel (Ni) and mercury (Hg) concentrations measured from F1 show with the resistivity (Re). Pb is negatively correlated with Cr and Hg. The rest of the metals are positively correlated, forming groups of correlations. The most significant is 0.9 the correlation between Cr and Hg in F1.

F2 presented different behaviour. In this deposit, the resistivity showed a moderate correlation with the metal concentrations. CE and pH do not present relevant features. Cu and As contents were strongly correlated as well as As and Pb contents. The most significant correlation is 0.92 occurring between Zn and Cu. Cr presents relevant correlation with Ni, Hg, and Cd. The rest of the significant correlations are positive above 0.60.

Therefore, we performed a PCA to detect the relationships among the variables. Identifying groups of variables that account for at least of the total variance. A scree plot of the components is displayed in Fig. 3 d where is shown the percentage of variance accounted for each principal component. As a criterion, a number of components with a cumulative percentage of variance at least 70% is retained.

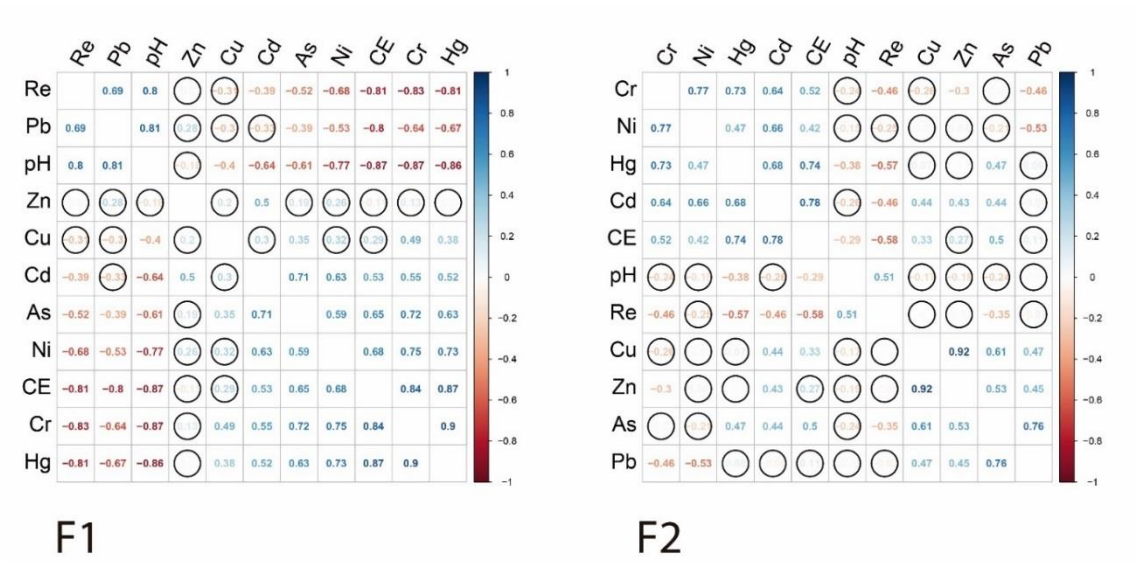

Fig. 4. Pearson's correlation coefficients matrix of all the variables measured. Circled values are the non-significant correlations.

Hence, the first three principal components (PCs) were considered, which covered 74% of the variability of all the studied variables. The score and correlation plots associated with these components are represented in Fig. 5 a; the score plot represents the dataset into the low-dimensional space defined by the PCs, while the correlation plot indicates the correlation of the original variables with the PCs where the concentric circles represent 50% and 100% explained variance of the variables by the PCs. The corresponding loading values are given in Table 2, where boldly marked values correspond to the most influential variables for each principal component.

Table 2. Loading values of the most relevant principal components.

	Cu	As	Pb	Zn	Cr	Ni	Cd	Hg	pH	EC*	Re**	Depth
PC1	0.123	0.182	-0.048	0.077	**0.389**	**0.327**	**0.368**	**0.405**	-0.288	**0 387**	-0.173	**-0.351**
PC2	**0.493**	**0.445**	**0.387**	**0.501**	-0.208	-0.183	0.131	-0.054	-0.021	0.03	-0.089	0.23
PC3	0.056	-0.122	**0.378**	0.019	0.046	0.284	0.078	0.002	**-0.375**	-0.282	**0.726**	-0.053

*Electrical conductivity, **Electrical Resistivity

Fig. 3 a-c gives the contributions, as a percentage, for each variable to each principal component. As can be seen, the PC1 was associated to Hg, Cr, CE, Cd, Depth and Ni, and explained the 40.4% of the total variance, while PC2 representing the 23.6% of the total variance was defined by Zn, Cu, As and Pb. As indicated, PC1 and PC2 explained 64% of the variance, and are not capable of discriminating one deposit from the other.

Since the PC3 (~10% of the variance) separated the samples from the deposits. Values above zero, marked by a horizontal dashed line, belong to pond F1 (red circles), and the rest to F2 (blue squares). Resistivity is the most influential variable, and it governs the separation occurring in PC3. Resistivity is on the positive side of the Y-axis, within the crown at ≈ 0.73 in the range -1 to 1, see fig.5 a.

PLS-DA is a PLS regression method where the response variable is a categorical variable, defined as a dummy variable, and the latent variables are defined by a linear combination of the explanatory variables that maximize the information of the covariance between the response variable and the explanatory variables. For the PLS-DA application, the dataset was splitting into two sets: the first was used to construct the model (training set), while the second to evaluate the performance of the model (test set). The training set was randomly extracted from the dataset (75% of the data), and the remaining was used as the test set.

Next, PLS-DA was applied to the training set and validated by the test set. Thus, two components were extracted (variability explained of the explanatory variables: R^2X = 35.1%; variability explained of the response variable: R^2Y = 83.3%) and the results were represented in score and correlation plots (Fig. 5 b). As can be seen, there is clear discrimination between the two deposits and the first component was responsible for the separation of the samples.

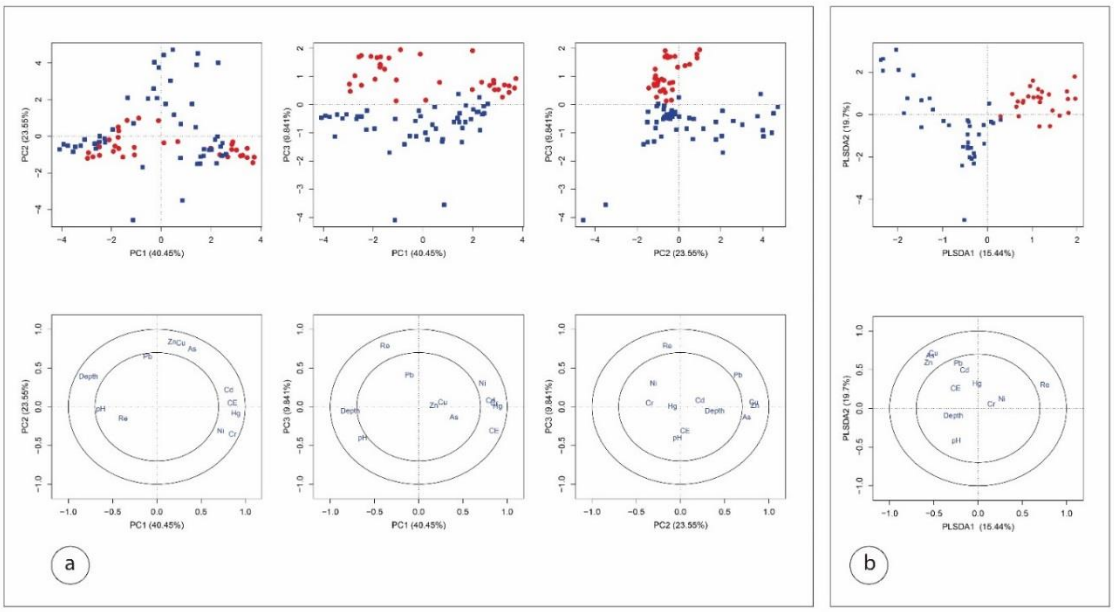

Fig. 5. Results of multivariate analysis applied to the chemical and geoelectrical parameters measured. Score plot (top). Red circles represent F1 and blue squares F2. Correlation plot (bottom). Circles represent r^2 = 50% and 100% variability explained by the components. **a.** The first three components of the PCA. **b.** The first two components of the PLS-DA.

Resistivity (Re) was the variable highly correlated with the first component and with the highest VIP score (see Fig. 6). Zn, As and Cu showed similar VIP values and were positively correlated with the second component. The performance of the PLS-DA model provided an error rate of 4.8 % for the test set; 20 samples were correctly classified while one sample from F2 was misclassified.

Consequently, the statistical study reveals that ERT could be a tool to determine the sites more affected by heavy metals contamination.

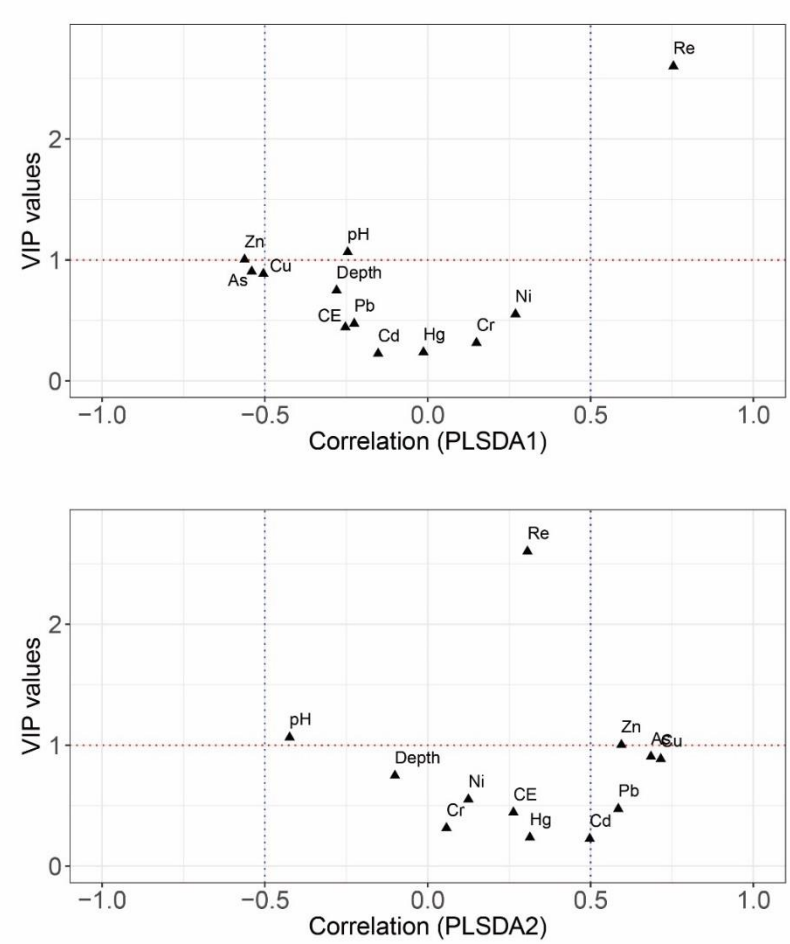

Fig. 6. Variable importance in the projection (VIP) and the correlation coefficients for the first two components of PLS-DA.

5.4 Conclusions

ERT provided the geometry of the deposits, confirming that the deposits were formed by accumulation being the top layer the most contaminated. Also, the distribution of electrical resistivity values under the top layer suggested that a leach phenomenon could be happening, but further studies will need to be conducted to confirm it. Chemically, F2 is identified as the most contaminated deposit by the analysed heavy metals being the arsenic the most concentrated within the deposit. While in F1, the arsenic concentration is 14 times lower. This suggested that the phosphoric rock was not attacked with the same acid. We can consider that waste present in F1 comes from HCl while F2 holds waste generated with H_2SO_4. Therefore, in future management, they have to be treated differently.

By combining ERT, chemical analysis of the borehole core samples and a statistical study, we have attained satisfactory results in the characterisation of waste deposits, yielding an accurate methodology. ERT provides the first site overview revealing the potentially contaminated zones. This information allows us to map out the most suitable location for drilling the boreholes. The statistics tools merge the data revealing the contaminant behaviour facilitating the data interpretation reporting at conclusions. Consequently, it can be concluded that this study is an efficient methodology to determine the location and the extent of heavy metal contamination in phosphoric waste deposits, and it is entirely applicable elsewhere beyond our study area.

CHAPTER 6

6. Conclusions

Since the specific objectives of this dissertation were conceived as scientific articles and these are divided per chapters; then, conclusions are given per chapters as well.

Chapter three is devoted to a physical characterisation of the waste deposits. The methodology achieved with the research gave satisfactory results for calculating an existing volume within a deposit. This methodology combined LiDAR point cloud with electrical resistivity tomography. LiDAR point cloud provided metric accuracy on the top surface of the deposit, and the electrical resistivity tomography allowed computing the bottom surface of the deposit. This methodology is utterly exportable to any deposit without a significant investment due to it was employed commercial software.

Chapter four deals with the chemical characterisation. Electrical resistivity tomography showed the geometry of the deposit. The electrical contrast of the deposit guided the most suitable position of where borehole might be drilled. As expected, phosphogypsum showed high acidic and saline values. The metallic concentration of the all analysed metals but lead exceeded by far the local legal threshold.

Non-linear regression models found a significant relationship between resistivity and metallic concentrations. The model allowed to determine that chromium is the most concentrated metal in the pond. The statistic tools allowed identifying where the chromium was located within the pond. This information is valuable; we can predict which part of the deposit holds chromium with a concentration of above 800 mg kg^{-1}.

Chapter five bears out earlier findings; the methodology previously employed was improved with more sophisticated statistic tools. Despite that deposits house similar waste chemically talking. Waste deposits presented different concentrations of metals. Deposit F1 presents 14 times lower arsenic than deposit F2. This variation on the chemical concentration suggested that F1 was attacked with a different acid. Then, an unsupervised and a supervised technique were applied for recognising and classifying the two-population found. Consequently, in future remediation of the site, deposit F1 and deposit F2 must be treated differently.

By using the modelling and statistical methods, electrical resistivity tomography can produce spatiotemporal data unavailable from only using standard traditional methods. Not only did ERT provided a map of resistivity, but it also computed concentration maps or precise volume data.

In a whole, the aims of the thesis were successfully completed. The combination of electrical resistivity tomography with chemical analysis resulted in suitable and reliable to characterise phosphogypsum deposits. However, incorporating statistic tools have demonstrated significant advances in engineering. This synergic combination permitted inferring new information beyond a simple characterisation; it allowed to provide useful information and understandable information to the researchers.

Consequently, it can be considered that this thesis has contributed to science due to all methodologies used are proven and completely exportable beyond the study area. This thesis exposes the first steps in the further growth of assessing phosphogypsum with electrical resistivity tomography to generate useful models of this problematic waste.

Challenges and recommendations

A more significant challenge continues regarding the electrical resistivity tomography (ERT) applications in complex waste as phosphogypsum. The research in this thesis demonstrated that it is entirely feasible to infer more information from electrical resistivity tomography; showing that the most influential variable to infer that information was the resistivity. However, the ERT technique is an indirect measure that needs to be supported with direct measurements.

Shortly the efforts can be oriented to achieve a methodology that reduces to a minimum the direct measures needed to support ERT. One possible suggestion is to combine some geophysical techniques, such as Induced Polarization (IP), Ground Penetrating Radar (GPR), etcetera. IP could provide additional valuable data to ERT.

Further studies still need to be conducted to extract more information from the datasets. One suggestion is to use sophisticated software and hardware; it may be beneficial only with reinversion of the dataset, it could produce modern outputs or even 3D models.

Another promising step in correlating ERT data with physical properties of the deposits is using radioactivity data. High values of radioactivity are inherently linked to phosphogypsum. Hence, another suggestion is to study how radioactivity behaves and correlate it with the ERT.

The step ahead in this line of investigation is the monitoring and 4D models. Planting permanent and georeferenced electrodes provide spatiotemporal information not only information of a campaign. With 4D models, researchers can analyse the global behaviour of the area and observe how the studied material evolves in the time. Continuous monitoring of a site might provide earlier alerts and might avoid potential disasters.

Ultimately, this research has presented new paths for obtaining additional useful information from phosphogypsum deposits by using electrical resistivity tomography. This research set a milestone in my professional career, and with a bit of chance, it could help other colleagues of research.

CHAPTER 7

7. References

Acosta, J. A., Martínez-Pagán, P., Martínez-Martínez, S., Faz, A., Zornoza, R., & Carmona, D. M. (2014). Assessment of environmental risk of reclaimed mining ponds using geophysics and geochemical techniques. *Journal of Geochemical Exploration*, *147*, 80–90. https://doi.org/10.1016/J.GEXPLO.2014.04.005

AEMET. (2018). Agencia Estatal de Meteorología - AEMET. Gobierno de España. Retrieved December 10, 2018, from http://www.aemet.es/es/portada

Agency for Toxic Substances and Disease Registry. (2011). ATSDR - Substance Listing Page. Retrieved May 31, 2019, from https://www.atsdr.cdc.gov/substances/indexAZ.asp

Agilent Technologies. (2006). *Agilent 7500 Series ICP-MS-Power, Flexibility, Sensitivity The Ultimate in Metals Analysis Specifications*. Retrieved from https://www.agilent.com/cs/library/Support/Documents/F05009.pdf

Al-Fariss, T. F., Ozbelge, H. O., & El-Shall, H. S. H. (1992). Process technology for phosphoric acid production in Saudi Arabia. *Magallat Gamiat Al-Malik Saud. Al-Ulum Al-Handsiyyat*, *4*(2), 239–255. https://doi.org/10.1016/s1018-3639(18)30567-1

Alamry, A. S., van der Meijde, M., Noomen, M., Addink, E. A., van Benthem, R., & de Jong, S. M. (2017). Spatial and temporal monitoring of soil moisture using surface electrical resistivity tomography in Mediterranean soils. *CATENA*, *157*, 388–396. https://doi.org/10.1016/J.CATENA.2017.06.001

Andrades, M. (1996). *Prácticas de Edafología y Climatología* (Universida). Logroño. La Rioja, España.

Austin, G. T. (1992). *Manual de procesos químicos en la industria*. McGraw-Hill.

Baniel, A., & Blumberg, R. (1959). *U.S. Patent Nº 2,880,063*. Israel.

Bisone, S., Gautier, M., Chatain, V., & Blanc, D. (2017). Spatial distribution and leaching behavior of pollutants from phosphogypsum stocked in a gypstack: Geochemical characterization and modeling. *Journal of Environmental Management*, *193*, 567–575. https://doi.org/10.1016/J.JENVMAN.2017.02.055

BOE. REAL DECRETO 9/2005, de 14 de enero, por el que se establece la relación de actividades potencialmente contaminantes del suelo y los criterios y estándares para la declaración de suelos contaminados (2005). Spain.

BOE. RESIDUOS . Establece la relación de actividades potencialmente contaminantes del suelo y los criterios y estándares para la declaración de suelos contaminados . MINISTERIO PRESIDENCIA (2005). Spain.

BOE 18 enero 2005, núm. 15. RESIDUOS, Pub. L. No. Real Decreto núm. 9/2005, de 14 de enero, 1833 (2005). España.

Bortnikova, S. B., Olenchenko, V. V., Gaskova, O. L., Chernii, K. I., Devyatova, A. Y., & Kucher, D. O. (2017). Evidence of trace element emission during the combustion of sulfide-bearing metallurgical slags. *Applied Geochemistry*, *78*, 105–115. https://doi.org/10.1016/j.apgeochem.2016.12.016

Bortnikova, S., Olenchenko, V., Gaskova, O., Yurkevich, N., Abrosimova, N., Shevko, E., … Eder, L. (2018). Characterization of a gold extraction plant environment in assessing the hazardous nature of accumulated wastes (Kemerovo region, Russia). *Applied Geochemistry*, *93*, 145–157. https://doi.org/10.1016/j.apgeochem.2018.04.009

Brillante, L., Mathieu, O., Bois, B., Van Leeuwen, C., & Lévêque, J. (2015). The use of soil electrical resistivity to monitor plant and soil water relationships in vineyards, *1*, 273–286. https://doi.org/10.5194/soil-1-273-2015

British Geological Survey. (2020). Digital geoscience. Retrieved November 15, 2020, from https://www.bgs.ac.uk/geological-research/digital-geoscience/

Cánovas, C. R., Macías, F., Pérez-López, R., Basallote, M. D., & Millán-Becerro, R. (2018). Valorization of wastes from the fertilizer industry: Current status and future trends. *Journal of Cleaner Production*, *174*, 678–690. https://doi.org/10.1016/J.JCLEPRO.2017.10.293

Cardarelli, E., De Donno, G., Oliveti, I., & Scatigno, C. (2018). Three-dimensional reconstruction of a masonry building through electrical and seismic tomography validated by biological analyses. *Near Surface Geophysics*, *16*(1), 53–65.

https://doi.org/10.3997/1873-0604.2017040

Cárdenas-Escudero, C., Morales-Flórez, V., Pérez-López, R., Santos, A., & Esquivias, L. (2011). Procedure to use phosphogypsum industrial waste for mineral CO 2 sequestration. *Journal of Hazardous Materials*, *196*, 431–435. https://doi.org/10.1016/j.jhazmat.2011.09.039

Caterina, D., Flores Orozco, A., & Nguyen, F. (2017). Long-term ERT monitoring of biogeochemical changes of an aged hydrocarbon contamination. *Journal of Contaminant Hydrology*, *201*, 19–29. https://doi.org/10.1016/j.jconhyd.2017.04.003

Certified Reference Material BAM-U110 Contaminated Soil Certified Values. (2006).

Chalupa, V., Pánek, T., Táborík, P., Klimeš, J., Hartvich, F., & Grygar, R. (2018). Deep-seated gravitational slope deformations controlled by the structure of flysch nappe outliers: Insights from large-scale electrical resistivity tomography survey and LiDAR mapping. *Geomorphology*, *321*, 174–187. https://doi.org/10.1016/j.geomorph.2018.08.029

Chambers, J. E., Gunn, D. A., Wilkinson, P. B., Meldrum, P. I., Haslam, E., Holyoake, S., … Wragg, J. (2014). 4D electrical resistivity tomography monitoring of soil moisture dynamics in an operational railway embankment. *Near Surface Geophysics*, *12*(1), 61–72. https://doi.org/10.3997/1873-0604.2013002

CHAREYRON Bruno. (2007). *Contrôles radiologiques sur les lagunes de stockage de phosphogypse et la décharge CRI-9*. Retrieved from https://inis.iaea.org/collection/NCLCollectionStore/_Public/42/052/42052466.pdf

Chen, T., Chang, Q., Clevers, J. G. P. W., & Kooistra, L. (2015). Rapid identification of soil cadmium pollution risk at regional scale based on visible and near-infrared spectroscopy. https://doi.org/10.1016/j.envpol.2015.07.009

Chen, Y., Wei, Z., Irfan, M., Xu, J., & Yang, Y. (2018). Laboratory investigation of the relationship between electrical resistivity and geotechnical properties of phosphate tailings. *Measurement*. https://doi.org/10.1016/j.measurement.2018.05.095

Climate-data.org. (2018). Clima Cartagena: Temperatura, Climograma y Tabla climática

para Cartagena - Climate-Data.org. Retrieved April 5, 2018, from https://es.climate-data.org/location/3213/

Clynes, T. (2018). Guatemala's Maya Society Featured Huge "Megalopolis," LiDAR Data Show. Retrieved December 18, 2018, from https://news.nationalgeographic.com/2018/02/maya-laser-lidar-guatemala-pacunam/

Concejalía de Nuevas Tecnologías. (2018). Ayuntamiento de Cartagena. Retrieved February 27, 2018, from https://www.cartagena.es/barrios_diputaciones.asp

Cortada, U., Martínez, J., Rey, J., Hidalgo, M. C., & Sandoval, S. (2017). Assessment of tailings pond seals using geophysical and hydrochemical techniques. *Engineering Geology*, *223*, 59–70. https://doi.org/10.1016/j.enggeo.2017.04.024

Dirección General del Instituto Geográfico Nacional. (2016). Plan Nacional de Ortofotografía Aérea. Retrieved January 3, 2019, from http://pnoa.ign.es/especificaciones-tecnicas

Domènech, C., Canals, À., Soler, A., Sabanès, A., & Dumestre, A. (2017). Evolution Assessment of Soils Contaminated by Roasted Pyrite Wastes. *Procedia Earth and Planetary Science*, *17*, 432–435. https://doi.org/10.1016/J.PROEPS.2016.12.109

Drahor, M. G. (2011). A review of integrated geophysical investigations from archaeological and cultural sites under encroaching urbanisation in İzmir, Turkey. *Physics and Chemistry of the Earth*, *36*(16), 1294–1309. https://doi.org/10.1016/j.pce.2011.03.010

El Zrelli, R., Rabaoui, L., Abda, H., Daghbouj, N., Pérez-López, R., Castet, S., … Courjault-Radé, P. (2019). Characterization of the role of phosphogypsum foam in the transport of metals and radionuclides in the Southern Mediterranean Sea. *Journal of Hazardous Materials*, *363*, 258–267. https://doi.org/10.1016/j.jhazmat.2018.09.083

EMGRISA. (1998). *Proyecto de investigación de suelos contaminados de las fincas, propiedad del I.C.O., en la zona del Hondón (Cartagena)*. Murcia.

Espejo Marín, C. (2005). Antecedentes históricos y situación actual de la industria en la Región de Murcia. Retrieved February 28, 2018, from

http://www.ingeba.org/lurralde/lurranet/lur28/28espejo/28espejo.htm

Esri. (2016). ArcGIS for Desktop. *Esri*, 1. Retrieved from http://desktop.arcgis.com/en/arcmap/10.3/manage-data/las-dataset/what-is-lidar-data-.htm

European Chemicals Agency. (2018). Cadmium - Substance Information - ECHA. Retrieved November 9, 2018, from https://echa.europa.eu/substance-information/-/substanceinfo/100.028.320

European Communities, C. of. (1991). Council Directive of 18 March 191 amending Directive 75/442/ECC on waste, (L), 1–53.

European Environment Agency. (1998). *MEDIO AMBIENTE EN EUROPA : Segunda evaluación. Degradación del suelo*.

European Environment Agency. (2015). Progress in management of contaminated sites — European Environment Agency. Retrieved from http://www.eea.europa.eu/data-and-maps/indicators/progress-in-management-of-contaminated-sites/progress-in-management-of-contaminated-1

Evangelista, L., de Silva, F., d'Onofrio, A., Di Fiore, V., Silvestri, F., Scotto di Santolo, A., … Tarallo, D. (2017a). Application of ERT and GPR geophysical testing to the subsoil characterization of cultural heritage sites in Napoli (Italy). *Measurement: Journal of the International Measurement Confederation*, *104*, 326–335. https://doi.org/10.1016/j.measurement.2016.07.042

Evangelista, L., de Silva, F., d'Onofrio, A., Di Fiore, V., Silvestri, F., Scotto di Santolo, A., … Tarallo, D. (2017b). Application of ERT and GPR geophysical testing to the subsoil characterization of cultural heritage sites in Napoli (Italy). *Measurement: Journal of the International Measurement Confederation*, *104*, 326–335. https://doi.org/10.1016/j.measurement.2016.07.042

Everett, M. E. (2013). Electrical resistivity method. In *Near-Surface Applied Geophysics* (pp. 70–102). Cambridge University Press.

Frid, V., Averbach, A., Frid, M., Dudkinski, D., & Liskevich, G. (2017). Statistical

Analysis of Resistivity Anomalies Caused by Underground Caves. *Pure and Applied Geophysics*, *174*(3), 997–1012. https://doi.org/10.1007/s00024-015-1106-x

Frid, Vladimir, Sharabi, I., Frid, M., & Averbakh, A. (2017). Leachate detection via statistical analysis of electrical resistivity and induced polarization data at a waste disposal site (Northern Israel). *Environmental Earth Sciences*, *76*(6), 233. https://doi.org/10.1007/s12665-017-6554-4

Friedman, S. P. (2005). Soil properties influencing apparent electrical conductivity: a review. *Computers and Electronics in Agriculture S.P. Friedman / Computers and Electronics in Agriculture*, *46*(46), 45–70. https://doi.org/10.1016/j.compag.2004.11.001

Gabarrón, M., Faz, A., & Acosta, J. A. (2018). Use of multivariable and redundancy analysis to assess the behavior of metals and arsenic in urban soil and road dust affected by metallic mining as a base for risk assessment. *Journal of Environmental Management*, *206*, 192–201. https://doi.org/10.1016/j.jenvman.2017.10.034

García-menéndez, O., Ballesteros, B. J., Renau-Pruñonosa, A., & Morell, I. (2018). Using electrical resistivity tomography to assess the effectiveness of managed aquifer recharge in a salinized coastal aquifer. *Environ Monit Assess*. https://doi.org/10.1007/s10661-017-6446-9

Golden Software. (2018). Surfer®. Retrieved December 18, 2018, from https://www.goldensoftware.com/products/surfer/features

Gómez-García, C., Martin-Hernandez, F., López García, J. Á., Martínez-Pagán, P., Manteca, J. I., & Carmona, C. (2015). Rock magnetic characterization of the mine tailings in Portman Bay (Murcia, Spain) and its contribution to the understanding of the bay infilling process. *Journal of Applied Geophysics*, *120*, 48–59. https://doi.org/10.1016/j.jappgeo.2015.06.008

Gómez-Ortiz, D., Martín-Velázquez, S., Martín-Crespo, T., José, C. D. I.-S., & Lillo, J. (2010). Application of electrical resistivity tomography to the environmental characterization of abandoned massive sulphide mine ponds (Iberian Pyrite Belt, SW Spain). *Near Surface Geophysics*, *8*(1), 65–74. https://doi.org/10.3997/1873-

0604.2009052

Guerrero, J. L., Gutiérrez-Álvarez, I., Mosqueda, F., Olías, M., García-Tenorio, R., & Bolívar, J. P. (2019). Pollution evaluation on the salt-marshes under the phosphogypsum stacks of Huelva due to deep leachates. *Chemosphere*, *230*, 219–229. https://doi.org/10.1016/j.chemosphere.2019.04.212

Halihan, T., Sefa, V., Sale, T., & Lyverse, M. (2017). Mechanism for detecting NAPL using electrical resistivity imaging. *Journal of Contaminant Hydrology*, *205*, 57–69. https://doi.org/10.1016/j.jconhyd.2017.08.007

Hazreek, Z. A. M., Azhar, A. T. S., Tun, U., Onn, H., Johor, B. P., & Rosli, S. (2018). FIELD MINIATURE STUDY ON HEAVY METAL DETECTION USING ELECTRICAL RESISTIVITY IMAGING (ERI), *9*(5), 284–292.

IRIS Instruments. (2018). Syscal R1 plus Switch. Retrieved April 9, 2018, from http://www.iris-instruments.com/syscal-r1plussw.html

Isaac, B. J., Song, B., Pinna, S., Coldren, L. A., & Klamkin, J. (2019). Indium Phosphide Photonic Integrated Circuit Transceiver for FMCW LiDAR. *IEEE Journal of Selected Topics in Quantum Electronics*, *25*(6), 1–7. https://doi.org/10.1109/JSTQE.2019.2911420

Juan Carlos I Rey de España. LEY 10/1998, de 21 de abril, de Residuos (1998). Spain: BOE num. 96. Retrieved from https://www.boe.es/boe/dias/1998/04/22/pdfs/A13372-13384.pdf

Kargar Shouroki, F., Shahtaheri, S. J., Golbabaei, F., Barkhordari, A., & Rahimi-Froushani, A. (2018). Biological Monitoring and Lung Function Assessment among Workers Exposed to Chromium in the Ceramic Industry. *Journal of Research in Health Sciences*, *18*(1), e00408.

Kemna, A., Kulessa, B., & Vereecken, H. (2002). Imaging and characterisation of subsurface solute transport using electrical resistivity tomography (ERT) and equivalent transport models. *Journal of Hydrology*, *267*(3–4), 125–146. https://doi.org/10.1016/S0022-1694(02)00145-2

Kottek, M., Grieser, J., Beck, C., Rudolf, B., & Rubel, F. (2006). World Map of the Köppen-Geiger climate classification updated. *Meteorologische Zeitschrift*, *15*(3), 259–263. https://doi.org/10.1127/0941-2948/2006/0130

Lenntech. (2018). Lead (Pb) - Chemical properties, Health and Environmental effects. Retrieved November 9, 2018, from https://www.lenntech.com/periodic/elements/pb.htm

Liang, H., Jin, Z., & Depaoli, D. (2018). Rare-earth leaching from Florida phosphate rock in wet-process phosphoric acid production, *34*(3).

Lin, J., Sun, W., Desmarais, J., Chen, N., Feng, R., Zhang, P., … Pan, Y. (2018). Uptake and speciation of uranium in synthetic gypsum (CaSO4•2H2O): Applications to radioactive mine tailings. *Journal of Environmental Radioactivity*, *181*, 8–17. https://doi.org/10.1016/J.JENVRAD.2017.10.010

Loke, M. H. (2015). Tutorial:2-D and 3-D Electrical Imaging Surveys. *Tutorial*. Retrieved from http://citeseerx.ist.psu.edu/viewdoc/download?doi=10.1.1.454.4831&rep=rep1&type=pdf

Loke, M. H., & Barker, R. D. (1996). Rapid least-squares inversion of apparent resistivity pseudosections by a quasi-Newton method. *Geophysical Prospecting*, *44*(1), 131–152. https://doi.org/10.1111/j.1365-2478.1996.tb00142.x

Ma, B., Lu, W., Su, Y., Li, Y., Gao, C., & He, X. (2018). Synthesis of α-hemihydrate gypsum from cleaner phosphogypsum. https://doi.org/10.1016/j.jclepro.2018.05.228

Macías, F., Cánovas, C. R., Cruz-Hernández, P., Carrero, S., Asta, M. P., Nieto, J. M., & Pérez-López, R. (2017). An anomalous metal-rich phosphogypsum: Characterization and classification according to international regulations. *Journal of Hazardous Materials*, *331*, 99–108. https://doi.org/10.1016/J.JHAZMAT.2017.02.015

Mahmoud, E., & Abd El-Kader, N. (2015). Heavy Metal Immobilization in Contaminated Soils using Phosphogypsum and Rice Straw Compost. *Land Degradation and Development*, *26*(8), 819–824. https://doi.org/10.1002/ldr.2288

Martín-Crespo, T., Gómez-Ortiz, D., Martín-Velázquez, S., Martínez-Pagán, P., De Ignacio, C., Lillo, J., & Faz, Á. (2018a). Geoenvironmental characterization of unstable abandoned mine tailings combining geophysical and geochemical methods (Cartagena-La Union district, Spain). *Engineering Geology*, *232*(May 2017), 135–146. https://doi.org/10.1016/j.enggeo.2017.11.018

Martín-Crespo, T., Gómez-Ortiz, D., Martín-Velázquez, S., Martínez-Pagán, P., De Ignacio, C., Lillo, J., & Faz, Á. (2018b). Geoenvironmental characterization of unstable abandoned mine tailings combining geophysical and geochemical methods (Cartagena-La Union district, Spain). *Engineering Geology*, *232*(May 2017), 135–146. https://doi.org/10.1016/j.enggeo.2017.11.018

Martín-Crespo, T., Gómez-Ortiz, D., Martínez-Pagán, P., De Ignacio-San José, C., Martín-Velázquez, S., Lillo, J., & Faz, A. (2012). Geoenvironmental characterization of riverbeds affected by mine tailings in the Mazarrón district (Spain). *Journal of Geochemical Exploration*, *119–120*, 6–16. https://doi.org/10.1016/J.GEXPLO.2012.06.004

Martinez-Pagan, P., Cano, A. F., Aracil, E., & Arocena, J. M. (2009). Electrical Resistivity Imaging Revealed the Spatial Properties of Mine Tailing Ponds in the Sierra Minera of Southeast Spain. *Journal of Environmental & Engineering Geophysics*, *14*(2), 63–76. https://doi.org/10.2113/JEEG14.2.63

Martínez-Pagán, P., Cano, A. F., Aracil, E., & Arocena, J. M. (2009). Electrical Resistivity Imaging Revealed the Spatial Properties of Mine Tailing Ponds in the Sierra Minera of Southeast Spain. *Journal of Environmental & Engineering Geophysics*, *14*(2), 63–76. https://doi.org/10.2113/JEEG14.2.63

Martínez-Pagán, P., Faz, A., Acosta, J. A., Carmona, D. M., & Martínez-Martínez, S. (2011). A multidisciplinary study for mining landscape reclamation: A study case on two tailing ponds in the Region of Murcia (SE Spain). *Physics and Chemistry of the Earth*, *36*(16), 1331–1344. https://doi.org/10.1016/j.pce.2011.02.007

Martínez-Pagán, Pedro. (2006). *" Aplicación De Diferentes Técnicas No Destructivas De Prospección Geofísica a Actividades Antrópicas En La Región De Murcia ."*

Martínez-Segura, M. A., Vásconez-Maza, M. D., & García-Nieto, M. C. (2020). Volumetric characterisation of waste deposits generated during the production of fertiliser derived from phosphoric rock by using LiDAR and electrical resistivity tomography. *Science of The Total Environment*, 137076. https://doi.org/10.1016/j.scitotenv.2020.137076

Martínez Pagán, P. (2006). *Aplicación de diferentes técnicas no destructivas de prospección geofísica a problemas relacionados con contaminación ambiental producidas por diferentes actividades antrópicas en la Región de Murcia*. Pedro Martínez Pagán. https://doi.org/10.31428/10317/975

Mashifana, T., Ntuli, F., & Okonta, F. (2018). Leaching kinetics on the removal of phosphorus from waste phosphogypsum by application of shrinking core model. https://doi.org/10.1016/j.sajce.2018.11.001

Matys Grygar, T., Nováková, T., Bábek, O., Elznicová, J., & Vadinová, N. (2013). Robust assessment of moderate heavy metal contamination levels in floodplain sediments: A case study on the Jizera River, Czech Republic. *Science of the Total Environment*, *452–453*, 233–245. https://doi.org/10.1016/j.scitotenv.2013.02.085

Millán-Becerro, R., Pérez-López, R., Macías, F., Cánovas, C. R., Papaslioti, E.-M., & Dolores Basallote, M. (2019). Assessment of metals mobility during the alkaline treatment of highly acid phosphogypsum leachates. *Science of The Total Environment*, *660*, 395–405. https://doi.org/10.1016/j.scitotenv.2018.12.305

Oliveira, M. L. S., Ward, C. R., Izquierdo, M., Sampaio, C. H., de Brum, I. A. S., Kautzmann, R. M., … Silva, L. F. O. (2012a). Chemical composition and minerals in pyrite ash of an abandoned sulphuric acid production plant. *Science of The Total Environment*, *430*, 34–47. https://doi.org/10.1016/J.SCITOTENV.2012.04.046

Oliveira, M. L. S., Ward, C. R., Izquierdo, M., Sampaio, C. H., de Brum, I. A. S., Kautzmann, R. M., … Silva, L. F. O. (2012b). Chemical composition and minerals in pyrite ash of an abandoned sulphuric acid production plant. *Science of The Total Environment*, *430*, 34–47. https://doi.org/10.1016/J.SCITOTENV.2012.04.046

Papastefanou, C., Stoulos, S., Ioannidou, A., & Manolopoulou, M. (2006). The application

of phosphogypsum in agriculture and the radiological impact. *Journal of Environmental Radioactivity*. https://doi.org/10.1016/j.jenvrad.2006.05.005

Pedrera-Parrilla, A., Pachepsky, Y. A., Taguas, E. V., Martos-Rosillo, S., Giráldez, J. V., & Vanderlinden, K. (2017). Concurrent temporal stability of the apparent electrical conductivity and soil water content. *Journal of Hydrology*, *544*, 319–326. https://doi.org/10.1016/j.jhydrol.2016.10.017

Pérez-López, R., Macías, F., Cánovas, C. R., Sarmiento, A. M., & Pérez-Moreno, S. M. (2016). Pollutant flows from a phosphogypsum disposal area to an estuarine environment: An insight from geochemical signatures. *Science of The Total Environment*, *553*, 42–51. https://doi.org/10.1016/j.scitotenv.2016.02.070

Perrone, A., Lapenna, V., & Piscitelli, S. (2014). Electrical resistivity tomography technique for landslide investigation: A review. *Earth-Science Reviews*, *135*, 65–82. https://doi.org/10.1016/j.earscirev.2014.04.002

R Core Team. (2019). R: A language and environment for statistical computing. R Foundation for Statistical Computing. Retrieved October 30, 2019, from https://www.r-project.org/

R Core Team. (2020). What is R? Retrieved November 14, 2020, from https://www.r-project.org/about.html

Región de murcia digital. (2009). GEOLOGÍA-Cuencas Neógenas - Región de Murcia Digital. Retrieved November 8, 2018, from http://www.regmurcia.com/servlet/s.Sl?sit=c,365,m,108&r=ReP-16274-DETALLE_REPORTAJESPADRE

Romero-Hermida, M. I., Borrero-López, A. M., Alejandre, F. J., Flores-Alés, V., Santos, A., Franco, J. M., & Esquivias, L. (2018). Phosphogypsum waste lime as a promising substitute of commercial limes: A rheological approach. https://doi.org/10.1016/j.cemconcomp.2018.11.007

Rosales Aranda, R. M. (2013). *Detection and evaluation of hydrocarbons soil contamination by underground storage tanks at petrol stations*. Rosa María Rosales Aranda. https://doi.org/10.31428/10317/3892

Rosales, R. M., Martínez-Pagan, P., Faz, A., & Moreno-Cornejo, J. (2012). Environmental Monitoring Using Electrical Resistivity Tomography (ERT) in the Subsoil of Three Former Petrol Stations in SE of Spain. *Water, Air, & Soil Pollution*, *223*(7), 3757–3773. https://doi.org/10.1007/s11270-012-1146-0

Roy, A., & Apparao, A. (1971). DEPTH OF INVESTIGATION IN DIRECT CURRENT METHODS. *GEOPHYSICS*, *36*(5), 943–959. https://doi.org/10.1190/1.1440226

Rutherford, P. M., Dudas, M. J., & Samek, R. A. (1994). Environmental impacts of phosphogypsum. *Science of The Total Environment*, *149*(1–2), 1–38. https://doi.org/10.1016/0048-9697(94)90002-7

Rychkov, V. N., Kirillov, E. V., Kirillov, S. V., Semenishchev, V. S., Bunkov, G. M., Botalov, M. S., … Malyshev, A. S. (2018). Recovery of rare earth elements from phosphogypsum. *Journal of Cleaner Production*, *196*, 674–681. https://doi.org/10.1016/j.jclepro.2018.06.114

Sadiqul Islam, G., Habib Chowdhury, F., Tanveer Raihan, M., Kumar Sikder Amit, S., & Rafiqul Islam, M. (2017). Effect of Phosphogypsum on the Properties of Portland Cement. *Procedia Engineering*, *171*, 744–751. https://doi.org/10.1016/j.proeng.2017.01.440

Sahu, S. K., Ajmal, P. Y., Bhangare, R. C., Tiwari, M., & Pandit, G. G. (2014). Natural radioactivity assessment of a phosphate fertilizer plant area. *Journal of Radiation Research and Applied Sciences*, *7*(1), 123–128. https://doi.org/10.1016/j.jrras.2014.01.001

Samouëlian, A., Cousin, I., Tabbagh, A., Bruand, A., & Richard, G. (2005). Electrical resistivity survey in soil science: A review. *Soil and Tillage Research*. https://doi.org/10.1016/j.still.2004.10.004

Siddiqui, F. I., & Osman, S. B. A. B. S. O. (2012). Simple and multiple regression models for relationship between electrical resistivity and various soil properties for soil characterization. https://doi.org/10.1007/s12665-012-2122-0

Simyrdanis, K., Papadopoulos, N., Soupios, P., Kirkou, S., & Tsourlos, P. (2018). Characterization and monitoring of subsurface contamination from Olive Oil Mills'

waste waters using Electrical Resistivity Tomography. *Science of The Total Environment*, *637–638*, 991–1003. https://doi.org/10.1016/j.scitotenv.2018.04.348

Soil Survey Staff. (2011). *Soil Survey Laboratory Information Manual Soil Survey Investigations Report No. 45*. Lincoln, Nebraska. Retrieved from https://www.nrcs.usda.gov/Internet/FSE_DOCUMENTS/nrcs142p2_052226.pdf

Sudha, K., Israil, M., Mittal, S., & Rai, J. (2009). Soil characterization using electrical resistivity tomography and geotechnical investigations. *Journal of Applied Geophysics*, *67*(1), 74–79. https://doi.org/10.1016/J.JAPPGEO.2008.09.012

Tayibi, H., Choura, M., López, F. A., Alguacil, F. J., & López-Delgado, A. (2009). Environmental impact and management of phosphogypsum. *Journal of Environmental Management*, *90*(8), 2377–2386. https://doi.org/10.1016/j.jenvman.2009.03.007

The Conference Board. (2019). Economic Data & Analysis. Retrieved January 10, 2019, from https://www.conference-board.org/data/

Tsokas, G. N., Tsourlos, P. I., Vargemezis, G., & Novack, M. (2008). Non-destructive electrical resistivity tomography for indoor investigation: the case of Kapnikarea Church in Athens. *Archaeological Prospection*, *15*(1), 47–61. https://doi.org/10.1002/arp.321

US-EPA. (2007). Method 3051A: Microwave Assisted Acid Digestion of Sediments, Sludges, Soils, and Oils. Retrieved from https://www.epa.gov/sites/production/files/2015-12/documents/3051a.pdf

Vanella, D., Cassiani, G., Busato, L., Boaga, J., Barbagallo, S., Binley, A., & Consoli, S. (2018). Use of small scale electrical resistivity tomography to identify soil-root interactions during deficit irrigation. *Journal of Hydrology*, *556*, 310–324. https://doi.org/10.1016/J.JHYDROL.2017.11.025

Vásconez-Maza, M. D., Martínez-Segura, M. A., Bueso, M. C., Faz, Á., García-Nieto, M. C., Gabarrón, M., & Acosta, J. A. (2019). Predicting spatial distribution of heavy metals in an abandoned phosphogypsum pond combining geochemistry, electrical resistivity tomography and statistical methods. *Journal of Hazardous Materials*, *374*,

392–400. https://doi.org/10.1016/j.jhazmat.2019.04.045

Virolainen, S., Repo, E., & Sainio, T. (2019). Recovering rare earth elements from phosphogypsum using a resin-in-leach process: Selection of resin, leaching agent, and eluent. *Hydrometallurgy*, *189*, 105125. https://doi.org/10.1016/j.hydromet.2019.105125

Walawalkar, M., Nichol, C. K., & Azimi, G. (2016). Process investigation of the acid leaching of rare earth elements from phosphogypsum using HCl, HNO3, and H2SO4. *Hydrometallurgy*. https://doi.org/10.1016/j.hydromet.2016.06.008

Wang, T.-P., Chen, C.-C., Tong, L.-T., Chang, P.-Y., Chen, Y.-C., Dong, T.-H., … Cheng, S.-N. (2015). Applying FDEM, ERT and GPR at a site with soil contamination: A case study. *Journal of Applied Geophysics*, *121*, 21–30. https://doi.org/10.1016/J.JAPPGEO.2015.07.005

Winters, G., Ryvkin, I., Rudkov, T., Moreno, Z., & Furman, A. (2015). Mapping underground layers in the super arid Gidron Wadi using electrical resistivity tomography (ERT). *Journal of Arid Environments*, *121*, 79–83. https://doi.org/10.1016/j.jaridenv.2015.05.008

Zrelli, R. El, Rabaoui, L., Daghbouj, N., Abda, H., Castet, S., Josse, C., … Courjault-Radé, P. (2018). Characterization of phosphate rock and phosphogypsum from Gabes phosphate fertilizer factories (SE Tunisia): high mining potential and implications for environmental protection. *Environmental Science and Pollution Research*. https://doi.org/10.1007/s11356-018-1648-4

APPENDIX

APPENDIX 1

IMPACT FACTOR OF THE SCIENTIFIC JOURNALS

ISI Web of Science. JCR section

Article 1

Vásconez-Maza, M.D., Martínez-Segura, M.A., Bueso, M.C., Faz, Á., García-Nieto, M.C., Gabarrón, M., Acosta, J.A., 2019. Predicting spatial distribution of heavy metals in an abandoned phosphogypsum pond combining geochemistry, electrical resistivity tomography and statistical methods. J. Hazard. Mater. 374, 392–400. https://doi.org/10.1016/j.jhazmat.2019.04.045; Q1; IF: 9.038.

25/9/2020 InCites Journal Citation Reports

Web of Science | InCites | Journal Citation Reports | Essential Science Indicators | EndNote | Publons

InCites Journal Citation Reports

Home > Journal Profile

JOURNAL OF HAZARDOUS MATERIALS

ISSN: 0304-3894
eISSN: 1873-3336
ELSEVIER
RADARWEG 29, 1043 NX AMSTERDAM, NETHERLANDS
NETHERLANDS

Go to Journal Table of Contents Go to Ulrich's Printable Version

TITLES
ISO: J. Hazard. Mater.
JCR Abbrev: J HAZARD MATER

CATEGORIES
ENVIRONMENTAL SCIENCES -- SCIE
ENGINEERING, ENVIRONMENTAL -- SCIE

LANGUAGES
English

PUBLICATION FREQUENCY
20 issues/year

2019 Journal Impact Factor & percentile rank in category for: JOURNAL OF HAZARDOUS MATERIALS

9.038
2019 Journal Impact Factor

JCR Impact Factor

JCR Year	ENGINEERING, ENVIRONMENTAL			ENVIRONMENTAL SCIENCES			ENGINEERING, CIVIL		
	Rank	Quartile	JIF Percentile	Rank	Quartile	JIF Percentile	Rank	Quartile	JIF Percentile
2019	4/53	Q1	93.396	8/265	Q1	97.170	n/a	n/a	n/a
2018	4/52	Q1	93.269	12/251	Q1	95.418	n/a	n/a	n/a
2017	5/50	Q1	91.000	13/242	Q1	94.835	n/a	n/a	n/a
2016	5/49	Q1	90.816	13/229	Q1	94.541	1/125	Q1	99.600
2015	7/50	Q1	87.000	19/225	Q1	91.778	2/126	Q1	98.810

Article 2

Martínez-Segura, M.A., **Vásconez-Maza, M.D.**, García-Nieto, M.C., 2020. Volumetric characterisation of waste deposits generated during the production of fertiliser derived from phosphoric rock by using LiDAR and electrical resistivity tomography. Sci. Total Environ. 716, 137076. https://doi.org/10.1016/j.scitotenv.2020.137076. Q1; IF: 6.551

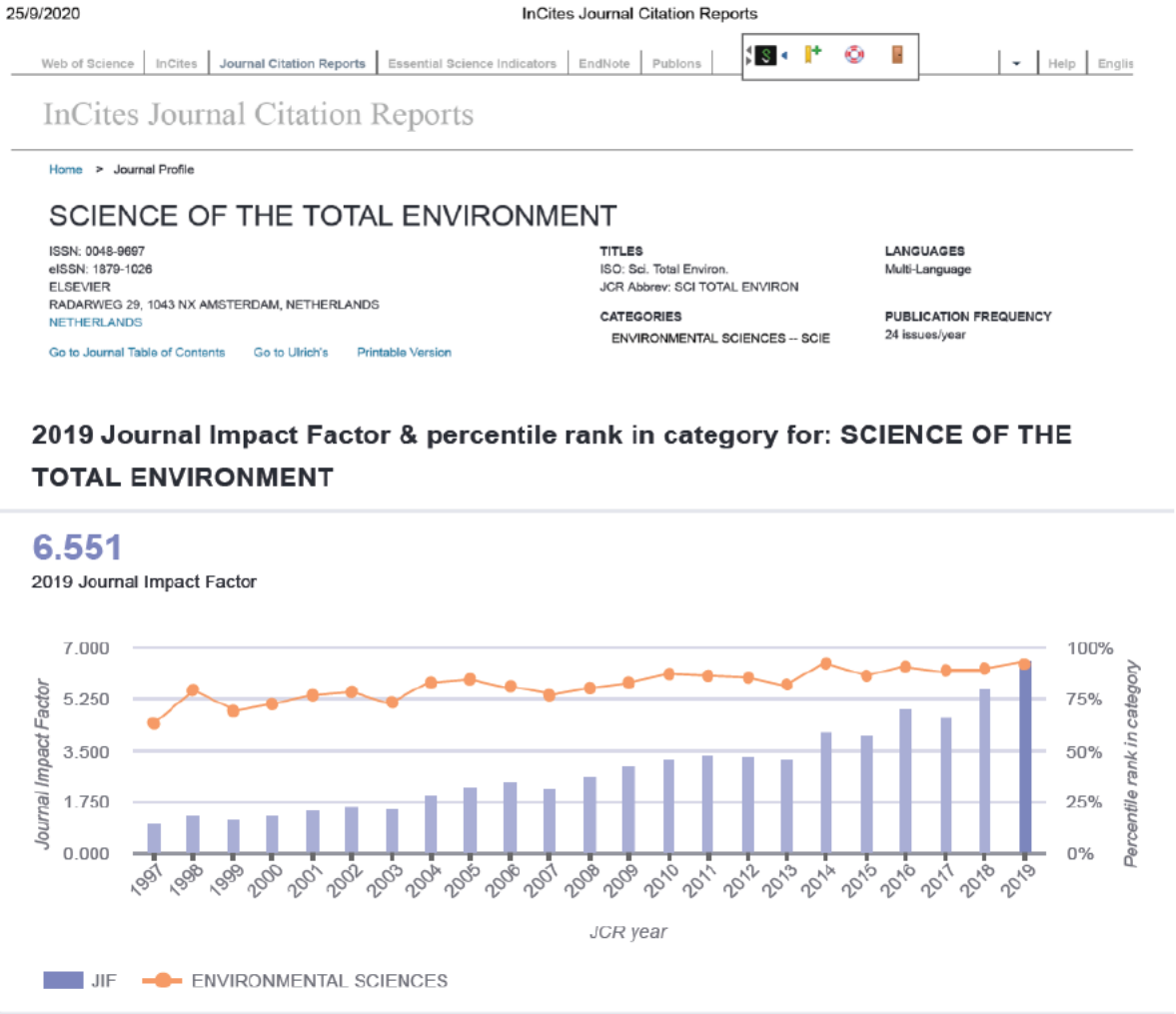

25/9/2020 InCites Journal Citation Reports

Web of Science | InCites | Journal Citation Reports | Essential Science Indicators | EndNote | Publons | Help | Englis

InCites Journal Citation Reports

Home > Journal Profile

SCIENCE OF THE TOTAL ENVIRONMENT

ISSN: 0048-9697
eISSN: 1879-1026
ELSEVIER
RADARWEG 29, 1043 NX AMSTERDAM, NETHERLANDS
NETHERLANDS

Go to Journal Table of Contents Go to Ulrich's Printable Version

TITLES
ISO: Sci. Total Environ.
JCR Abbrev: SCI TOTAL ENVIRON

CATEGORIES
ENVIRONMENTAL SCIENCES -- SCIE

LANGUAGES
Multi-Language

PUBLICATION FREQUENCY
24 issues/year

2019 Journal Impact Factor & percentile rank in category for: SCIENCE OF THE TOTAL ENVIRONMENT

6.551
2019 Journal Impact Factor

JCR Impact Factor

JCR Year	ENVIRONMENTAL SCIENCES		
	Rank	Quartile	JIF Percentile
2019	22/265	Q1	91.887
2018	27/251	Q1	89.442
2017	27/242	Q1	89.050
2016	22/229	Q1	90.611
2015	32/225	Q1	86.000

Article 3

Vásconez-Maza, M. D., Bueso, M.C., Faz, A., Acosta, J.A., Martínez-Segura, M.A., 2021. Assessing the behaviour of heavy metals in abandoned phosphogypsum deposits combining electrical resistivity tomography and multivariate analysis. J. Environ. Manage. 278, 301–4797. https://doi.org/10.1016/j.jenvman.2020.111517; Q1; IF: 5.647

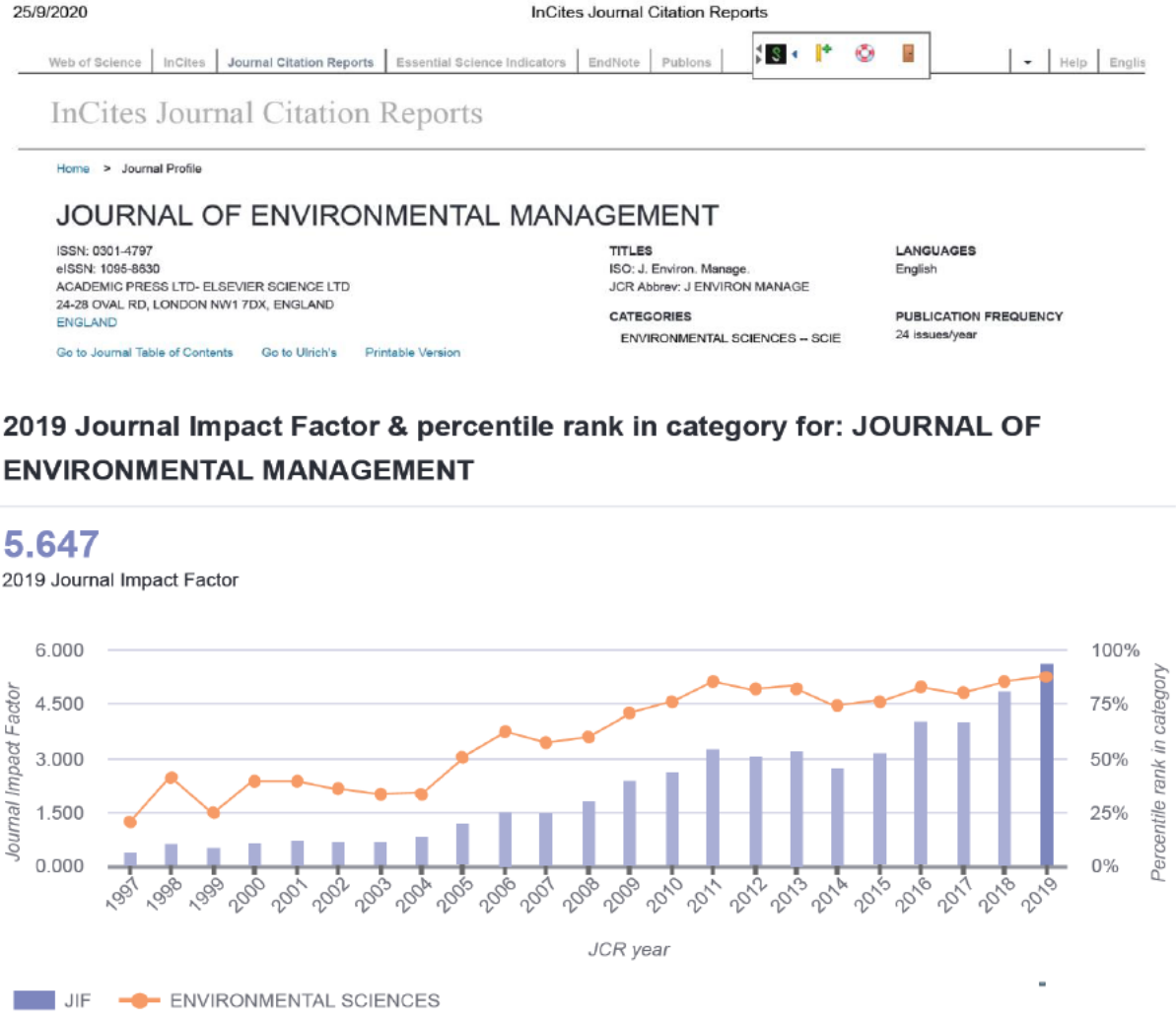

25/9/2020 InCites Journal Citation Reports

Web of Science | InCites | Journal Citation Reports | Essential Science Indicators | EndNote | Publons | Help | Englis

InCites Journal Citation Reports

Home > Journal Profile

JOURNAL OF ENVIRONMENTAL MANAGEMENT

ISSN: 0301-4797
eISSN: 1095-8630
ACADEMIC PRESS LTD- ELSEVIER SCIENCE LTD
24-28 OVAL RD, LONDON NW1 7DX, ENGLAND
ENGLAND

Go to Journal Table of Contents Go to Ulrich's Printable Version

TITLES
ISO: J. Environ. Manage.
JCR Abbrev: J ENVIRON MANAGE

CATEGORIES
ENVIRONMENTAL SCIENCES – SCIE

LANGUAGES
English

PUBLICATION FREQUENCY
24 issues/year

2019 Journal Impact Factor & percentile rank in category for: JOURNAL OF ENVIRONMENTAL MANAGEMENT

5.647
2019 Journal Impact Factor

JCR Impact Factor

JCR Year	ENVIRONMENTAL SCIENCES		
	Rank	Quartile	JIF Percentile
2019	33/265	Q1	87.736
2018	37/251	Q1	85.458
2017	48/242	Q1	80.372
2016	39/229	Q1	83.188
2015	54/225	Q1	76.222